INL/EXT-12-27228
Revision 2

CRITICAL CONFIGURATION AND PHYSICS MEASUREMENTS FOR BERYLLIUM REFLECTED ASSEMBLIES OF U(93.15)O2 FUEL RODS (1.506-CM PITCH AND 7-TUBE CLUSTERS)

Margaret Marshall
John D. Bess
J. Blair Briggs
Michael F. Murphy
John T. Mihalczo

March 2015

The INL is a U.S. Department of Energy National Laboratory
operated by Battelle Energy Alliance

INL/EXT-05-Error! Reference source not found.

CRITICAL CONFIGURATION AND PHYSICS MEASUREMENTS FOR BERYLLIUM REFLECTED ASSEMBLIES OF U(93.15)O2 FUEL RODS (1.506-CM PITCH AND 7-TUBE CLUSTERS)

Margaret Marshall
John D. Bess
J. Blair Briggs
Michael F. Murphy
John T. Mihalczo

March 2015

Idaho National Laboratory

Idaho Falls, Idaho 83415

http://www.inl.gov

Prepared for the
U.S. Department of Energy
Office of Nuclear Energy
Under DOE Idaho Operations Office
Contract DE-AC07-05ID14517

NEA/NSC/DOC(2006)1

Space Reactor - SPACE

SCCA-SPACE-EXP-003
CRIT-SPEC-REAC-RRATE

CRITICAL CONFIGURATION AND PHYSICS MEASUREMENTS FOR BERYLLIUM REFLECTED ASSEMBLIES OF U(93.15)O_2 FUEL RODS (1.506-CM PITCH AND 7-TUBE CLUSTERS)

Evaluator

Margaret A. Marshall
Idaho National Laboratory

Internal Reviewers

John D. Bess
J. Blair Briggs
Idaho National Laboratory

Independent Reviewers

Michael F. Murphy
Under Subcontract to the OECD NEA

John T. Mihalczo
Oak Ridge National Laboratory
(Section 1)

Space Reactor - SPACE

SCCA-SPACE-EXP-003
CRIT-SPEC-REAC-RRATE

Status of Compilation/Evaluation/Peer Review

Section 1	Compiled	Independent Review	Working Group Review	Approved
1.0 DETAILED DESCRIPTION				
1.1 Description of the Critical and/or Subcritical Configuration	YES	YES	YES	YES
1.2 Description of Buckling and Extrapolation-Length Measurements	NA	NA	NA	NA
1.3 Description of Spectral-Characteristics Measurements	YES	YES	YES	YES
1.4 Description of Reactivity-Effects Measurements	YES	YES	YES	YES
1.5 Description of Reactivity-Coefficient Measurements	NA	NA	NA	NA
1.6 Description of Kinetics Measurements	NA	NA	NA	NA
1.7 Description of Reaction-Rate Distribution Measurements	YES	YES	YES	YES
1.8 Description of Power-Distribution Measurements	NA	NA	NA	NA
1.9 Description of Isotopic Measurements	NA	NA	NA	NA
1.10 Description of Other Miscellaneous Types of Measurements	NA	NA	NA	NA
Section 2	**Evaluated**	**Independent Review**	**Working Group Review**	**Approved**
2.0 EVALUATION OF EXPERIMENTAL DATA				
2.1 Evaluation of Critical and/or Subcritical Configuration Data	YES	YES	YES	YES
2.2 Evaluation of Buckling and Extrapolation Length Data	NA	NA	NA	NA
2.3 Evaluation of Spectral-Characteristics Data	YES	YES	YES	YES
2.4 Evaluation of Reactivity-Effects Data	YES	YES	YES	YES
2.5 Evaluation of Reactivity-Coefficient Data	NA	NA	NA	NA
2.6 Evaluation of Kinetics-Measurements Data	NA	NA	NA	NA
2.7 Evaluation of Reaction-Rate Distributions	YES	YES	YES	YES
2.8 Evaluation of Power-Distribution Data	NA	NA	NA	NA
2.9 Evaluation of Isotopic Measurements	NA	NA	NA	NA
2.10 Evaluation of Other Miscellaneous Types of Measurements	NA	NA	NA	NA

Section 3	Compiled	Independent Review	Working Group Review	Approved
3.0 BENCHMARK SPECIFICATIONS				
3.1 Benchmark-Model Specifications for Critical and/or Subcritical Measurements	YES	YES	YES	YES
3.2 Benchmark-Model Specifications for Buckling and Extrapolation-length Measurements	NA	NA	NA	NA
3.3 Benchmark-Model Specifications for Spectral-Characteristics Measurements	YES	YES	YES	YES
3.4 Benchmark-Model Specifications for Reactivity-Effects Measurements	YES	YES	YES	YES
3.5 Benchmark-Model Specifications for Reactivity-Coefficient Measurements	NA	NA	NA	NA
3.6 Benchmark-Model Specifications for Kinetics Measurements	NA	NA	NA	NA
3.7 Benchmark-Model Specifications for Reaction-Rate Distribution Measurements	YES	YES	YES	YES
3.8 Benchmark-Model Specifications for Power-Distribution Measurements	NA	NA	NA	NA
3.9 Benchmark-Model Specifications for Isotopic Measurements	NA	NA	NA	NA
3.10 Benchmark-Model Specifications of Other Miscellaneous Types of Measurements	NA	NA	NA	NA
Section 4	**Compiled**	**Independent Review**	**Working Group Review**	**Approved**
4.0 RESULTS OF SAMPLE CALCULATIONS				
4.1 Results of Calculations of the Critical or Subcritical Configurations	YES	YES	YES	YES
4.2 Results of Buckling and Extrapolation Length Calculations	NA	NA	NA	NA
4.3 Results of Spectral-Characteristics Calculations	YES	YES	YES	YES
4.4 Results of Reactivity-Effect Calculations	YES	YES	YES	YES
4.5 Results of Reactivity-Coefficient Calculations	NA	NA	NA	NA
4.6 Results of Kinetics-Parameter Calculations	NA	NA	NA	NA
4.7 Results of Reaction-Rate Distribution	YES	YES	YES	YES
4.8 Results of Power-Distribution Calculations	NA	NA	NA	NA
4.9 Results of Isotopic Calculations	NA	NA	NA	NA
4.10 Results of Calculations of Other Miscellaneous Types of Measurements	NA	NA	NA	NA
Section 5	**Compiled**	**Independent Review**	**Working Group Review**	**Approved**
5.0 REFERENCES	YES	YES	YES	YES
Appendix A: Computer Codes, Cross Sections, and Typical Input Listings	YES	YES	YES	YES

CRITICAL CONFIGURATION AND PHYSICS MEASUREMENTS FOR BERYLLIUM REFLECTED ASSEMBLIES OF U(93.15)O_2 FUEL RODS (1.506-CM PITCH AND 7-TUBE CLUSTERS)

IDENTIFICATION NUMBER: SCCA-SPACE-EXP-003
CRIT-SPEC-REAC-RRATE

KEY WORDS: 1.506-cm pitch, 7-tube clusters, acceptable, assembly, beryllium-reflected, cadmium ratios, critical experiments, dioxide, fuel rods, highly enriched, medium power reactor experiment, reactivity worth measurements, small modular reactor, space reactor, un-moderated, uranium

SUMMARY INFORMATION

1.0 DETAILED DESCRIPTION

A series of small, compact critical assembly (SCCA) experiments were completed from 1962–1965 at Oak Ridge National Laboratory's (ORNL's) Critical Experiments Facility (CEF) in support of the Medium-Power Reactor Experiments (MPRE) program. In the late 1950s, efforts were made to study "power plants for the production of electrical power in space vehicles."[(a)] The MPRE program was a part of those efforts and studied the feasibility of a stainless-steel system, boiling potassium 1 MW(t), or about 140 kW(e), reactor. The program was carried out in [fiscal years] 1964, 1965, and 1966. A summary of the program's effort was compiled in 1967.[a] The delayed critical experiments were a mockup of a small, potassium-cooled space power reactor for validation of reactor calculations and reactor physics methods.

Initial experiments, performed in November and December of 1962, consisted of a core of un-moderated stainless-steel tubes, each containing 26 UO_2 fuel pellets, surrounded by a graphite reflector. Measurements were performed to determine critical reflector arrangements, fission-rate distributions, and cadmium ratio distributions. Subsequent experiments used beryllium reflectors and also measured the reactivity for various materials placed in the core. "The [assemblies were built] on [a] vertical assembly machine so that the movable part was the core and bottom reflector" (see Reference 1). The experiment studied in this evaluation was the third of the series and had the fuel in a 1.506-cm-triangular and 7-tube clusters leading to two critical configurations (see References 4 and 5). Once the critical configurations had been achieved, various measurements of reactivity, relative axial and radial activation rates of ^{235}U, and cadmium ratios were performed. The cadmium ratio, reactivity, and activation rate measurements were performed on the 1.506-cm-array critical configuration and are described in Sections 1.3, 1.4, and 1.7, respectively.

Information for this evaluation was compiled from References 1 through 5, from the experimental logbook,[b] and from communication with the experimenter, John T. Mihalczo.

---

[a] A. P. Fraas, "Summary of the MPRE Design and Development Program," ORNL-4048, Oak Ridge National Laboratory (1967).

[b] Radiation Safety Information Computation Center (RSICC), The ORNL Critical Experiments Logbooks, Book 75r, http://rsicc.ornl.gov/RelatedLinks.aspx?t=criticallist, logbook page 81-114.

1.1 Description of the Critical and/or Subcritical Configuration

(The criticality portion of this evaluation has been reviewed and approved by the International Criticality Safety Benchmark Evaluation Project (ICSBEP) and has been published under the following identifier: HEU-COMP-FAST-004.[a])

1.2 Description of Buckling and Extrapolation Length Measurements

Buckling and extrapolation-length measurements were not performed.

1.3 Description of Spectral Characteristics Measurements

1.3.1 Overview of Experiment

Cadmium ratios were measured with enriched uranium metal foils at various locations in the assembly with the fuel tube at the 1.506-cm spacing. They are described in the following subsections.

1.3.2 Geometry of the Experiment Configuration and Measurement Procedure

The experiment configuration was the same as the first critical configuration described in HEU-COMP-FAST-004 (Case 1). The experimenter placed 0.75-cm-diameter × 0.010-cm-thick 93.15%-^{235}U-enriched uranium metal foils[b] with and without 0.051-cm-thick cadmium covers at various locations in the core and top reflector. One part of the cadmium cover was cup shaped and contained the uranium foil. The other part was a lid that fit over the exposed side of the foil when it was in the cup shaped section of the cover.[c] As can be seen in the logbook (pages 103 and 105), two runs were required to obtain all the measurements necessary for the cadmium ratios. The bare foil measurements within the top reflector were performed first as part of the axial foil activation measurements. The results of these measurements are used for both the axial activation results and the cadmium ratios. Cadmium covered foils were then placed at the same locations through the top reflector in a different run. Three pairs of bare and cadmium covered foils were also placed through the core tank. One pair was placed at the midplane of the core 11.35 cm from the center of the core. Two pairs of foils were placed on top of fuel tubes 3.02 and 12.06 cm from the center of the core.[d]

Uranium foils were selected from hundreds of identical foils "according to their activity when exposed to the same neutron flux." Corresponding bare and covered foils had the same activity to less than 1% after activation in the same neutron flux for the same time."[e] The activation of the uranium metal foils was measured after removal from the assembly using two lead-shielded NaI scintillation detectors as follows.

The NaI scintillators were carefully matched and had detection efficiencies for counting delayed-fission-product gamma rays with energies above 250 KeV within 5%. In all foil activation measurements, one foil at a specific location was used as a normalizing foil to remove the effects of the decay of fission products during the counting measurements with the NaI detectors. The normalization foil was placed on one NaI scintillator and the other foil on the other NaI detector and the activities measured

---

[a] International Handbook of Evaluated Criticality Safety Benchmark Experiments, NEA/NSC/DOC(95)03, OECD-NEA, Paris (2012).

[b] Reference 4 reports the foil enrichment as 93.2 wt.%, but according to the experimenter, it was 93.15 wt.% (September 19, 2011).

[c] Personal communication with J.T. Mihalczo, August 14, 2012.

[d] Radiation Safety Information Computation Center (RSICC), The ORNL Critical Experiments Logbooks, Book 75r, http://rsicc.ornl.gov/RelatedLinks.aspx?t=criticallist, logbook page 103 and 105.

[e] Personal communication with J.T. Mihalczo, November 9, 2012.

simultaneously. The activation of a particular foil was compared to that of the normalization foil by dividing the count rate for each foil by that of the normalization foil. "Use of a normalization foil corrects for the time decay after irradiation since it is decaying at the same rate as the foil of interest. So the relative distribution is measured with respect to the normalization foil position."[a] To correct for the differing efficiencies of the two NaI detectors, the normalization foil was counted in Detector 1 simultaneously with the foil at position *x* in Detector 2, and then the normalization foil was counted simultaneously in Detector 2 with the foil from position *x* in Counter 1. The activity of the foil from position *x* was divided by the activity of the normalization foil counted simultaneously. This resulted in two values of the ratio that were then averaged. This procedure essentially removed the effect of the differing efficiencies of the two NaI detectors. Differing efficiencies of 10% resulted in errors in the ratios measured to less than 1%. The background counting rates obtained with the foils used for the measurements on the NaI detectors before their irradiation measurement were subtracted from all count rates. [b] The results of the cadmium ratio measurements are given in Table 1.3-1 and some results are shown in Figure 1.3-1. "No correction has been made for self-shielding in the foils" (Reference 4).

[a] Personal email communication with J.T. Mihalczo, December 3, 2013.

[b] Personal email communication with J. T. Mihalczo, September 27, 2011, and November 23, 2011. The experimenter believes a 250-KeV threshold was used "so as to not count the natural activity of the uranium foils" (November 14, 2011).

Table 1.3-1. Cadmium Ratio (see Reference 4).

Distribution through Top Reflector[a]	
Distance from Center of Fuel Tube (cm)[b]	Cadmium Ratio[c]
15.91	1.37
17.18	1.56
18.45	1.70
19.72	1.76
20.99	1.97
22.26	2.06
Measurement at Axial Core Midplane	
Distance from Core Center (cm)	Cadmium Ratio[c]
11.35[d]	1.24
Measurement at 15.44 cm Above Core Midplane[e]	
Distance from Core Center (cm)	Cadmium Ratio[c]
3.02	1.39
12.06	1.87

(a) These ratios coincide with the position of the relative activation of ^{235}U fission foils in the top reflector measurements in Table 1.7-1.
(b) Foils were placed horizontally between sections of reflector at ½ inch spacing.
(c) The cadmium ratio is defined as the ratio of the bare-to-cadmium-covered foil activity.
(d) This is foil location 9 on Figure 1.4-2.
(e) Foils were placed on top of the fuel tubes. *The foils actually sat at the bottom of the 0.249 cm deep end cap wells. (Personal email communication with J.T. Mihalczo, March 12, 2014.)*

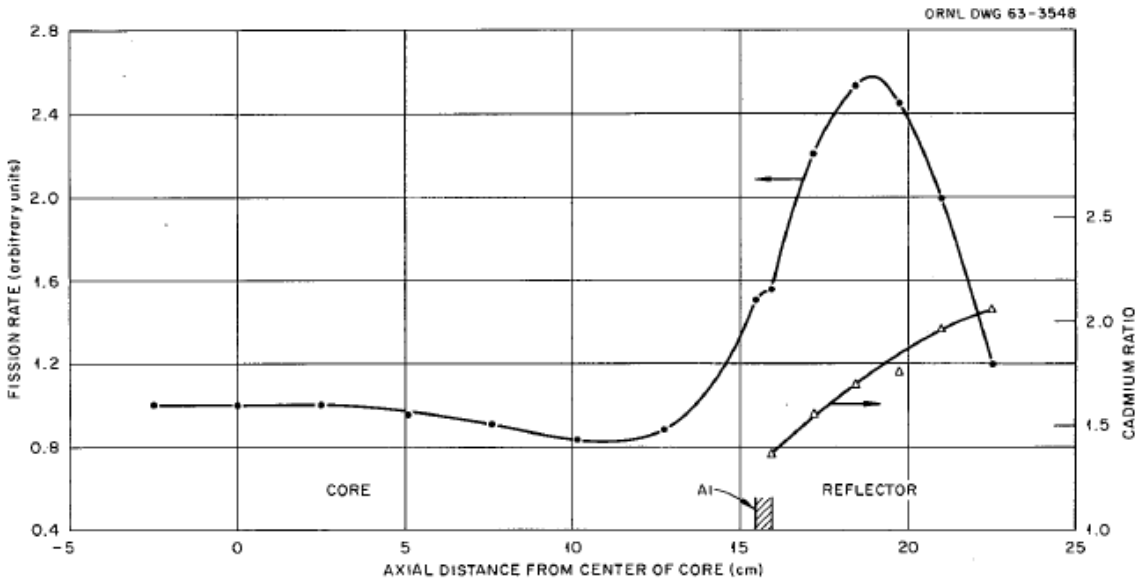

Figure 1.3-1. Plot of Relative Activation of ^{235}U Fission Foils (see Section 1.7) and Cadmium Ratios in the Top Reflector (see Reference 4).

1.3.3 Material Data

The uranium foils were 93.15 wt.% enriched. No impurity data were given for the uranium foils but according to the experimenter, the impurity content of the uranium foil was similar to that for the uranium metal described in HEU-MET-FAST-051.[a] The composition of the cadmium covers was not specified. Material data for the core and reflector parts are the same as those given in Section 1.3 of HEU-COMP-FAST-004.

1.3.4 Temperature Data

The temperature is the same as for the critical configuration, 72°F (22°C).[b]

1.3.5 Additional Information Relevant to Spectral Characteristics Measurements

Additional information was not identified.

[a] International Handbook of Evaluated Criticality Safety Benchmark Experiments, NEA/NSC/DOC(95)03, OECD-NEA, Paris (2012).

[b] Personal email communication with J. T. Mihalczo, May 23, 2011.

1.4 Description of Reactivity Effects Measurements

1.4.1 Overview of Experiment

Various reactivity measurements were performed. The reactivity of fuel tubes at various locations in the core and the effect of fuel tube movement at the periphery of the core were measured. The worth of various neutron absorbing and moderating materials inserted into the core and the worth of adding thickness to the top reflector were also measured. Finally the worth of adding potassium to the core was measured, which also led to some other worth measurements as the core was reconfigured to accommodate the potassium. These reactivity effect measurements are described and summarized below.

1.4.2 Geometry of the Experiment Configuration and Measurement Procedure

All worth measurement were performed by measuring the stable reactor period of the system before and after the system was perturbed. The stable reactor period was then converted to a system reactivity in unit of dollars (see Section 2.4). The change in the system reactivity is the worth of the perturbation.

1.4.2.1 Fuel Effect Reactivity Measurements

The worth of fuel tubes at various radial locations in the core was measured by "observing the change in the stable reactor period when the fuel tube was removed" (Reference 4). Fuel tube reactivities were measured relative to the center fuel tube reactivity.[a] The worth of fuel tubes versus radial position is given in Table 1.4-1 and Figure 1.4-1. The locations of the fuel tubes are shown in Figure 1.4-2.

Table 1.4-1. Fuel Tube Reactivity Worth
Versus Radial Position (see Reference 4).

Fuel Tube Position(a)	Distance From Core Center	Reactivity (¢)
1	0	32.0
2	2.59	32.0
3	5.23	30.8
4	7.75	27.2
5	10.48	25.5
6	10.56	25.6
7	11.78	22.6

(a) Positions given in Figure 1.4-2

[a] It is not clear what it means to be measured relative to the center fuel tube. The reported results are not relative to the center fuel tube. It should be noted that the effect of removing the fuel tubes represents a negative change in the reactivity, however the worth of the rod itself is positive.

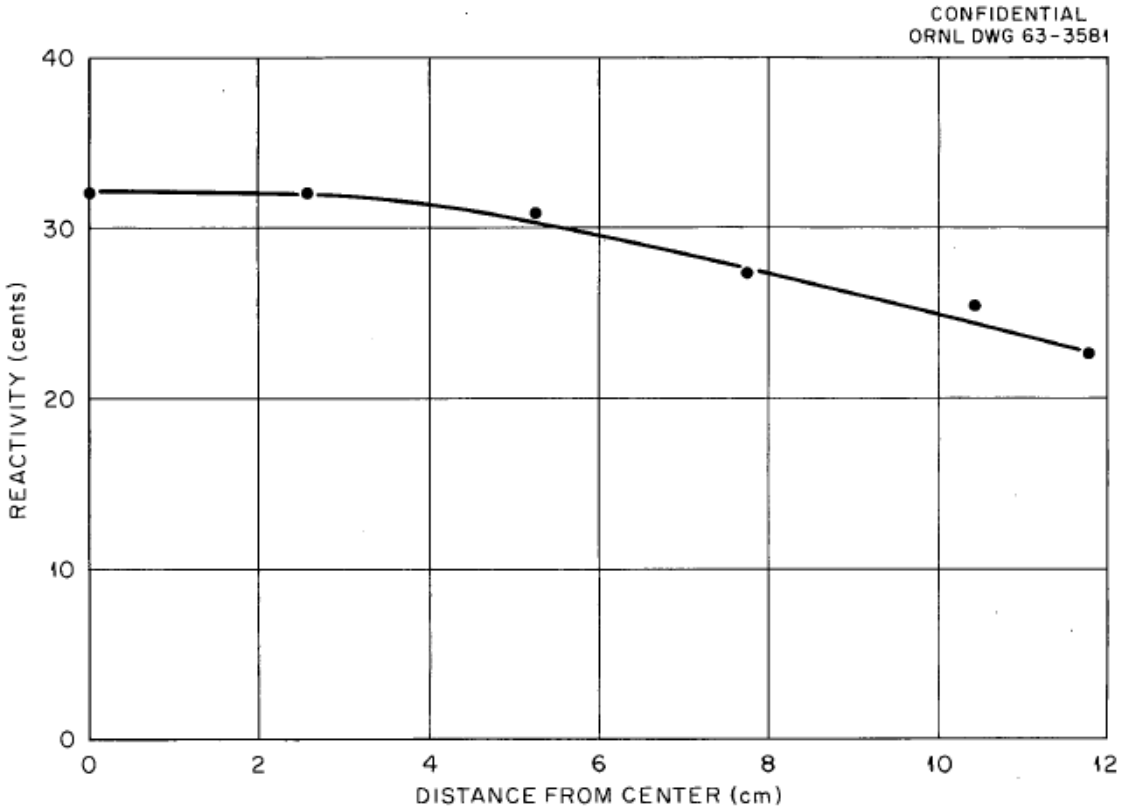

Figure 1.4-1. Reactivity Worth of Fuel Tube Versus Radius (see Reference 4).

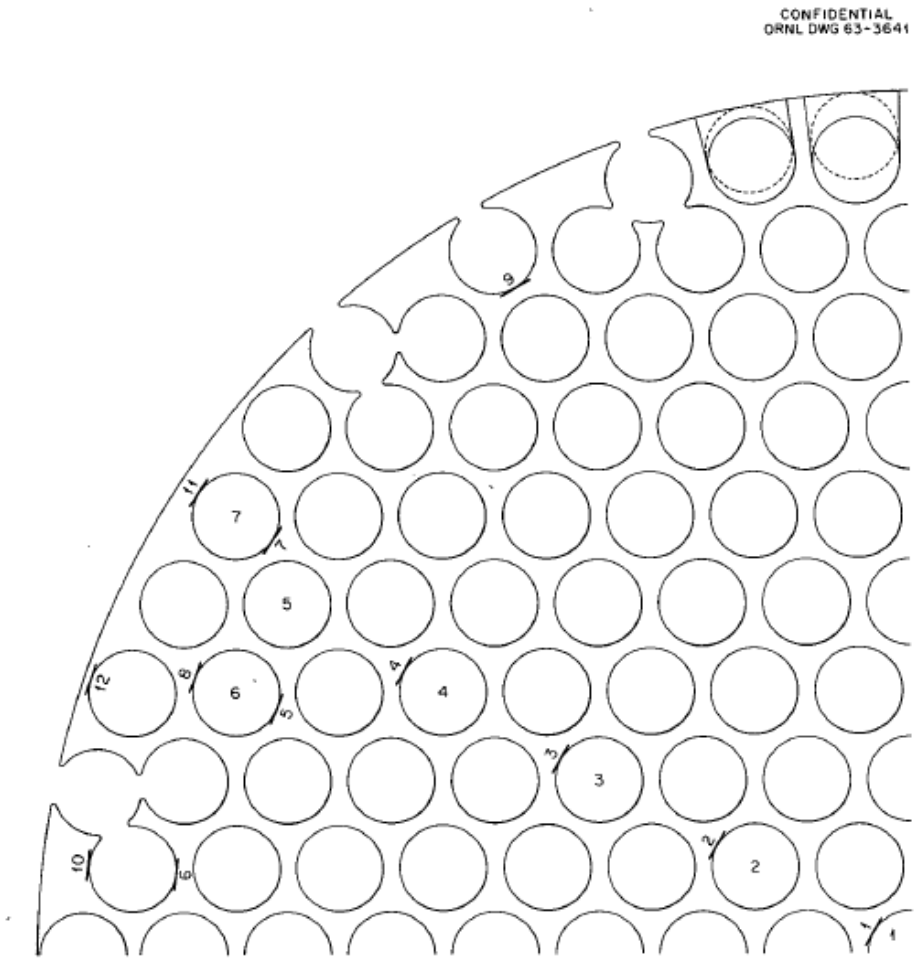

Figure 1.4-2. Foil Locations for Radial Fission Rate Distribution and Fuel Tube Locations for Fuel Reactivity Measurements (see Reference 4).

A credible accident condition where twenty fuel tubes at the periphery of the core were moved from their normal location in the lattice out to the edge of the core was simulated. An example of this movement is shown for two fuel tubes in Figure 1.4-2. It is clear from the grid plate, Figure 1.4-3, which twenty rods were moved. The measured reactivity effect was -8.2 ¢ for displacement of twenty fuel tubes.

An additional reactivity worth was measured for changing the fuel tubes from a regular lattice assembly to a 7-tube cluster assembly. The grid plate for this assembly is shown in Figure 1.4-4. This change was evaluated as an additional critical configuration and is described in HEU-COMP-FAST-004.

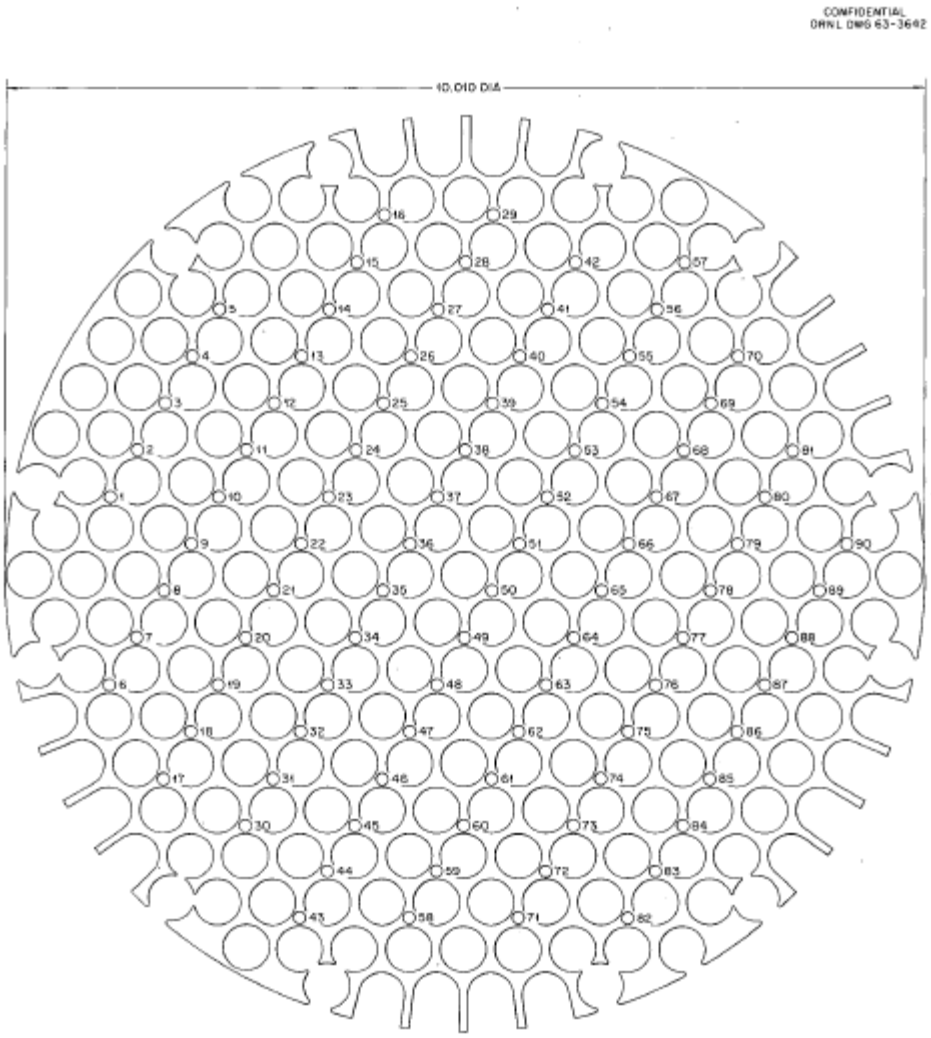

Figure 1.4-3. Locations of Samples in Reactivity Coefficient Measurements (see Reference 4).

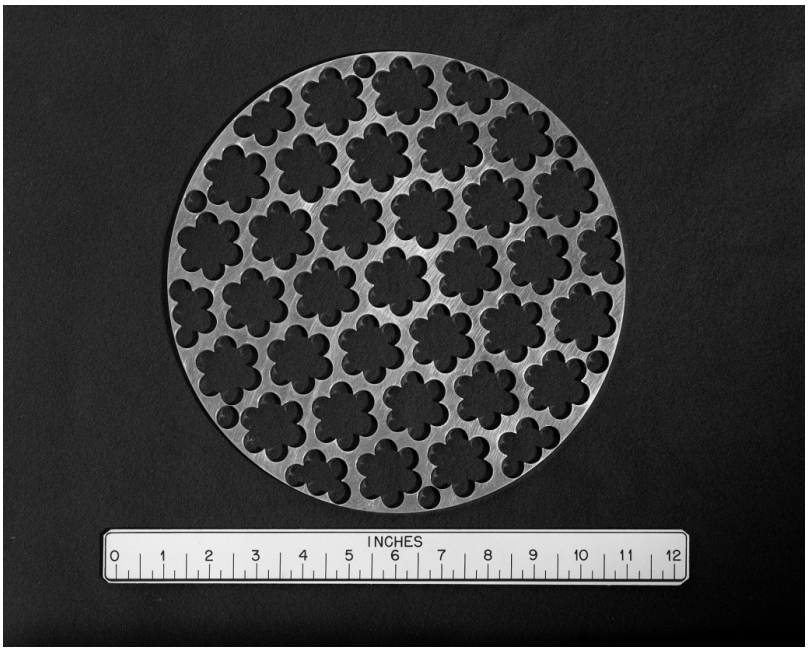

Figure 1.4-4. Grid Plate for 7-Tube-Cluster Assembly (see Reference 4).

1.4.2.2 Neutron Absorbing and Moderating Material Reactivity Measurements

The effect of adding various neutron absorbing and moderating materials was also measured. Materials were added to the core as rods, filled stainless steel tubes, and discs or lids that fit between the top of the fuel tubes and the top of the core tank.[a] The results of the reactivity measurements, reported in cents per kilogram material, from Reference 4 as well as the total reactivity, found in the logbook, are summarized in Table 1.4-2. Any discrepancies between the logbook and Reference 4 data are footnoted in Table 1.4-2. Rod locations are shown in Figure 1.4-3.

[a] Personal communication with J.T. Mihalczo, September 27, 2012.

Table 1.4-2. Reactivity Effects of Absorbing and Moderating Material in the Core

Material	Form	Number	Location	Total Weight (g)	Total Reactivity [a] (cents)	Reactivity Coefficient (cents/kg)	Logbook Reference Pages
Type 347 Stainless Steel	0.317 cm dia rods 30.5 cm long	90	All positions filled	1704	14.8	8.7	94
	0.317 cm dia rods 30.5 cm long	46	Every other position	871	7.92	9.1	84, 86
W	0.317 cm dia rods 30.5 cm long	46	Every other position	2110	-4.27	-2.0	86, 87
Nb[b]	3/32 inch dia rods 30.48 cm long[c]	90[d]	All positions	1050	4.9	4.7	86, 107
CH_2	0.317 cm dia rods 30.5 cm long	8	Odd number holes between 43-57	18.42[e]	24.43	1320	86, 88
C	0.120 inch dia rods 30.5 cm long[f]	23	Every 4th position	82	7.5	91	86, 94
B_4C	Filled with B_4C[g]	1	Center fuel tube position	30.5	-6.65	-220	91, 92
Stainless Steel[h]	Disc 0.317 cm thick for top of core tank	1	Top of core	1290	7.97[i]	6.2[j]	85, 86
Al[h]	Lid for top of core tank, 0.317 cm thick	1	Top of core	464	16.62[k]	36	85, 86
Al[h]	Lid for top of core tank, 0.159 cm thick	1	Top of core	226	8.14[l]	36[m]	85, 86
Cd[h]	Lid for top of core, 0.066 cm thick[n]	1	Top of core	286.5[o]	-45.7	-160[p]	91, 92

(a) These values are reported in the logbook.
(b) Reference 4 and the logbook use the element name columbium, Cb, which is now known is niobium, Nb.
(c) Reference 4 gives the rod diameter as 0.317 cm but the logbook gives the diameter as 3/32" which is used in this table. The logbook gives a rod length of 12" or 30.48 cm which rounds to 30.5 cm, as was given in Reference 4. The un-rounded value is given in this table.
(d) Reference 4 gives this value as 46 but the logbook gives it as 90. The reported mass corresponds to 90 rods.
(e) In Reference 4 this mass was rounded to18.4 g.
(f) The logbook gives a rod diameter of 0.120" or 0.3048 cm which rounds to 0.305 cm, as was given in Reference 4. The un-rounded value is given in this table.
(g) An empty fuel tube was filled with B_4C powder and placed in the center fuel tube position. The reactivity was compared to the reactivity of an empty fuel tube in the center fuel tube position to find the reactivity of just the B_4C. (Personal email communication with J.T. Mihalczo, December 16, 2014)
(h) The lids had a diameter slightly smaller than the core tank inner diameter. The lids sat on top of the fuel pins
(i) This value was calculated by the evaluator by taking the difference of the reactivity of the system with the stainless steel lid in place, 12.23 cents, and the reactivity of the system without the lid, 4.26 cents.
(j) The reactivity coefficient given in Reference 4 and the reactivity reported in the logbook do not agree. Reference 4 gives a reactivity of 18 cents per kg but using values from the logbook a reactivity of 6.2 cents per kg is calculated. The correct value is 6.2 cents per kg as calculated from the logbook and as confirmed by the experimenter. (Personal communication with J.T. Mihalczo, September 27, 2012.)
(k) This value was calculated by the evaluator by taking the difference of the reactivity of the system with the stainless steel lid in place, 20.88 cents, and the reactivity of the system without the lid, 4.26 cents.
(l) This value was calculated by the evaluator by taking the difference of the reactivity of the system with the stainless steel lid in place, 12.4 cents, and the reactivity of the system without the lid, 4.26 cents.
(m) Reference 4 incorrectly reports this value as 35 cents per kg. (Personal communication with J.T. Mihalczo, September 27, 2012.)
(n) The cadmium lid "was from a stock sheet with a thickness of 26 mills to within 1/2 of a mill." Where a mill is 0.001 inches. (Personal email communication with J.T. Mihalczo, December 16, 2014).
(o) In Reference 4 this was rounded to 287 g.
(p) In Reference 4 this value is reported as a positive value but it should be a negative worth.

1.4.2.3 Potassium Reactivity Measurements

The reactivity effect of adding potassium to the core was also studied. The critical configuration was changed by first switching the aluminum core tank for a calandria type vessel made of Type 304 and 307 Stainless Steel (13,372 g of stainless steel). This core tank is shown in Figure 1.4-5. The fuel and reflector arrangement was not changed. The change of the core tank resulted in a reactivity change of +28 ¢. The thickness of the top beryllium reflector was then decreased to 6.35 cm to compensate for the increased reactivity. The system then had a reactivity of +13.4 ¢. When 3,403 g of potassium was added to the core the reactivity was +32 ¢, i.e. an increase of 18.6 ¢. The resulting potassium reactivity coefficient was reported as +5.4 ¢/kg in Reference 4. The calandria type vessel was sent to Y-12 for filling. The experimenter believes that the potassium was pumped into the tank through a tube at the bottom, until the potassium filled the tank and overflowed through a tube, at the top of the tank, which was then sealed, all the while keeping the potassium liquid. The tank was probably X-rayed to check that there was no air at the top of the tank.[a] In the logbook two mass measurements were reported. The first reported the empty core mass as 13,372 g and the filled with potassium core mass as 16,765 grams. This difference gives a potassium mass of 3,393 g. The potassium mass of 3,403 g used in Reference 4 was reported "as per X-10 [Hofman]" in the logbook.[b]

[a] Personal email communication with J.T. Mihalczo, January 3, 2012.

[b] Radiation Safety Information Computation Center (RSICC), The ORNL Critical Experiments Logbooks, Book 75r, http://rsicc.ornl.gov/RelatedLinks.aspx?t=criticallist, logbook page 111. It is not known exactly what "as per X-10 [Hofman]" means, but Hofman was probably responsible for the measurement.

Figure 1.4-5. Potassium Filled Calandria (see Reference 4).[a]

1.4.3 Material Data

All core and reflector materials were the same as those used in the critical configuration as given in HEU-COMP-FAST-004 unless stated otherwise.

[a] ORNL Photo 39928.

1.4.3.1 Fuel Effect Reactivity Measurements

No additional material was used for the fuel effect reactivity measurements.

1.4.3.2 Neutron Absorbing and Moderating Material Reactivity Measurements

Various additional materials were added to the core region to test the reactivity worth of those materials. The materials investigated include Type 347 Stainless Steel, tungsten (W), niobium (Nb),[a] polyethylene (CH_2), graphite, boron carbide (B_4C), aluminum (Al), and cadmium (Cd). Impurity data for these materials were not given.

As can be seen in Table 1.4-2 the worth of a stainless steel disc was measured. The type of stainless steel used for this disc was not given.

1.4.3.3 Potassium Reactivity Measurements

The core tank was switched from a Type 1100 Aluminum core tank to a Type 304 and 347 Stainless Steel calandria type core tank for the potassium reactivity measurements. Tubes of the tank were Type 347 Stainless Steel and the end plates and tank were Type 304 Stainless Steel. Potassium was added to the core tank. The form and purity of the potassium was not given.

1.4.4 Temperature Data

The temperature is the same as for the critical configuration, 72°F (22°C).[b]

1.4.5 Additional Information Relevant to Reactivity Effects Measurements

Additional information was not identified.

1.5 Description of Reactivity Coefficient Measurements

The worths per gram of various materials placed in the core were given in Reference 4. These reactivity coefficients are based on the absolute measured worth of a sample and the sample mass. The measured absolute worth values were evaluated and not the calculated reactivity coefficients. For reference the reactivity coefficients calculated using the sample mass and measured reactivity are provided in Section 1.4.

1.6 Description of Kinetics Measurements

Kinetics measurements were not performed.

[a] The logbook and Reference 4 use the historical name of columbium (Cb) for niobium.

[b] Personal email communication with J. T. Mihalczo, May 23, 2011.

1.7 Description of Reaction-Rate Distribution Measurements

1.7.1 Overview of Experiment

Activation measurements were taken through the core and top reflector.

1.7.2 Geometry of the Experiment Configuration and Measurement Procedure

The activation measurements were performed for the critical assembly (as described in Section 1 of HEU-COMP-FAST-004). Measurements were performed using 93.15 wt.% enriched uranium metal foils that were 0.75-cm in diameter and 0.010-cm-thick.[a] These foils were taped tangent to the fuel tubes within the core, placed on top of fuel tubes, and placed between sections of reflector. The foils were stiff and did not curve around the fuel tube when taped tangentially to the side of the fuel tube. A small piece of Teflon tape was placed in the vertical direction, along the length of the fuel tube, to hold the foils in place.[b] For the foils in the core, the activation is a spatial average over the diameter of the foil. For the foils in the reflector they represent a point axially and are averaged over the foil dimensions in the radial direction. No correction for self-shielding in the foils was made when obtaining the results in Tables 1.7-1, 1.7-2 and 1.7-3. Results are plotted in Figures 1.7-1 and 1.7-2. From Figure 1.7-2 it can be seen that the "radial fission rate distribution at the core midplane is flat to within 2.54 cm of the side reflector, where it increases to a maximum, at the core boundary, about 3.7 greater than at the center" (Reference 4). Foil locations within the core are given in Figure 1.4-2.

[a] Reference 4 reports the foil enrichment as 93.2 wt.%, but according to the experimenter, it was 93.15 wt.% September 19, 2011).

[b] Personal email communication with J.T. Mihalczo, December 4, 2013.

Table 1.7-1. Axial Activation Fission Rate Distribution (see Reference 4).

Axial Fission Rate Distribution[a]	
Distance from Center of Fuel Tube (cm)[b]	Relative Fission Rate (Arbitrary Units)
-2.54	1.02
0	1.00
2.54	1.00
5.08	0.95
7.62	0.91
10.16	0.83
12.7	0.88
15.44	1.51
15.91	1.56
17.18	2.21
18.45	2.53
19.72	2.45
20.99	2.00
22.26	1.20

(a) Activation foils were 0.010-cm-thick by 0.75-cm-dia HEU metal foil.

(b) Foils in the core were taped tangent to the center fuel tube. Foils in the top reflector were placed between beryllium blocks at ½ inch spacing.

Table 1.7-2. Radial Activation Fission Rate Distribution (see Reference 4).

Radial Fission Rate Distribution at Core Midplane[a]		
Location[b]	Distance from Core Center (cm)	Relative Fission Rate (Arbitrary Units)
1	0.635	1.0
2	3.25	0.98
3	5.87	0.99
4	8.53	1.04
5	9.93	1.06
6	10.74	1.12
7	11.12	1.21
8	11.2	1.55
9	11.35	1.45
10	12.06	3.04
11	12.47	3.68
12	12.62	3.56

(a) Activation foils were 0.010-cm-thick by 0.75-cm-dia HEU metal foil taped tangent to the fuel tubes.
(b) Foil locations within the core are given in Figure 1.4-2.

Table 1.7-3. Radial Activation Fission Rate Distribution (see Reference 4).

Radial Fission Rate Distribution at 15.44 cm Above Core Midplane[a]		
Location[b]	Distance from Core Center (cm)	Relative Fission Rate[c] (Arbitrary Units)
13	0	1.51
14	3.02	1.63
15	12.06	2.50

(a) Activation foils were 0.010-cm-thick by 0.75-cm-dia HEU metal foil.
(b) Foils were laid on top of fuel tubes. These locations are not shown in Figure 1.4-2. *The foils actually sat at the bottom of the 0.249 cm deep end cap wells. (Personal email communication with J.T. Mihalczo, March 12, 2014.)*
(c) *These fission rates were normalized to the same normalization foil as in Table 1.7-2,*

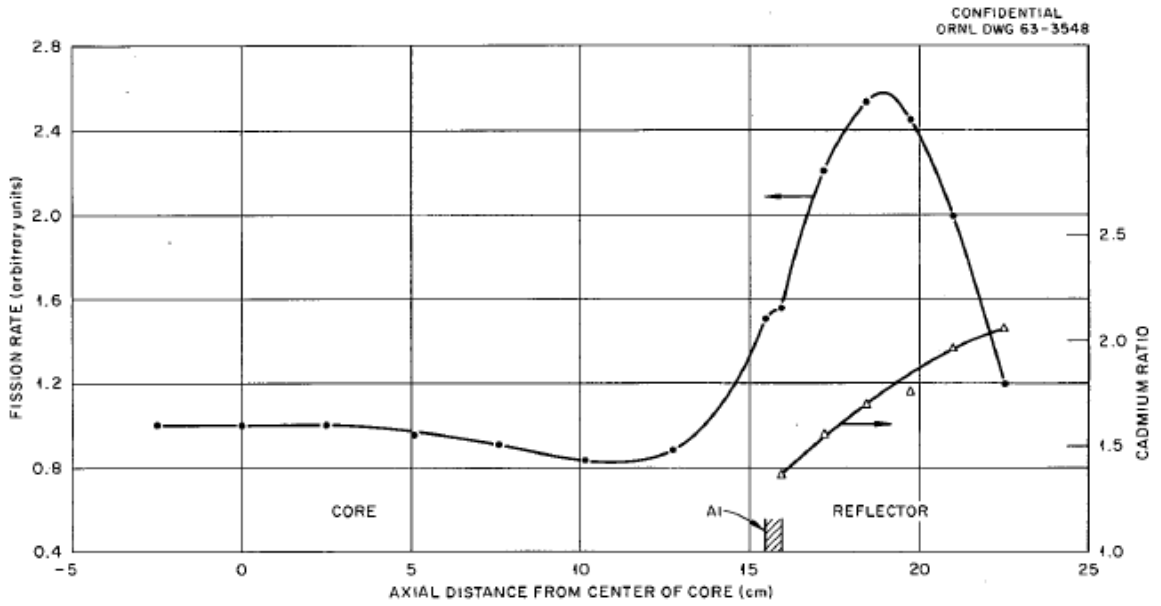

Figure 1.7-1. Plot of Axial Relative Activation of ^{235}U Fission Foils and Cadmium Ratios (see Section 1.3) (see Reference 4).

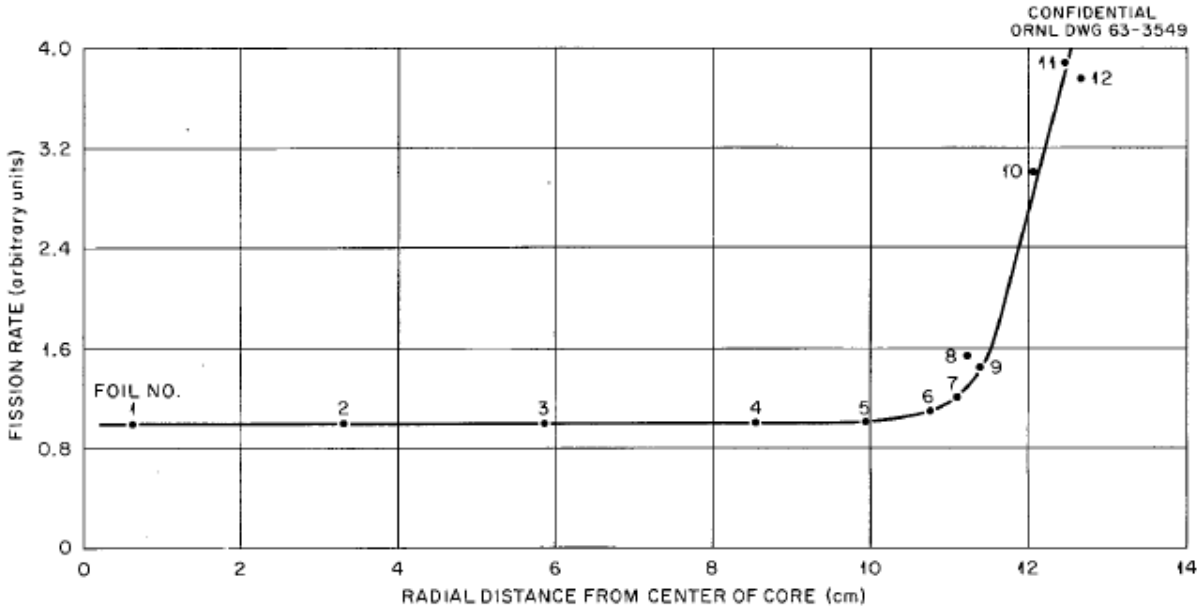

Figure 1.7-2. Plot of Radial Relative Activation of ^{235}U Fission Foils at the Core Midplane (see Reference 4).

1.7.3 Material Data

Material data for the core and reflector parts are the same as those given for the critical configuration (see Section 1.3 of HEU-COMP-FAST-004). The uranium metal foils were the same foils used for the cadmium ratio measurements (see Section 1.3.3).

1.7.4 Temperature Data

The temperature is the same as for the critical configuration, 72°F (22°C).[a]

1.7.5 Additional Information Relevant to Reaction-Rate Distribution Measurements

Additional information is not available.

1.8 Description of Power Distribution Measurements

The axial and radial relative power distribution is the same as the relative fission rate that was measured in the core region of Assembly 1 (see Section 1.7).

1.9 Description of Isotopic Measurements

Isotopic measurements were not performed.

1.10 Description of Other Miscellaneous Types of Measurements

Other miscellaneous types of measurements were not performed.

[a] Personal email communication with J. T. Mihalczo, May 23, 2011.

2.0 EVALUATION OF EXPERIMENTAL DATA

2.1 Evaluation of Critical and/or Subcritical Configuration Data

(The criticality portion of this evaluation has been reviewed and approved by the International Criticality Safety Benchmark Evaluation Project (ICSBEP) and has been published under the following identifier: HEU-COMP-FAST-004.[a])

2.2 Evaluation of Buckling and Extrapolation Length Data

Buckling and extrapolation-length measurements were not performed.

2.3 Evaluation of Spectral Characteristics Data

The cadmium ratio measurements were a ratio of the activation of bare 93.15 wt% ^{235}U metal foils to the activation of 93.15 wt% ^{235}U metal foils with cadmium covers. The uncertainty in the uranium foils and cadmium covers dimensions, materials, and placements are the same as for the cadmium ratios in SCCA-SPACE-EXP-002. The effects of these uncertainties have been reevaluated using the detailed benchmark model described in Section 3.3. In order to obtain statistically significant results for perturbation calculations a scaling factor was used. The uncertainty values were scaled by 1, 5, 10, 50, and/or 100. An uncertainty is considered negligible if the effect was less than 0.0057, the rounding uncertainty ($0.01/\sqrt{3}$).

According to the experimenter, the measurement uncertainty in the cadmium ratio would have been 0.5 %. It is believed that this uncertainty is based on the number of counts taken for each foil, 100,000. (i.e., the square root of the number of counts is divided by the number of counts). This yields the measurement uncertainty in a single foil. Because a ratio of activations is taken, this uncertainty is then added to itself in quadrature giving a total measurement uncertainty of about 0.447%. It is believed that this value is arbitrarily rounded up to 0.5%.This value was taken as the total measurement uncertainty. There is also an additional uncertainty in the measurements of $\pm 0.01/\sqrt{3}$ for rounding; however, this uncertainty is negligible in relation to the other evaluated uncertainties.

In the benchmark models, the uranium foils and cadmium covers were modeled without impurities. The effect of adding impurities is treated as an uncertainty. According to the experimenter, the effect of foil composition would have been negligible because the cadmium ratio is a ratio.[b] However, to calculate the effect of impurities in the uranium foils the uranium composition from HEU-MET-FAST-051[c] was used. A scaling factor was used to determine the effect of the uranium foil impurities. It was found that the effect was negligible. The uranium foils were modeled at the nominal density of 18.75 g/cm^3 given in HEU-MET-FAST-051. Using the mass and dimensions of the various uranium parts used in that evaluation, it is found that the density of the parts had a standard deviation of ±0.04 g/cm^3; this value was taken to be the 1σ uncertainty in the uranium foil density. The calculated effect of the uncertainty in uranium density is negligible.

Since the composition of the cadmium covers was not specified, pure cadmium was assumed. The effect of possible impurities in the cadmium covers was determined by replacing the pure cadmium with a 5N

---

[a] International Handbook of Evaluated Criticality Safety Benchmark Experiments, NEA/NSC/DOC(95)03, OECD-NEA, Paris (2012).

[b] Personal communication with J.T. Mihalczo, August 14, 2012.

[c] *International Handbook of Evaluated Criticality Safety Benchmark Experiments*, NEA/NSC/DOC(95)03, OECD-NEA, Paris (2012).

cadmium composition.[a] Using a scaling factor, it was determined that the effect of impurities in the cadmium was negligible. The cadmium was modeled with a nominal density of 8.65g/cm^3. The uncertainty in the density was taken to be ±0.01 g/cm^3.[b] The calculated effect of the uncertainty in cadmium density is negligible.

The uncertainty in the thickness for the 0.051-cm-thick cadmium covers is ± 0.001 cm. The uncertainty in the thickness of the 0.01 cm thick uranium foil is ±0.001 cm. The uncertainty in the cadmium diameter is ±0.001 cm. The uncertainty in the uranium foil diameter is ±0.01 cm. Using scaling factors for the perturbation calculations, it was determined that the uncertainty in the cadmium and uranium thicknesses and diameters all had a negligible effect.

It has been suggested that a ± 0.001 cm uncertainty for the 0.051-cm-thick cadmium cover may be too low. However, even if the 2% uncertainty is arbitrarily increased to 10% the effect on the cadmium ratio is still negligible.

The experimental, material, and dimension uncertainties are summarized in Table 2.3-1.

Table 2.3-1. Uncertainty Effect in Cadmium Ratio due to Uranium and Cadmium Material Properties.

Uncertainty		Effect
Measurement	±	0.5%
Uranium Composition	±	NEG
Uranium Density	±	NEG
Cadmium Composition		NEG
Cadmium Density	±	NEG
Uranium Foil Thickness	±	NEG
Uranium Foil Diameter	±	NEG
Total	±	0.5%
Rounding	±	0.01/√3

The foil positions were reported to two decimal places; however, it is believed that, in many cases. position was calculated based on dimensions of the assembly rather than measured locations. When necessary, the location of the foils was adjusted from the given value to ensure correct location in the benchmark model. For example, two cadmium ratios were measured for foils laid on top of the fuel tubes, the heights of which are given as 15.44 cm above the core midplane. No definition of the core midplane is given and it is assumed that it is the axial center of the fuel tubes (15.24 cm above the bottom of the fuel tubes). If this is true, the foils located at a height of 15.44 cm above the midplane of the core would be floating 0.2 cm above the top of the 30.48-cm-long fuel tubes rather than resting at the bottom of the end-cap well. The height of these foils, in the benchmark models, was adjusted so they sat on top of the fuel tubes (see Section 3.3). The positions of the foils in the upper reflector were shifted up so that the bottom most foil was sitting on the inside bottom surface of the upper reflector tank and not in the middle of the bottom plate of the reflector tank. All other foils in the upper reflector were also shifted to maintain a 1.27 cm spacing. The uncertainty in the foil position is taken to be ±0.1 cm.

[a] "High Purity Cadmium," ESPI Metals, http://www.espimetals.com/index.php/online-catalog/346-cadmium-cd accessed June 28, 2012.

[b] PROTEUS-GCR-EXP-001.

The position uncertainty for the cadmium ratios in the upper beryllium reflector were evaluated separately from the cadmium ratios in the core tank region. To determine the uncertainty in the cadmium ratios in the upper reflector, the distribution of cadmium ratios in the upper reflector was calculated. The cadmium ratio distribution was obtained using the detailed benchmark model. The bare and cadmium covered foils in the upper reflector were shifted axially by 0.05 cm; all foils were shifted to maintain the 1.27 cm spacing between foils. This created multiple models. Each model was calculated using MCNP seven times with seven different random numbers. The results of these seven runs were averaged with a variance weighting. A polynomial was fit to the cadmium ratio distribution. This equation was used to determine the uncertainty in the cadmium ratio within the upper reflector as a function of position. The trendline and the resulting uncertainty equation are given as Equation 2.3-1 where y is the cadmium ratio, σ_y is the uncertainty in the cadmium ratio, x is the axial position in the upper reflector and σ_x is the uncertainty in the axial position. The x value must be as measured from the bottom of the fuel tubes and be between the values of 31.15 and 38.105 cm. The uncertainty in the position is 0.1 cm. The calculated distribution is shown in Figure 2.3-1. This method was used rather than a direct perturbation analysis due to the high variability and noise seen in the distribution of the Monte Carlo results for a single calculation where the reported statistical uncertainty was considered negligible.

$$y = -0.01083274x^2 + 0.82570802x - 13.83639373$$
$$\sigma_y = (-2 \cdot 0.01083274x + 0.82570802) \cdot \sigma_x$$

Equation 2.3-1

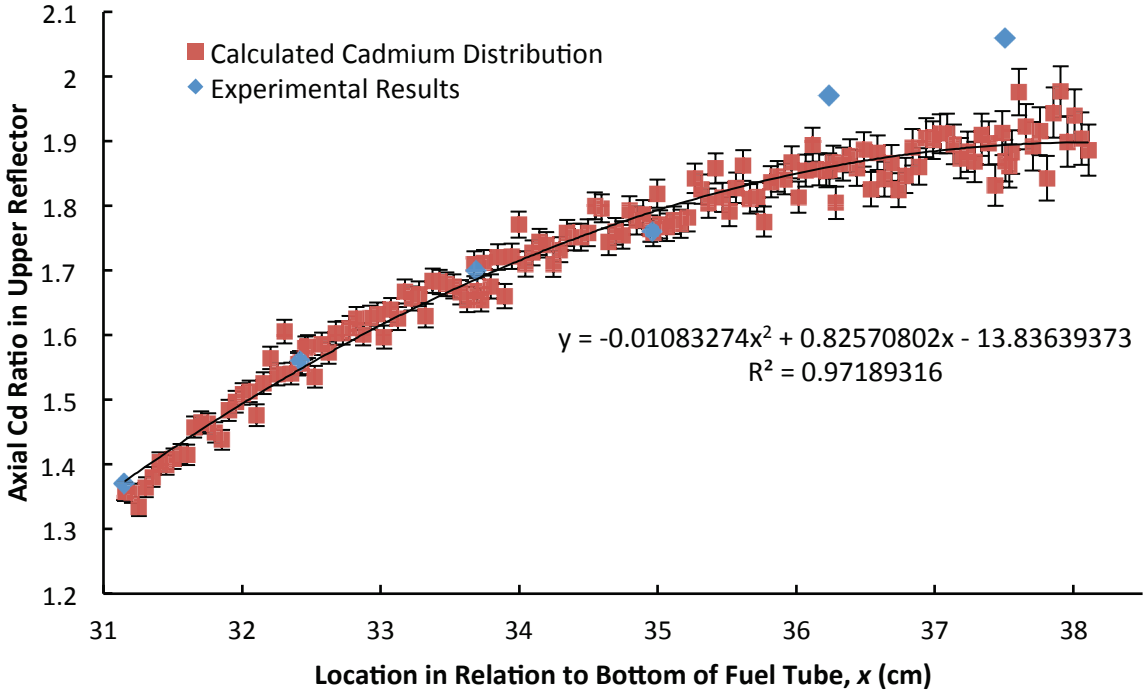

Figure 2.3-1. Calculated Distribution of Cadmium Ratio in Upper Beryllium Reflector.

The uncertainty in the axial position was calculated using Equation 2.3-1. The effect of the uncertainty in the radial position of the cadmium ratios was also evaluated and found to be negligible.

For the single cadmium ratio measurement at the midplane of the fuel, near the edge of the core, the position was evaluated by moving the foil from the inner surface of the fuel tube, to which it was tangentially taped, to the outer surface of the fuel tube one position closer to the center of the core. The

effect of doing this was 0.14 ± 0.015 ΔCd Ratio. This was taken to be a bounding uncertainty with a uniform distribution, thus the 1σ uncertainty in the position for the cadmium ratio measurement at the midplane of the core was 0.081 or 6.8%.

The uncertainty in the two cadmium ratios at the top of the fuel tubes was evaluated by shifting the positions of the foils radially. When the change in cadmium ratio was scaled to the 1σ position uncertainty of 0.1 cm, it was found that the position uncertainty in the cadmium ratio was negligible for the cadmium ratio near the radial center of the core (R=3.02 cm) and approximately 1% for the cadmium ratio near the edge of the core (R=12.06 cm).

The effects of the positional uncertainties are given in Table 2.3-2 for each cadmium ratio. Both the given and adjusted foil locations are given in Table 2.3-2.

Table 2.3-2. Uncertainty in Cadmium Ratio Position.

Cadmium Ratio				Effect	
Cd Ratio	Given Location (cm)[(a)]		Modified Location (cm)[(b)]	Position	
Distribution in Top Beryllium Reflector					
1	H	15.91	15.915	0.015	1.10%
2	H	17.18	17.185	0.012	0.76%
3	H	18.45	18.455	0.010	0.56%
4	H	19.72	19.725	0.007	0.39%
5	H	20.99	20.995	NEG	
6	H	22.26	22.265	NEG	
Cadmium Ratio at Core Midplane					
7	R	11.35	11.413	0.081	6.5%
Distribution at 15.24 cm Above Core Midplane[(c)]					
8	R	3.02	3.02	NEG	
9	R	12.06	12.06	0.021	1.0%

(a) Locations were given as axial distance from the center of the fuel tube, height (H), or radial distance from the core center, radius (R).
(b) Many of the foil locations were modified so that the foil was in a feasible location, i.e. not floating in air or in the middle of a solid mass of material. To obtain the position in the top reflector in relation to the bottom of the fuel tube, 15.24 cm must be added to the modified location.
(c) This height was given as 15.44 cm but was modified so foils lay on top of the fuel tubes and not 0.2 cm above.

The total experimental uncertainties are given in Table 2.3-3.[a]

[a] As discussed in Section 1.3 the foils were selected such that the foils were the same "to less than 1% for activation in the same neutron flux". This would lead to an uncertainty in the ratio or normalized measurements of less than 1% in foil properties due to foil correlation. For the benchmark experimental uncertainty each property was perturbed individually thus the actual uncertainty is probably somewhere between the 1% suggested by the experimenter and the benchmark experimental uncertainty.

Table 2.3-3. Total Uncertainty in Cadmium Ratio.

Cadmium Ratio				Effect			
Cd Ratio		Given Location (cm)[a]	Modified Location (cm)[b]	Cadmium Ratio			
Distribution in Top Beryllium Reflector							
1	H	15.91	15.915	1.37	±	0.017	(1.28%)
2	H	17.18	17.185	1.56	±	0.015	(0.99%)
3	H	18.45	18.455	1.70	±	0.014	(0.84%)
4	H	19.72	19.725	1.76	±	0.013	(0.72%)
5	H	20.99	20.995	1.97	±	0.011	(0.58%)
6	H	22.26	22.265	2.06	±	0.012	(0.57%)
Cadmium Ratio at Core Midplane							
7	R	11.35	11.413	1.24	±	0.081	(6.57%)
Distribution at 15.24 cm Above Core Midplane[c]							
8	R	3.02	3.02	1.39		0.009	(0.65%)
9	R	12.06	12.06	1.87		0.024	(1.27%)

(a) Locations were given as axial distance from the center of the fuel tube, height (H), or radial distance from the core center, radius (R).
(b) Many of the foil locations were modified so that the foil was in a feasible location, i.e. not floating in air or in the middle of a solid mass of material.
(c) This height was given as 15.44 cm but was modified so foils lay on top of the fuel tubes and not 0.2 cm above them.

2.4 Evaluation of Reactivity Effects Data

Worth, or reactivity, measurements were performed by measuring the system reactivity with and without the material of interest within the core or by measuring the system reactivity before and after a fuel tube location is changed within a core. The system reactivity was measured by "observing the change in the stable reactor period" when a change was made to the system (Reference 4). Though not explicitly given, the method is the same as that used by the experimenter for other experiments performed (ORSPHERE-FUND-EXP-001). To convert the stable reactor period to a reactivity in units of dollars an equation derived from the Inhour equation was used. This equation required the delayed neutron parameters and fission fractions and was independent of β_{eff}. The stable reactor periods and constants used in this calculation were not given thus the calculation could not be recreated. The derivation and use of this method are explained in more detail in Section 1.4 and Appendix B of ORSPHERE-FUND-EXP-001.

In Section 2.1 of HEU-COMP-FAST-004[a] the uncertainty of the system reactivity measurement is given as ±10% for the measurement and a ±1.2 ¢ repeatability uncertainty. These uncertainties would also apply to these system reactivity measurements. For every worth measurement, two system reactivity measurements were required. Because the two measurements were typically made within the same day, it is assumed that the repeatability uncertainty can be considered systematic to both measurements; thus, the contribution to the change in reactivity of the repeatability uncertainty is negligible. This leaves the ±10% uncertainty for each system reactivity measurement. Because a worth measurement is the difference between two system reactivities the measurements uncertainties must be combined in quadrature. Thus, for every worth measurement the measurement uncertainty is taken to be ±10%√2.

[a] International Handbook of Evaluated Criticality Safety Benchmark Experiments, NEA/NSC/DOC(95)03, OECD-NEA, Paris (2012).

The uncertainty in dimensions, locations, and material composition were also evaluated. When needed, the effect of uncertainty on the worth measurement was evaluated using Monte Carlo N-Particle (MCNP) versions 5-1.60[a] and ENDF/B-VII.0[b] neutron cross section libraries to calculated the k_{eff} of the system. Unless stated otherwise, the simple or detailed benchmark models, as described in Section 3.4, were used. The effect of the uncertainty in all measured parameters was found individually by increasing and decreasing the specified value by a given amount.

The reactivity of the system for the benchmark and perturbed models was calculated using Equation 2.4-1. The first term in Equation 2.4.1 calculates the system reactivity, denoted by the symbol ρ, in relation to exactly delayed critical, k_{eff} =1. (The general reactivity equation is $\rho = (k_1 - k_2)/k_1 k_2$)). The last two terms convert the reactivity to units of cents (¢) using β_{eff}. For system reactivities less than delayed critical, ρ will be negative and, conversely, for system reactivities above delayed critical, ρ will be positive.

$$\rho = \frac{k_{eff} - 1}{k_{eff}} * \frac{1}{\beta_{eff}} * 100 \qquad \text{Equation 2.4-1}$$

In Section 2.1 of HEU-COMP-FAST-004 β_{eff} for the system is determined to be 0.0073 with a ±5% uncertainty.

When the benchmark models were perturbed for the uncertainty effect evaluation, often the magnitude of the perturbation was increased from the 1σ uncertainty in order to obtain statistically significant results. The ratio of the perturbation to the 1σ uncertainty is the "scaling factor". The scaling factor is used to convert the calculated effect on the worth to a 1σ uncertainty effect. All models were calculated such that the statistical uncertainty in k_{eff} was no more than ±0.00006. An uncertainty was considered to have a negligible effect (NEG) when the effect was less than 0.1¢ . Often the calculated effect was less than the statistical uncertainty in the calculated effect and the parameter either could not be scaled or could not be scaled more than it already was. When this happened, the statistical uncertainty was taken to be the uncertainty effect.

The fuel effect reactivity and material reactivity measurements were evaluated and both judged to be acceptable and benchmark experiments. The potassium worth measurement was not evaluated.

2.4.1 Fuel Effect Reactivity Measurements

Fuel effect reactivity measurements include the measurements of the worth of individual fuel rods at varying radii in the core and the worth of moving twenty fuel rods from their designated position to the edge of the core tank, henceforth called the "accident configuration".

The uncertainty in the fuel and fuel tube dimensions and composition were evaluated as part of the evaluation of the critical configuration (Section 2, HEU-COMP-FAST-004). It was found that all parameters had a negligible effect on the critical system reactivity except for the fuel tube composition and the fuel mass. The fuel tube composition uncertainty was judged to be systematic across all fuel tubes. The effect of perturbing all fuel tubes simultaneously was ± 0.00025 Δk_{eff}. Because this uncertainty is rather small when perturbing all 253 fuel rods in the critical configuration and because the uncertainty is systematic across all fuel tubes, the effect of the fuel tube composition on the worth measurement of a single fuel tube would be negligible.

---

[a] F.B. Brown, R.F. Barrett, T.E. Booth, J.S. Bull, L.J. Cox, R.A. Forster, T.J. Goorley, R.D. Mosteller, S.E. Post, R.E. Prael, E.C. Selcow, A. Sood, and J. Sweezy, "MCNP Version 5," LA-UR-02-3935, Los Alamos National Laboratory (2002).

[b] M.B. Chadwick, et al., "ENDF/B-VII.0: Next Generation Evaluated Nuclear Data Library for Nuclear Science and Technology," *Nucl. Data Sheets*, **107**: 2931-3060 (2006).

The uncertainty effect of the mass of fuel per fuel tube was 0.00010 Δk_{eff} or ±1.37 ¢. For the fuel tube worth measurements, this was added in quadrature to the 10%√2 measurement uncertainty.

For the accident configuration, the fuel tube composition and the fuel mass uncertainties would have a negligible effect because no fuel was removed but only moved. The fuel position uncertainty was evaluated for the critical configurations and was found to have a negligible effect. Thus, only the 10%√2 measurement uncertainty applied to the accident configuration worth measurement.

The experimental uncertainty for the fuel effect reactivity measurements is summarized in Table 2.4-1.

Table 2.4-1. Fuel Effect Reactivity Measurements and Uncertainties

Distance from Core Center (Fuel Tube Position)	Experimental Worth with Experimental Uncertainty (¢)		
0 cm (1)	-32.0	±	4.73
2.59 cm (2)	-32.0	±	4.73
5.23 cm (3)	-30.8	±	4.57
7.75 cm (4)	-27.2	±	4.08
10.48 cm (5)	-25.5	±	3.86
10.56 cm (6)	-25.6	±	3.87
11.78 cm (7)	-22.6	±	3.48
Accident Configuration Worth	-8.2	±	1.79

2.4.2 Neutron Absorbing and Moderating Material Reactivity Measurements

Worth measurements were performed for neutron absorbing and moderating material, inserted in to the core as rods and as core tank lids. The uncertainty in measured dimensions and masses was taken to be one in the last significant digit (HEU-COMP-FAST-004). For the compositions, often a standard composition had to be used for a material. When calculating atom densities from material impurity data or standard composition data, typically three types of values were given: a single value (i.e., 15 ppm or 20 wt.%), which gives the actual content of the element in the material, a maximum value (i.e., < 15 ppm or < 20 wt.%), which gives the maximum amount of an element present in the material, and a range of values (i.e., 15 -17 ppm or 20 – 22 wt.%), which gives the minimum and maximum amount of an element present in the material. When calculating atom densities for models, the actual content of the element, one half of the maximum element content, and/or the middle of the range of element content were used for the material composition, respectively. The effect of material impurities was evaluated by perturbing compositions. To do this, single values were perturbed by plus or minus the square root of the value,[a] maximum values were varied between zero and the maximum, and range values were varied between the top and bottom of the range. These uncertainties are assumed to be bounding with uniform distribution probability. Additionally, the uncertainty in the material type was also evaluated by switching out the material type; for example, Aluminum 1100 was switched for Aluminum 6061.

[a] Using the square root of the content as the uncertainty was used because compositions come from spectrographic results, which report contents in 'counts'. The uncertainty in the composition can then be defined as the square root of the value, as is commonly assumed for spectrographic measurements with a Poisson distribution. It is believed that this method provides an overestimate of the actual uncertainty.

When an uncertainty in a rod was evaluated, all rods were perturbed simultaneously. For the dimensions uncertainties the given uncertainty of 0.01 inches or 0.0254 cm was taken to be 25% systematic and 75% random, as was done for the critical configuration dimensional uncertainties (Section 2, HEU-COMP-FAST-004). The 1σ uncertainty effect was calculated using Equation 2.4-2 where *N* is the number of rods present in the core.

$$\Delta\rho_{1\sigma} = \frac{1}{Scaling\ Factor}\sqrt{\left((\Delta\rho \cdot 25\%)^2 + \frac{(\Delta\rho \cdot 75\%)^2}{N}\right)} \qquad \text{Equation 2.4-5}$$

$\Delta\rho_{1\sigma}$ is the combined 1σ effect on k_{eff} and $\Delta\rho$ is the change in reactivity worth when all N rods were perturbed simultaneously.

2.4.2.1 Stainless Steel 347 Rod Worth

The worth of adding 90 and 46 stainless steel rods to the core tank was measured. The dimensional uncertainty was ± 0.0254 cm (25%/75% systematic/random). The effect of the uncertainty in the rod diameter and length were negligible.

The uncertainty in the fuel tube position was ±0.001 cm (HEU-COMP-FAST-004). This uncertainty is based on the measurement of the fuel tube pitch (1.506-cm). The rods are held in place between fuel tubes using holes added to the grid plates. The position and diameter of these holes are not explicitly given although from Figure 1.4-3 it appears that the holes are centered between fuel tubes. Because of this the uncertainty in the fuel tube position, ±0.001cm, was arbitrarily increased to ±0.01 cm for the rod position uncertainty. This uncertainty was taken to be 25% systematic and 75% random. The effect of the uncertainty in the rod position in both the x and y directions were negligible.

The mass of the stainless steel rods was given as 1704 g for the 90 rods and 871 g for the 46 rods. The calculated density of the 90 and 46 rods was very close at 7.865 g/cm^3 and 7.866 g/cm^3. The effect of this density difference is negligible so all stainless steel 347 rods were modeled at a density of 7.865 g/cm^3. The uncertainty in mass was ±1 g. The effect of the uncertainty in the mass was negligible.

The uncertainty in the material impurities was evaluated as described in Section 2.4.2. The stainless steel 347 composition is given in Table 2.4-2. This approach yields a bounding uncertainty effect. To obtain results above the statistical uncertainty of the calculation the impurities were perturbed simultaneously using a scaling factor of five. Only a one-sided perturbation could be performed when a scaling factor was applied. Additionally, because all nine impurities were perturbed simultaneously the results must also be scaled by √9. The perturbation had a change in k_{eff} of 2.77 ¢ for the 90 rods and 2.08 ¢ for the 46 rods. The 1σ uncertainty in the material impurities was ±0.1 ¢ (2.77/(5√9√3) ¢) for the 90 rods and was negligible for the 46 rods.

Table 2.4-2. Type 347 Stainless Steel Composition.

Element	Standard Composition[(a)(b)]	Model Composition
Iron, Fe	Balance	68.7225 wt.%
Carbon, C	0.08 wt.%	0.04 wt.%
Manganese, Mn	2.00 wt.%	1.00 wt.%
Silicon, Si	1.00 wt.%	0.50 wt.%
Chromium, Cr	17.0-19.0 wt.%	18.0 wt.%
Nickel, Ni	9.0-13.0 wt.%	11.0 wt.%
Phosphorus, P	0.045 wt.%	0.0225 wt.%
Sulfur, S	0.030 wt.%	0.0150 wt.%
Tantalum+Niobium, Ta + Nb	10×C min.[(c)], 1.0 wt.% max	0.7 wt.% total 0.644 wt.% Nb, 0.056 wt.% Ta[(d)]

(a) R.H. Perry and D.W. Green, editors, "Perry's Chemical Engineers' Handbook," McGraw-Hill, 7th ed. (1997) .
(b) Single values are maximum values.
(c) The sum of the tantalum and niobium content is at most 1.0 wt.% and at least ten times the carbon content. The maximum carbon content is 0.08 wt.% but is 0.04 wt.% in the model thus the minimum tantalum plus niobium content is 0.4 wt.%.
(d) The split between Nb and Ta was determined based on the natural abundances of Nb and Ta in the earth's crust, 8 and 0.7 ppm, respectively. Shaw, R., Goodenough, K., et. al., "Niobium-tantalum," British Geological Survey, April 2011, www.MineralsUK.com, (accessed June 8, 2012).

The non-negligible experimental uncertainty for the 90 stainless steel 347 rod worth measurement are the 10%√2 measurement uncertainty and the ±0. 1 ¢ impurity uncertainty. The worth of adding 90 stainless steel 347 rods to the core tank was measured as being 14.8 ¢ with a ±2.10 ¢ uncertainty.

There was an additional uncertainty in the 46 stainless steel 347 rod worth measurement. The rod location is given as 'every other position'. There is some ambiguity to this statement. Two configurations where 46 rods fit in 'every other position' are possible, see Figure 2.4-1. The change in worth between these two configurations was 2.49 ¢. This is taken to be a bounding uncertainty in rod location.

The non-negligible experimental uncertainties for the 46 stainless steel 347 rod worth measurement are the 10%√2 measurement uncertainty and the ± 2.49/√3 ¢ rod location uncertainty. The worth of adding 46 stainless steel 347 rods to the core tank was measured as being 7.92¢ with a ±1.82¢ uncertainty.

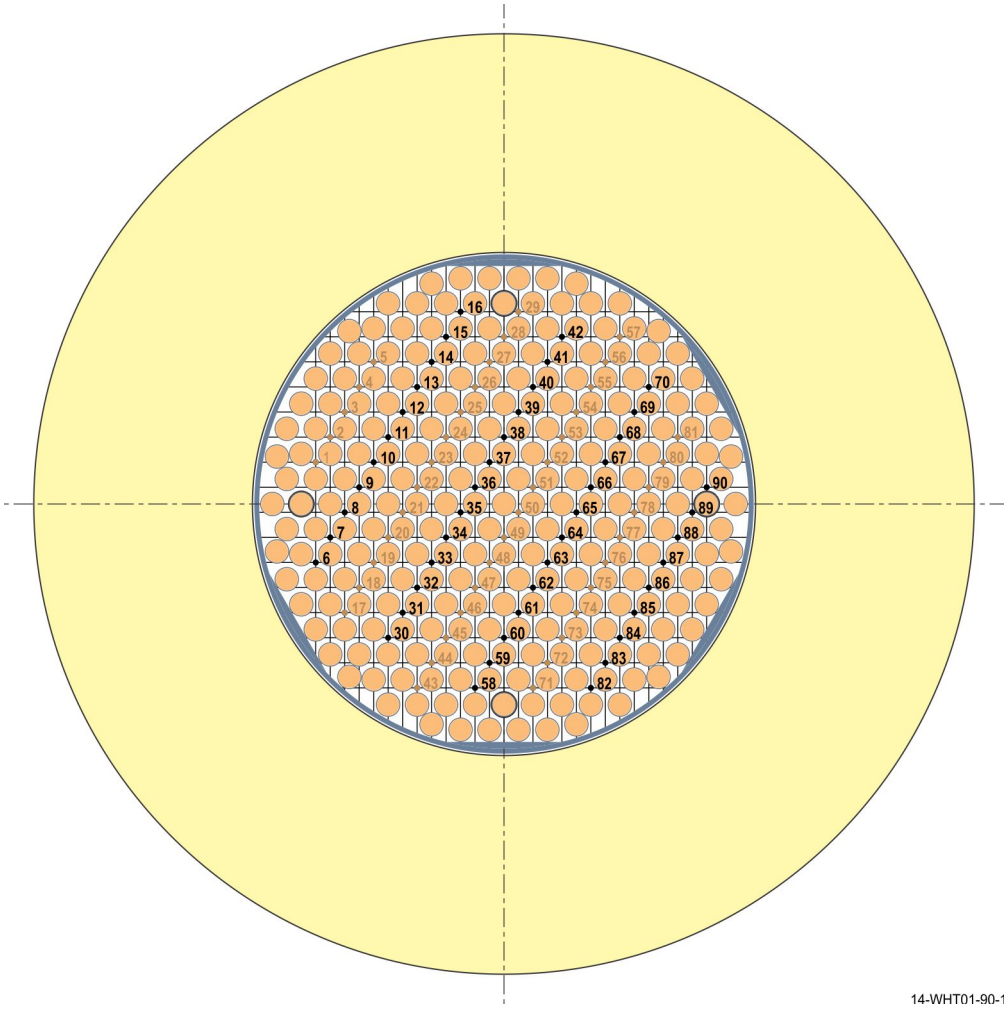

Figure 2.4-1a. Possible Configurations of 46 Rods.

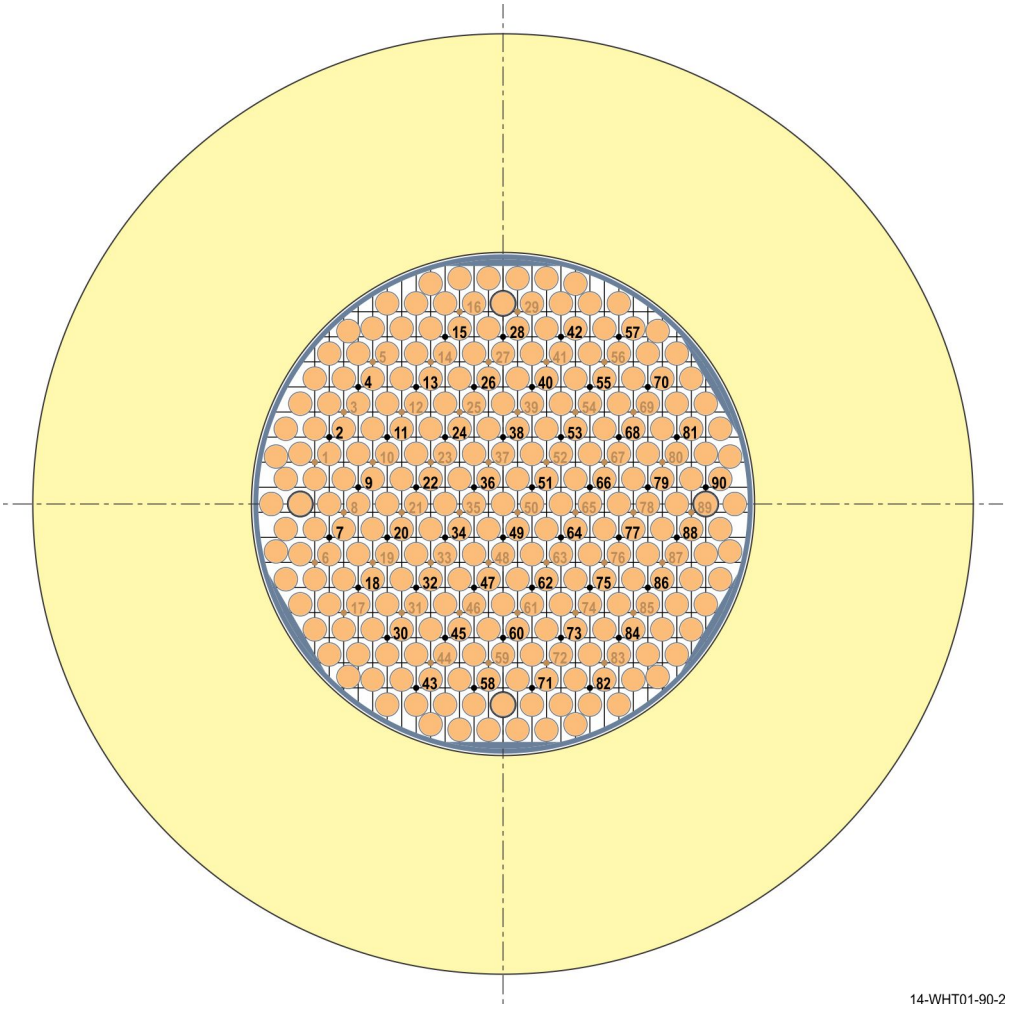

Figure 2.4-1b. Possible Configurations of 46 Rods.

2.4.2.2 Tungsten Rod Worth

The worth of adding 46 tungsten rods to the core was measured. The dimensional uncertainty was ± 0.0254 cm (25%/75% systematic/random). The effect of the uncertainty in the rod diameter and length were negligible.

The uncertainty in the fuel tube position was ±0.001 cm (HEU-COMP-FAST-004). This uncertainty is based on the measurement of the fuel tube pitch (1.506-cm). The rods are held in place between fuel tubes using holes added to the grid plates. The position and diameter of these holes are not explicitly given although from Figure 1.4-3 it appears that the holes are centered between fuel tubes. Because of this the uncertainty in the fuel tube position, ±0.001cm, was arbitrarily increased to ±0.01 cm for the rod position uncertainty. This uncertainty was taken to be 25% systematic and 75% random. The effect of the uncertainty in the rod position in both the x and y directions were negligible.

The mass of the tungsten was given as 2110 g. The uncertainty in mass was ±1 g. The effect of the uncertainty in the mass was negligible.

Because the type, purity or composition of tungsten was not given it was assumed that the tungsten was of purity 3N8, see Table 2.4-3 for tungsten composition. To evaluate the effect of the uncertainty in the tungsten purity the 3N8 tungsten composition was switched for the purer 4N tungsten. The effect of switching the tungsten purities was less than the statistical uncertainty of the calculation. So the tungsten purity was evaluated by perturbing the impurities of the 3N8 tungsten. The uncertainty in the material

impurities was evaluated as described in Section 2.4.2. This approach yields a bounding uncertainty effect. The tungsten composition is given in Table 2.4-3. To obtain results above the statistical uncertainty of the calculation the impurities were perturbed simultaneously using a scaling factor of 20. Only a one-sided perturbation could be performed when a scaling factor was applied. The uncertainty in the material impurities and thus the tungsten purity was negligible.

It has been suggested that molybdenum and oxygen impurities were also present in tungsten in the 1970's. To determine the effect of possible impurities, 150 ppm of molybdenum and oxygen impurities were added to the tungsten rods, individually, and had a negligible effect.

Table 2.4-3. Tungsten Purity and Model Composition.

Element	Standard Composition[(a)(b)]		Model Composition
	3N8	4N	
Tungsten, W	Balance	Balance	99.982 wt%
Potassium, K	< 20	< 10	10 ppm
Chromium, Cr	< 10	< 10	10 ppm
Nickel, Ni	130	30	130 ppm
Copper, Cu	< 20	< 10	10 ppm
Iron, Fe	20	10	20 ppm

(a) http://www.espimetals.com/index.php/online-catalog/467-tungsten-w (accessed on Oct. 9, 2014)
(b) Impurities in ppm.

There was an additional uncertainty in the 46 tungsten rod worth measurement. The rod location is given as 'every other position'. There is some ambiguity to this statement. Two configurations where 46 rods fit in 'every other position' are possible, see Figure 2.4-1. The change in worth between these two configurations was 0.83 ¢. This is taken to be a bounding uncertainty in rod location.

The non-negligible experimental uncertainties for the 46 tungsten rod worth measurement are the 10%√2 measurement uncertainty and the ± 0.83/√3 ¢ rod location uncertainty. The worth of adding 46 tungsten rods to the core tank was measured as being -4.27¢ with a ±0.77 ¢ uncertainty.

2.4.2.3 Columbium/Niobium Rod Worth

Henceforth the columbium rods will be referred to using the contemporary name, niobium. The worth of adding 90 niobium rods to the core was measured. The dimensional uncertainty was ± 0.0254 cm (25%/75% systematic/random). The effect of the uncertainty in the rod diameter and length were negligible.

The uncertainty in the fuel tube position was ±0.001 cm (HEU-COMP-FAST-004). This uncertainty is based on the measurement of the fuel tube pitch (1.506-cm). The rods are held in place between fuel tubes using holes added to the grid plates. The position and diameter of these holes are not explicitly given although from Figure 1.4-3 it appears that the holes are centered between fuel tubes. Because of this the uncertainty in the fuel tube position, ±0.001cm, was arbitrarily increased to ±0.01 cm for the rod position uncertainty. This uncertainty was taken to be 25% systematic and 75% random. The effect of the uncertainty in the rod position in both the x and y directions were negligible.

The mass of the niobium was given as 1050 g. The uncertainty in mass was ±1 g. The effect of the uncertainty in the mass was negligible.

Because the type, purity or composition of niobium was not given, it was assumed that the niobium was of purity 3N, see Table 2.4-4 for niobium composition. To evaluate the effect of the uncertainty in the niobium purity the 3N niobium composition was switched for the less pure 2N5 niobium. This approach yields a bounding uncertainty effect. Additionally, the niobium impurity uncertainty effect was evaluated. The uncertainty in the material impurities was evaluated as described in Section 2.4.2. This approach yields a bounding uncertainty effect. The effect of both these perturbations was less than the calculation's statistical uncertainty. So the perturbation of the impurity content was increased by a scaling factor of 30. The result was still within the statistical uncertainty of the calculation, thus it was judged that the effect of composition and impurity of niobium was negligible.

Table 2.4-4. Niobium Purity and Model Composition.

Element	Standard Composition[(a)(b)]		Model Composition
	2N5	3N	
Niobium, Nb	Balance	Balance	99.956 wt%
Iron, Fe	100	30	30 ppm
Nickel, Ni	175	50	50 ppm
Silicon, Si	30	10	10 ppm
Tin, Sn	<100	<50	25 ppm
Tantalum, Ta	500	300	300 ppm
Tungsten, W	<100	<50	

(a) http://www.espimetals.com/index.php/online-catalog/400-niobium-nb (accessed on Oct. 9, 2014)
(b) Impurities in ppm.

The only non-negligible experimental uncertainties for the 90 niobium rod worth measurement is the 10%√2 measurement uncertainty. The worth of adding 90 niobium rods to the core tank was measured as being 4.9¢ with a ±0.69 ¢ uncertainty.

2.4.2.4 Polyethylene, CH_2, Rod Worth

The worth of adding 8 polyethylene rods to the core was measured. The dimensional uncertainty was ± 0.0254 cm (25%/75% systematic/random). The effect of the uncertainty in the rod diameter and length were negligible.

The uncertainty in rod position was assumed to be the same as the fuel tube position uncertainty: ±0.001 cm (HEU-COMP-FAST-004). This uncertainty was taken to be 25% systematic and 75% random. There is the possibility of some additional uncertainty in rod position due to the flexibility of a polyethylene rod. The maximum movement possible was ±0.085 cm in the x direction and ±0.075 in the y direction. Even when the rod is moved the maximum amount the effect is still negligible thus it is judged that any additional uncertainty in the rod positions due to the flexibility of the 0.317-cm-diameter would be negligible. The effect of the uncertainty in the rod position in both the x and y directions were negligible.

The mass of the polyethylene was given as 18.42 g. The uncertainty in mass was ±0.01 g. The effect of the uncertainty in the mass was negligible.

The uncertainty in the hydrogen to carbon ratio in the polyethylene was evaluated. An arbitrary uncertainty of 2 ±0.05 in the ratio was taken to represent a bounding uncertainty in the value. The effect of perturbing the hydrogen to carbon ratio was ±0.23¢.

No impurities were given for the polyethylene. The possible effect of impurities on the worth measurement were evaluated by modeling 1 ppm of boron in the polyethylene. The effect of 1 ppm boron on the polyethylene worth was negligible; thus, it can be inferred that any impurities totaling 1 ppm boron equivalent or less would have a negligible effect on the polyethylene worth measurement.

The non-negligible experimental uncertainties for the 8 polyethylene rods worth measurement are the 10%√2 measurement uncertainty and the ±0.23 ¢ hydrogen to carbon ratio uncertainty The worth of adding 8 polyethylene rods to the core tank was measured as being 24.43¢ with a ±3.46 ¢ uncertainty.

2.4.2.5 Graphite Rod Worth

The worth of adding 23 graphite rods to the core was measured. The dimensional uncertainty was ±0.0254 cm (25%/75% systematic/random). The effect of the uncertainty in the rod diameter and length were negligible.

This uncertainty is based on the measurement of the fuel tube pitch (1.506-cm). The rods are held in place between fuel tubes using holes added to the grid plates. The position and diameter of these holes are not explicitly given although from Figure 1.4-3 it appears that the holes are centered between fuel tubes. Because of this the uncertainty in the fuel tube position, ±0.001cm, was arbitrarily increased to ±0.01 cm for the rod position uncertainty. This uncertainty was taken to be 25% systematic and 75% random. The effect of the uncertainty in the rod position in both the x and y directions were negligible.

The mass of the graphite was given as 82 g. The uncertainty in mass was ±1 g. The effect of the uncertainty in the mass was ± 0.19 ¢.

The graphite rods were assumed to be Type ATL graphite which was used as reflector in the previous two experiments in this series (HEU-COMP-FAST-001 and HEU-COMP-FAST-002). The composition of the graphite is given in Table 2.4-5. The uncertainty in the material impurities was evaluated as described in Section 2.4.2. This approach yields a bounding uncertainty effect. To obtain results above the statistical uncertainty of the calculation the impurities were perturbed simultaneously using a scaling factor of 20. Only a one-sided perturbation could be performed when a scaling factor was applied. Even with a scaling factor of 20, the result was still within the statistical uncertainty of the calculation, thus it was judged that the effect of impurities in graphite were negligible.

Table 2.4-5. Graphite Composition.

Element	Given Content	Model Composition	Element	Given Content	Model Composition
C	Balance	99.4536 wt.%	Mg	1	1 ppm
Al	270	270 ppm	Mn	1	1 ppm
Ba	22	22 ppm	Mo	5	5 ppm
B	< 1	0.5 ppm	Na	3	3 ppm
Ca	820	820 ppm	Ni	27	27 ppm
Co	3	3 ppm	Si	54	54 ppm
Cr	16	16 ppm	Sr	5	5 ppm
Cu	1	1 ppm	Ti	54	54 ppm
Fe	3940	3940 ppm	V	220	220 ppm
K	5	5 ppm	Y	11	11 ppm
Li	2	2 ppm	Yb	3	3 ppm
Lu	1	1 ppm			

There was an additional uncertainty in the 23 graphite rods worth measurement. The rod location is given as ‘every fourth position’. There is some ambiguity to this statement. Four configurations where 23 rods fit in ‘every fourth position’ are possible, see Figure 2.4-2. The change in worth between these four configurations has a maximum effect of 0.42 ¢. This is taken to be a bounding uncertainty in rod location.

The non-negligible experimental uncertainties for the 23 graphite rods worth measurement are the 10%√2 measurement uncertainty, the 0.19 ¢ mass uncertainty, and the ± 0.42/√3 ¢ rod location uncertainty. The worth of adding 23 graphite rods to the core tank was measured as being 7.5¢ with a ±1.10 ¢ uncertainty.

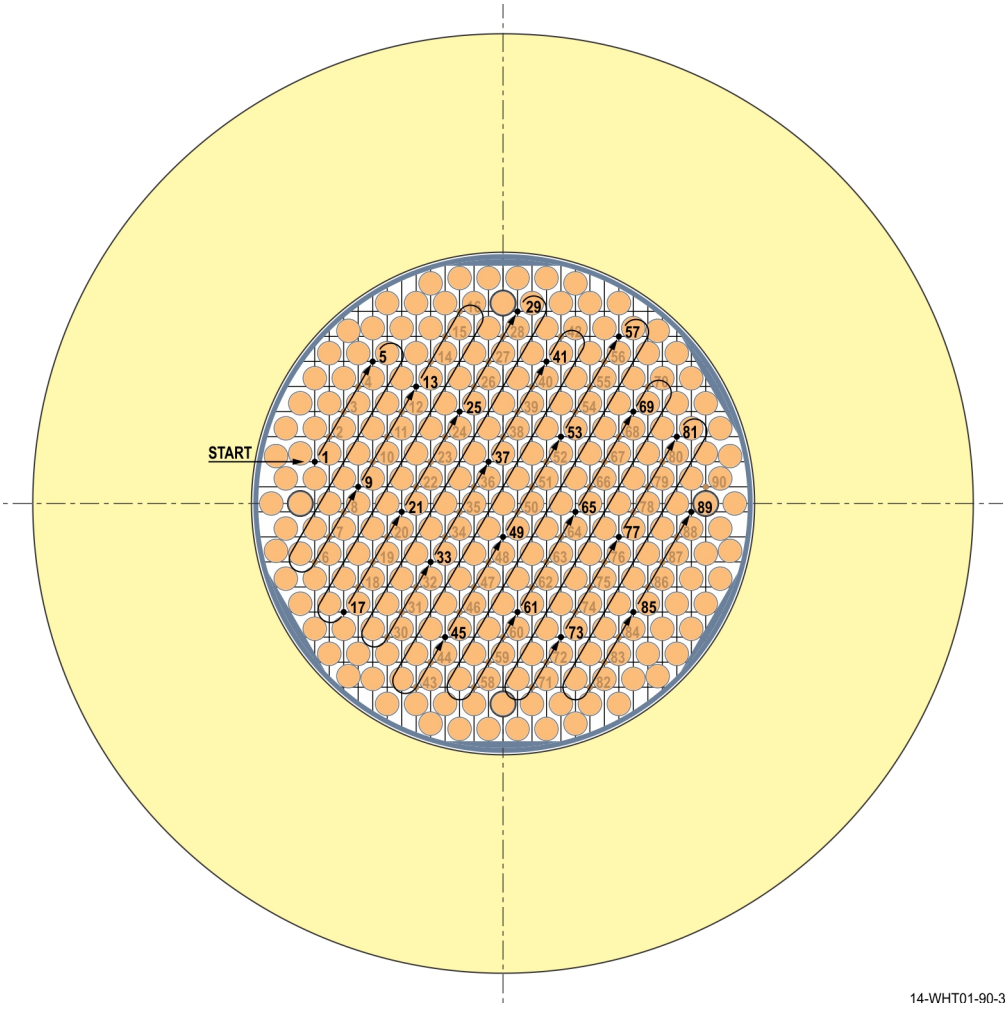

Figure 2.4-2a. Possible Configurations of 23 Rods.

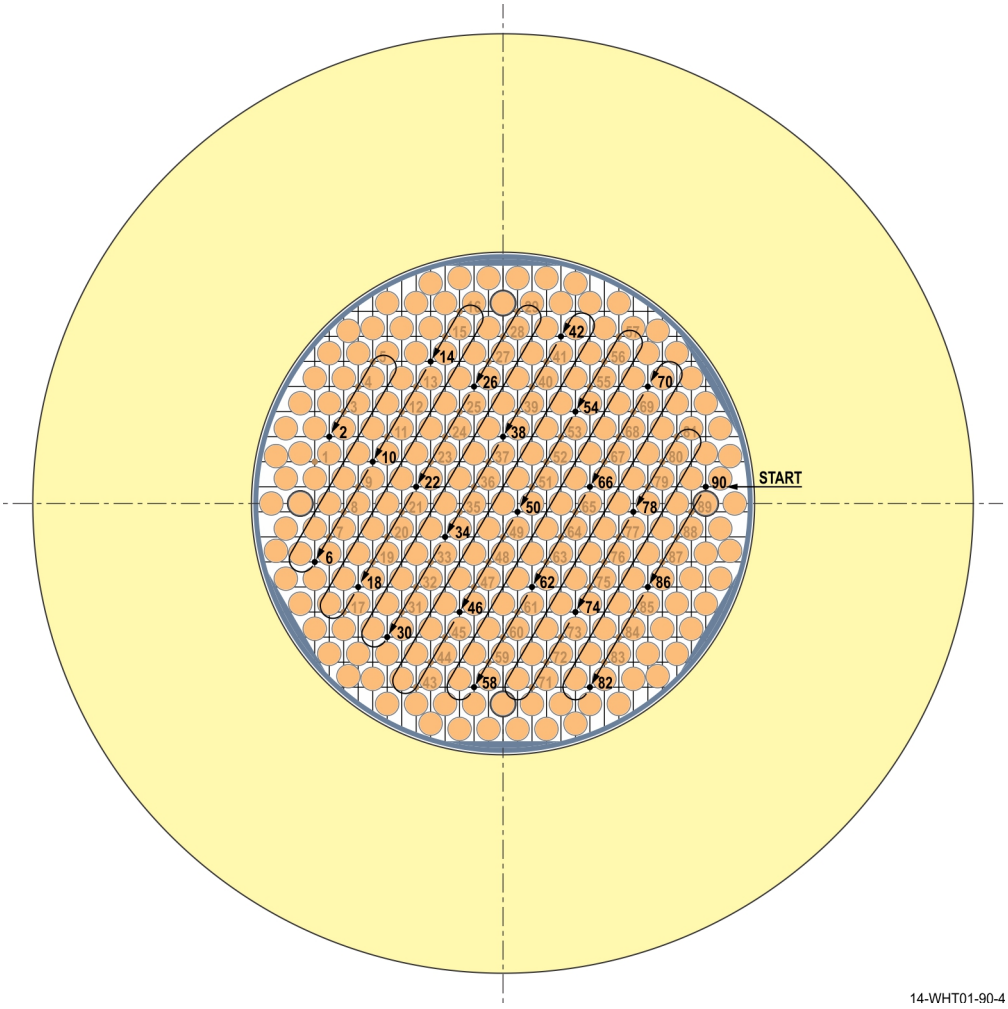

Figure 2.4-2b. Possible Configurations of 23 Rods.

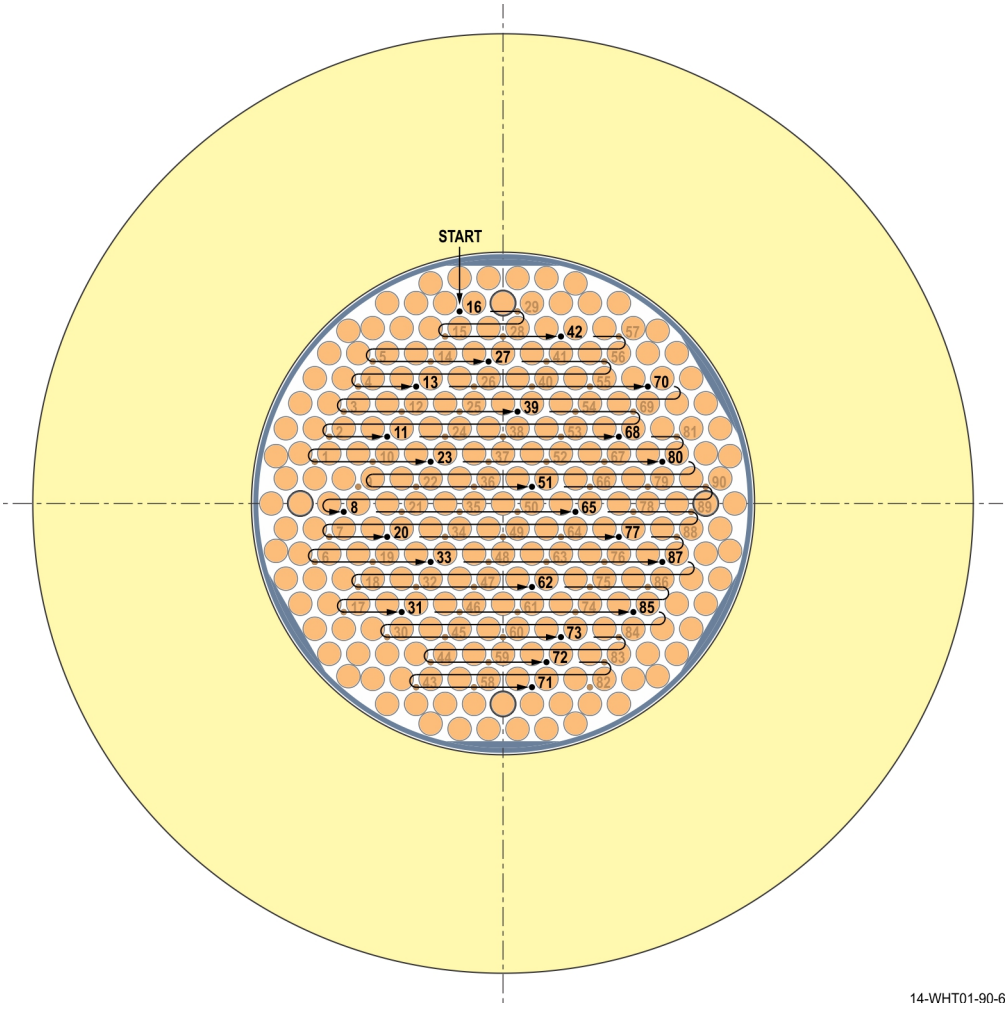

Figure 2.4-2c. Possible Configurations of 23 Rods.

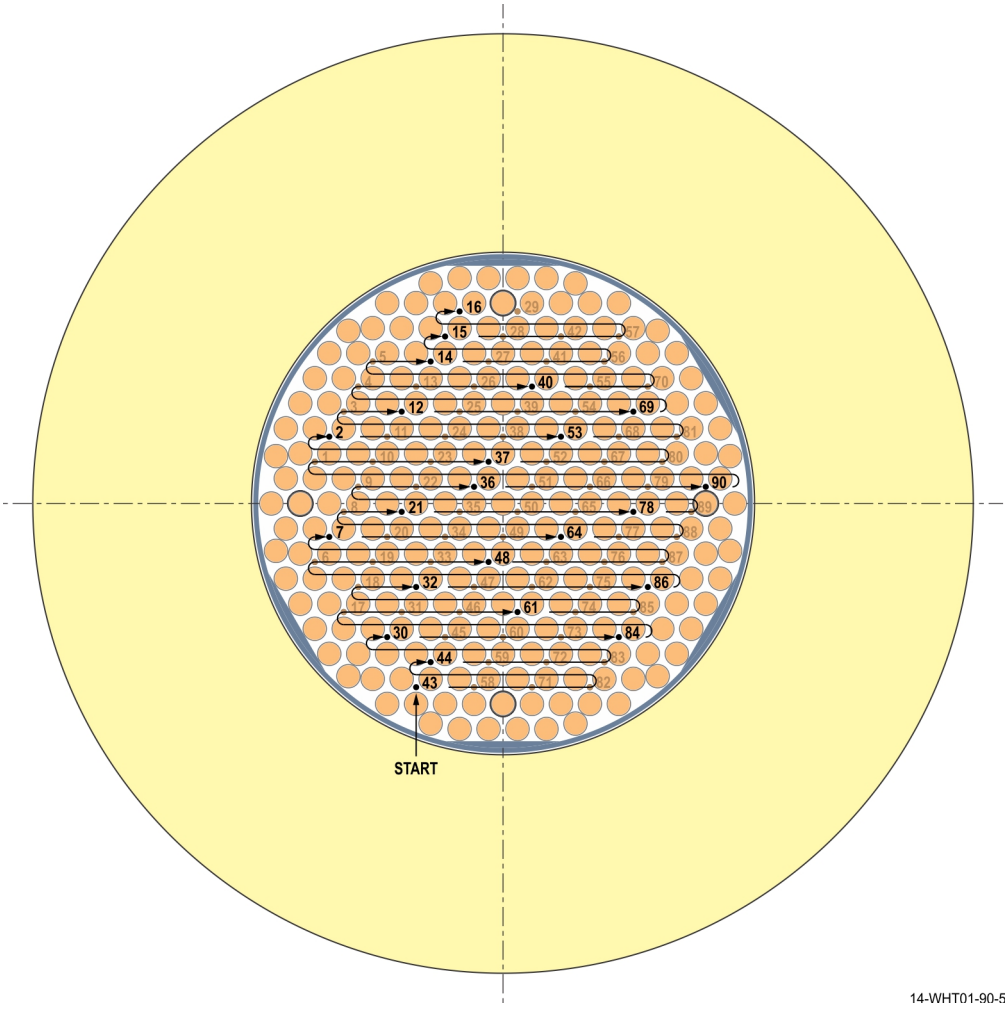

Figure 2.4-2d. Possible Configurations of 23 Rods.

2.4.2.6 Boron Carbide, B_4C, Worth

The worth of filling the fuel zone of an empty fuel tube with B_4C powder was measured. The fuel tube replaced the center fuel tube. The system reactivity was measured when an empty tube was in the center position and again when the filled tube was in the center position. The reactivity of the B_4C was the difference between the empty and filled tube system reactivities. The dimensions of the B_4C were assumed to be the inner dimensions of a fuel tube: 1.168-cm-diameter×29.88-cm-length.

The dimensional uncertainty for the B_4C was probably less than the dimensional uncertainties for the other material rods. This was because the fuel tube dimensions were measured very accurately (±0.00254 cm). The dimensional uncertainty of ±0.0254 cm was retained but is treated as a bounding uncertainty. The effect of the uncertainty in the B_4C diameter and length were negligible.

The uncertainty in B_4C tube position was assumed to be the same as the fuel tube position uncertainty: ±0.001 cm (HEU-COMP-FAST-004). Because the B_4C tube was place in a fuel tube position this is a reasonable assumption. The effect of the uncertainty in the rod position in both the x and y directions were negligible.

The mass of the B_4C was given as 30.5 g. The uncertainty in mass was ±0.1 g. The effect of the uncertainty in the mass was negligible.

The weights percent of boron in B_4C, based on the boron to carbon ratio of 4, was 77.263 wt.%. An uncertainty in the boron content of ± 1wt.% was assumed (NRAD-FUND-RESR-001). The effect of the uncertainty in the boron content was negligible.

The B_4C was in powder form. Based on the inside dimensions of a fuel tube and the mass of B_4C the density was 0.953 g/cm^3. There was a potential for settling of the B_4C, to evaluate this uncertainty the powder was modeled at an increased density of 1.6 g/cm^3.[a] Mass was conserved, thus the height was decreased to 17.7909 cm. The effect of settling of the B_4C powder was negligible.

The only non-negligible experimental uncertainties for the B_4C tube was the 10%√2 measurement uncertainty. The worth of the B_4C in the center position was -6.65 ¢ with a ±0.94 ¢ uncertainty.

2.4.2.7 Stainless Steel Lid Worth

The worth of placing a 0.317-cm-thick stainless steel disc in the top of the core tank, resting on top of the fuel pins, was measured. It was assumed that the stainless steel lid was made from stock sheet like the cadmium lid was. The uncertainty of the cadmium lid thickness was ± 1/2 mill or 0.00127 cm; however, the uncertainty in the stainless steel lid thickness was increased to 0.0254 cm because of the assumptions made. The diameter of the lid was only slightly less than the core tank diameter. The lid was modeled as having a diameter equal to the core tank inner diameter. The effect of this is believed to be captured by the uncertainty in the lid diameter. The dimensional uncertainty was ± 0.0254 cm. The effect of the uncertainties in the lid diameter and thickness were negligible.

The mass of the stainless steel lid was given as 1290 g. The uncertainty in mass was ±1 g. The effect of the uncertainty in the mass was negligible.

The report and logbook do not report what type of stainless steel was used for the lid. It was assumed that stainless steel 347 was used because it was also used for the stainless steel rod worth measurements. The worth was evaluated using a variety of types of stainless steel including: stainless steel 201, stainless steel 304, stainless steel 310, stainless steel 316, and stainless steel 321.[b,c] The effects of switching the stainless steel type were all below the statistical uncertainty of the calculation. Thus, it was judged that effect of the uncertainty in the stainless steel type was negligible.

The uncertainty in the material impurities was evaluated as described in Section 2.4.2. The stainless steel 347 composition is given in Table 2.4-2. This approach yields a bounding uncertainty effect. The effect of the material impurities was ±0.80 ¢.

The non-negligible experimental uncertainty for the stainless steel 347 lid measurement are the 10%√2 measurement uncertainty and the ±0.80 ¢ impurity uncertainty. The worth of a 0.317-cm-thick stainless steel 347 disc in the top of the core tank, resting on top of the fuel pins, was measured as being 7.97 ¢ with a ±1. 38 ¢ uncertainty.

2.4.2.8 Aluminum Lid Worth

The worth of placing 0.317-cm-thick and 0.159-cm-thick aluminum lids in the top of the core tank, resting on top of the fuel pins, was measured. Each lid was put into the core individually. It was assumed that the aluminum lids were made from stock sheet like the cadmium lid was. The uncertainty of the cadmium lid thickness was ± 1/2 mill or 0.00127 cm; however, the uncertainty in the aluminum lid thicknesses was increased to 0.0254 cm because of the assumptions made. The diameter of the lid was only slightly less than the core tank diameter. The lid was modeled as having a diameter equal to the core tank inner diameter. The effect of this is believed to be captured by the uncertainty in the lid diameter.

---

[a] G.A. Freund, P. Elias, D.R. MacFarlane, J.D. Geier, "Design Summary Report on the Transient Reactor Test Facility Treat," ANL-6034, Argonne National laboratory (1960).

[b] R.H. Perry and D.W. Green, editors, "Perry's Chemical Engineers' Handbook," McGraw-Hill, 7th ed. (1997).

[c] ASTM Standard A 312M -09.

The dimensional uncertainty was ±0.0254 cm. The effect of the uncertainties in the lid diameter and thickness were negligible.

The mass of the 0.317-cm-thick and 0.159-cm-thick aluminum lids was given as 464 g and 226 g, respectively. The uncertainty in mass was ±1 g per lid. The effect of the uncertainty in the mass was ±0.14 ¢ for both lids.

The lid material was given as aluminum, no type was specified. It was assumed that aluminum 1100 was used because it was used for aluminum parts throughout the system. The effect of selecting aluminum 1100 was evaluated by switching the aluminum 1100 for aluminum 6061, aluminum 5083, aluminum 7075, and aluminum 3003. The maximum effect was for switching with aluminum 5083 and was ±2.0 ¢. This was taken to be a bounding uncertainty. The effect of switching the aluminum type is less ±2.0/√3 ¢ for both lids.

The uncertainty in the aluminum 1100 impurities was evaluated as described in Section 2.4.2. The stainless steel 347 composition is given in Table 2.4-6. This approach yields a bounding uncertainty effect. The uncertainty in the material impurities on the worth is less than the calculation's statistical uncertainty thus the perturbation of the impurity content was increased by a scaling factor of 15. Additionally because all five impurities were perturbed simultaneously the uncertainty was scaled by a factor of √5. The resulting uncertainty for the aluminum 1100 impurities was ±0.32 ¢ for both lids.

Table 2.4-6. Type 1100 Aluminum Composition.

Element	Standard Composition[(a)(b)]	Model Composition
Aluminum, Al	99.00 wt.% minimum	99.325 wt.%
Copper, Cu	0.05-0.20 wt.%	0.125 wt.%
Silicon, Si	0.95 wt.%	0.2375 wt.%
Iron, Fe	Si + Fe	0.2375 wt.%
Manganese, Mn	0.05 wt.%	0.025 wt.%
Zinc, Zn	0.1 wt.%	0.05 wt.%
Other[(c)]	0.03 wt.% each 0.015 wt. total	0.00 wt.%

(a) ASTM Standard B 209 - 07.
(b) Single values are maximum values.
(c) 'Other' impurities were assumed have a negligible effect on k_{eff} and thus were not included in the benchmark model.

The non-negligible experimental uncertainties for the stainless steel 347 lid measurement are the 10%√2 measurement uncertainty, the 0.14¢ aluminum mass uncertainty, the ±2.00/√3 ¢ aluminum type uncertainty, and the ±0.32 ¢ impurity uncertainty. The worth of the 0.317-cm-thick and 0.159-cm-thick aluminum lids in the top of the core tank, resting on top of the fuel pins, was measured as being 16.62¢ and 8.14 ¢, with a ±2.64 ¢ and ±1.66 ¢ uncertainty, respectively.

2.4.2.9 Cadmium Lid Worth

The worth of placing 0.066-cm-thick cadmium lids in the top of the core tank, resting on top of the fuel pins, was measured. The diameter of the lid was only slightly less than the core tank diameter. The lid was modeled as having a diameter equal to the core tank inner diameter. The effect of this is believed to be captured by the uncertainty in the lid diameter. The lid was reported as having a thickness uncertainty of ½ mill or 0.00127 cm. The diameter uncertainty was taken to be one in the last significant digit or ± 0.0254 cm. The effect of the uncertainties in the lid diameter and thickness were negligible.

The mass of the 0.066-thick cadmium lids was given as 268.5 g. The uncertainty in mass was ±0.1 g. The effect of the uncertainty in the mass was negligible.

Because the type, purity or composition of cadmium was not given, it was assumed that the cadmium was of purity 5N, see Table 2.4-4 for cadmium composition. To evaluate the effect of the uncertainty in the cadmium purity the 5N cadmium composition was switched for the purer 6N cadmium. This approach yields a bounding uncertainty effect. The effect of switching the cadmium purity was less than the statistical uncertainty of the calculation. So the cadmium purity was evaluated by perturbing the impurities of the 5N tungsten. The uncertainty in the material impurities was evaluated as described in Section 2.4.2. The cadmium composition is given in Table 2.4-7. The perturbation of the impurity content was increased by a scaling factor of 50. Because a scaling factor was used only a one-sided perturbation could be used. This approach yields a bounding uncertainty effect. The uncertainty in the material impurities, and thus the cadmium purity, was negligible.

Table 2.4-7. Cadmium Purity and Model Composition.

Element	Standard Composition[(a)(b)]		Model Composition
	5N	6N	
Cadmium, Cd	Balance	Balance	99.999110 wt%
Copper, Cu	<0.1 ppm	-	0.05 ppm
Iron, Fe	0.2 ppm	-	0.1 ppm
Lead, Pb	2 ppm	0.1 ppm	2 ppm
Magnesium, Mg	3 ppm	0.1 ppm	3 ppm
Aluminum, Al	0.2 ppm	-	0.2 ppm
Silicon, Si	0.2 ppm	0.2 ppm	0.2 ppm
Silver, Ag	< 0.1 ppm	0.1	0.05 ppm
Titanium, Ti	0.2 ppm	-	0.2 ppm
Bismuth, Bi	3 ppm	0.2 ppm	3 ppm
Calcium, Ca	0.1 ppm	-	0.1 ppm

(a) http://www.espimetals.com/index.php/online-catalog/346-cadmium-cd (accessed on June 28, 2012)
(b) Impurities in ppm.

The non-negligible experimental uncertainty for the cadmium lid measurement are the 10%√2 measurement uncertainty. The worth of the cadmium lid in the top of the core tank, resting on top of the fuel pins, was measured as being -45.7¢ with a ±6.46 ¢ uncertainty.

2.4.2.10 Summary of Material Reactivity Measurements and Experimental Uncertainties

Table 2.4-8. Material Reactivity Measurements and Uncertainties.

Absorbing or Moderating Material	Experimental Worth with Experimental Uncertainty (¢)		
90 Stainless Steel 347 Rods	14.8	±	2.10
46 Stainless Steel 347 Rods	7.92	±	1.82
46 Tungsten Rods	-4.27	±	0.77
90 Niobium Rods	4.9	±	0.69
8 Polyethylene Rods	24.43	±	3.46
23 Graphite Rods	7.5	±	1.10
B_4C Filled Tube	-6.65	±	0.94
Stainless Steel Lid	7.97	±	1.38
0.3175 cm Thick Al Lid	16.62	±	2.64
0. 15875 cm Thick Al Lid	8.14	±	1.66
Cadmium Lid	-45.7	±	6.46

2.4.3 Potassium Worth Measurement

The potassium worth measurement was not evaluated.

2.5 Evaluation of Reactivity Coefficient Data

The worths per gram of various materials placed in the core were given in Reference 4. These reactivity coefficients are based on the absolute measured worth of a sample and the sample mass. The measured absolute worth values were not evaluated. For reference, the reactivity coefficients calculated using the sample mass and measured reactivity are provided in Section 1.4.

2.6 Evaluation of Kinetics Measurements Data

Kinetics measurements were not performed

2.7 Evaluation of Reaction-Rate Distributions

The uncertainty in the uranium foils dimensions, materials, and placement used for the activation measurements are the same as for the radial measurements of the activation of ^{235}U fission foils in SCCA-SPACE-EXP-002. The effects of these uncertainties have been reevaluated using the simple benchmark model described in Section 3.7.

According to the experimenter the measurement uncertainty in the radial foil measurements in SCCA-SPACE-EXP-002 would have been 0.5 %. This is applied as the experimental uncertainty for this evaluation as well.

In the benchmark model, the uranium foils were modeled without impurities. To calculate the effect of impurities in the uranium foils the uranium composition from HEU-MET-FAST-051[a] was used. It was found that the maximum 1σ uncertainty effect for the uranium foil composition is 1.86 %. The density of the foils was 18.75 g/cm^3; the nominal density in HEU-MET-FAST-051. Using the mass and dimensions of the various uranium parts used in that evaluation it is found that the density of the parts had a standard deviation of ±0.04 g/cm^3; this value was taken to be the 1σ uncertainty in the uranium foil density. The effect of this uncertainty was ±0.83 %. The effect of foil enrichment was evaluated by comparing calculated neutron flux for 100 wt.% ^{235}U foils to 93.15 wt.% ^{235}U foils. It was found that this 6.8 wt.% change in enrichment yields a maximum change in the calculated normalized neutron flux results of only 2 %. Based on these results, it is assumed that the effect of uncertainty in the foil enrichment would be negligible.

The uncertainty in the uranium foil thickness is ±0.001 cm. The maximum 1σ effect of the uncertainty in the uranium foil thickness is ±0.90 %. The uncertainty in the uranium foil diameter is ±0.01 cm, which has a maximum 1σ effect of ±0.27 %.

Because the measurements were normalized to a foil in the top reflector, the uncertainty in all points is multiplied by $\sqrt{2}$. Since the same value is applied to all measurement points for the majority of the uncertainties, and the remaining position uncertainty is negligible for the normalization point, this simplified approach is justified. Additionally, because the relative activation values are rounded to two decimal places there is also an additional uncertainty in the measurements of ±0.01, bounding with a uniform distribution, due to the rounding of the measured values.

The foil dimension, material, and rounding uncertainties are summarized in Table 2.7-1.

Table 2.7-1. Summary of Experimental Uncertainty in Activation of ^{235}U Fission Foils.

Uncertainty		Effect
Measurement	±	0.5%
Uranium Composition	±	1.28%
Uranium Density	±	0.83%
Uranium Foil Enrichment	±	NEG
Uranium Foil Thickness	±	0.90%
Uranium Foil Diameter	±	0.27%
Total	±	$1.86\%\sqrt{2}^{(a)}$
Rounding	±	$0.01/\sqrt{3}$

(a) The $\sqrt{2}$ accounts for the added uncertainty from the normalization.

The foil position uncertainty is the same as for the cadmium ratio measurement, ±0.10 cm. The positions of the foils in the core tank were adjusted so that foils were touching the side of a fuel tube and not floating between fuel tubes or sitting on the top of the fuel tube. The positions of the foils in the upper reflector were shifted up so that the bottom most foil was sitting on the inside bottom surface of the upper reflector tank. All other foils in the upper reflector were also shifted to maintain a 1.27 cm spacing (see

[a] *International Handbook of Evaluated Criticality Safety Benchmark Experiments*, NEA/NSC/DOC(95)03, OECD-NEA, Paris (2012).

Section 2.3). The effect of the foil position varied widely between foils and the calculated effect of axial and radial foil position was preserved for each foil. Table 2.7-2 gives the axial and radial foil position uncertainties. The given and adjusted foil locations are given in Table 2.7-2.

Table 2.7-2. Calculated Effect of Uncertainty in Position of ^{235}U Fission Foils.

Foil[a]		Given Location (cm)[b]	Modified Location (cm)[c]	Axial Position	Radial Position	Total Position Uncertainty
Axial Foil Activation Distribution						
1	H	-2.54	-2.54	NEG	1.01%	1.01%
2	H	0	0.00	NEG	NEG	NEG
3	H	2.54	2.54	0.21%	0.71%	0.74%
4	H	5.08	5.08	NEG	0.47%	0.47%
5	H	7.62	7.62	0.27%	NEG	0.27%
6	H	10.16	10.16	NEG	0.91%	0.91%
7	H	12.7	12.70	0.45%	NEG	0.45%
8	H	15.44	15.24	0.42%	NEG	0.42%
9	H	15.91	15.915	5.57%	0.86%	5.63%
10	H	17.18	17.185	2.72%	1.88%	3.30%
11	H	18.45	18.455	0.17%	2.96%	2.97%
12	H	19.72	19.725	NEG	1.21%	1.21%
13	H	20.99	20.995	1.70%	0.36%	1.74%
14	H	22.26	22.265	7.21%	1.29%	7.32%
Radial Foil Activation Distribution at Core Midplane						
15[d]	R	0.635	0.635	-[d]	-[d]	-[d]
16	R	3.25	3.243	0.18%	0.64%	0.66%
17	R	5.87	5.852	0.35%	1.06%	1.11%
18	R	8.53	8.460	0.14%	1.00%	1.01%
19	R	9.93	9.907	0.45%	2.05%	2.10%
20	R	10.74	10.735	0.17%	1.45%	1.46%
21	R	11.12	11.127	0.26%	2.41%	2.42%
22	R	11.2	11.177	0.46%	2.12%	2.17%
23	R	11.35	11.413	0.53%	11.10%	11.11%
24	R	12.06	12.005	0.44%	6.45%	6.46%
25	R	12.47	12.397	1.07%	3.35%	3.52%
26	R	12.62	12.589	0.40%	NEG	0.40%
Foil Activation Distribution at 15.24 cm Above Core Midplane[e]						
27[f]	R	0	0	-[f]	-[f]	-[f]
28	R	3.02	3.02	0.89%	0.39%	0.97%
29	R	12.06	12.06	2.92%	3.57%	4.62%

(a) These foil numbers were assigned by the evaluator.
(b) Locations were given as axial distance from the center of the fuel tube, height (H), or radial distance from the core center, radius (R).
(c) Many of the foil locations were modified so that the foil was in a feasible location, i.e. not floating in air or in the middle of a solid mass of material.
(d) This foil is a duplicate of foil 2.
(e) This height was given as 15.44 cm but was modified so foils lay on top of the fuel tubes and not 0.2 cm above them.
(f) This foil is a duplicate of foil 8.

The effect of material, dimensional, normalization and rounding uncertainties in Table 2.7-1 and the effect of the positional uncertainties from Table 2.7-2 are added in quadrature to obtain the total experimental uncertainty. The experimental results and the total experimental uncertainty, given as an absolute change in foil activation and a percentage, are summarized in Table 2.7-3. The given and adjusted foil locations are given in Table 2.7-3.

Table 2.7-3. Experimental Results of Relative Activation of ^{235}U Fission Foils Distribution and Total Experimental Uncertainty Effect.

Foil[a]	Given Location (cm)[b]		Modified Location (cm)[c]	Relative Foil Activation with Experimental Uncertainty[d]			
Axial Foil Activation Distribution							
1	H	-2.54	-2.54	1.02	±	0.034	(2.82%)
2	H	0	0.00	1.00	±	0.025	(1.86%)
3	H	2.54	2.54	1.00	±	0.032	(2.73%)
4	H	5.08	5.08	0.95	±	0.031	(2.67%)
5	H	7.62	7.62	0.91	±	0.030	(2.64%)
6	H	10.16	10.16	0.83	±	0.029	(2.78%)
7	H	12.7	12.70	0.88	±	0.029	(2.67%)
8	H	15.44	15.24	1.51	±	0.044	(2.66%)
9	H	15.91	15.915	1.56	±	0.099	(6.22%)
10	H	17.18	17.185	2.21	±	0.095	(4.22%)
11	H	18.45	18.455	2.53	±	0.102	(3.97%)
12	H	19.72	19.725	2.45	±	0.073	(2.90%)
13	H	20.99	20.995	2.00	±	0.065	(3.15%)
14	H	22.26	22.265	1.20	±	0.095	(7.78%)
Radial Foil Activation Distribution at Core Midplane							
15[d]	R	0.635	0.635	1.00	±	-[e]	-[e]
16	R	3.25	3.243	0.98	±	0.032	(2.71%)
17	R	5.87	5.852	0.99	±	0.033	(2.86%)
18	R	8.53	8.460	1.04	±	0.034	(2.82%)
19	R	9.93	9.907	1.06	±	0.040	(3.36%)
20	R	10.74	10.735	1.12	±	0.038	(3.01%)
21	R	11.12	11.127	1.21	±	0.047	(3.57%)
22	R	11.2	11.177	1.55	±	0.056	(3.41%)
23	R	11.35	11.413	1.45	±	0.166	(11.42%)
24	R	12.06	12.005	3.04	±	0.213	(6.98%)
25	R	12.47	12.397	3.68	±	0.163	(4.39%)
26	R	12.62	12.589	3.56	±	0.096	(2.66%)
Foil Activation Distribution at 15.24 cm Above Core Midplane[f]							
27[f]	R	0	0	1.51	±	-[g]	-[g]
28	R	3.02	3.02	1.63	±	0.049	(2.80%)
29	R	12.06	12.06	2.50	±	0.134	(5.31%)

(a) These foil numbers were assigned by the evaluator.
(b) Locations were given as axial distance from the center of the fuel tube, height (H), or radial distance from the core center, radius (R).
(c) Many of the foil locations were modified so that the foil was in a feasible location, i.e. not floating in air or in the middle of a solid mass of material.
(d) The total experimental uncertainty is the sum of the effects of the composition and dimensional uncertainties (1.86%) and rounding and normalization foils from Table 2.7-1 and the effect of the positional uncertainty (Table 2.7-2). The normalization uncertainty was not applied to the normalization foil, foil 2.
(e) This foil is a duplicate of foil 2 and will be omitted from tables from this point forward.
(f) This height was given as 15.44 cm but was modified so foils lay on top of the fuel tubes and not 0.2 cm above them.
(g) This foil is a duplicate of foil 8 and will be omitted from tables from this point forward.

2.8 Evaluation of Power Distribution Data

The relative power distribution in the core is the same as the relative fission rate as was measured in the core region of Assembly 1.

2.9 Evaluation of Isotopic Measurements

Isotopic measurements were not performed.

2.10 Evaluation of Other Miscellaneous Types of Measurements

Other miscellaneous types of measurements were not performed.

3.0 BENCHMARK SPECIFICATIONS

3.1 Benchmark-Model Specifications for Critical and/or Subcritical Measurements

(The criticality portion of this evaluation has been reviewed and approved by the International Criticality Safety Benchmark Evaluation Project (ICSBEP) and has been published under the following identifier: HEU-COMP-FAST-004.[a]) Drawings of the Case 1 and Case 2 detailed benchmark models are given as Figure 3.1-1 and Figure 3.1-2 for reference. The full ICSBEP evaluation should be reviewed for full details.

[a] International Handbook of Evaluated Criticality Safety Benchmark Experiments, NEA/NSC/DOC(95)03, OECD-NEA, Paris (2012).

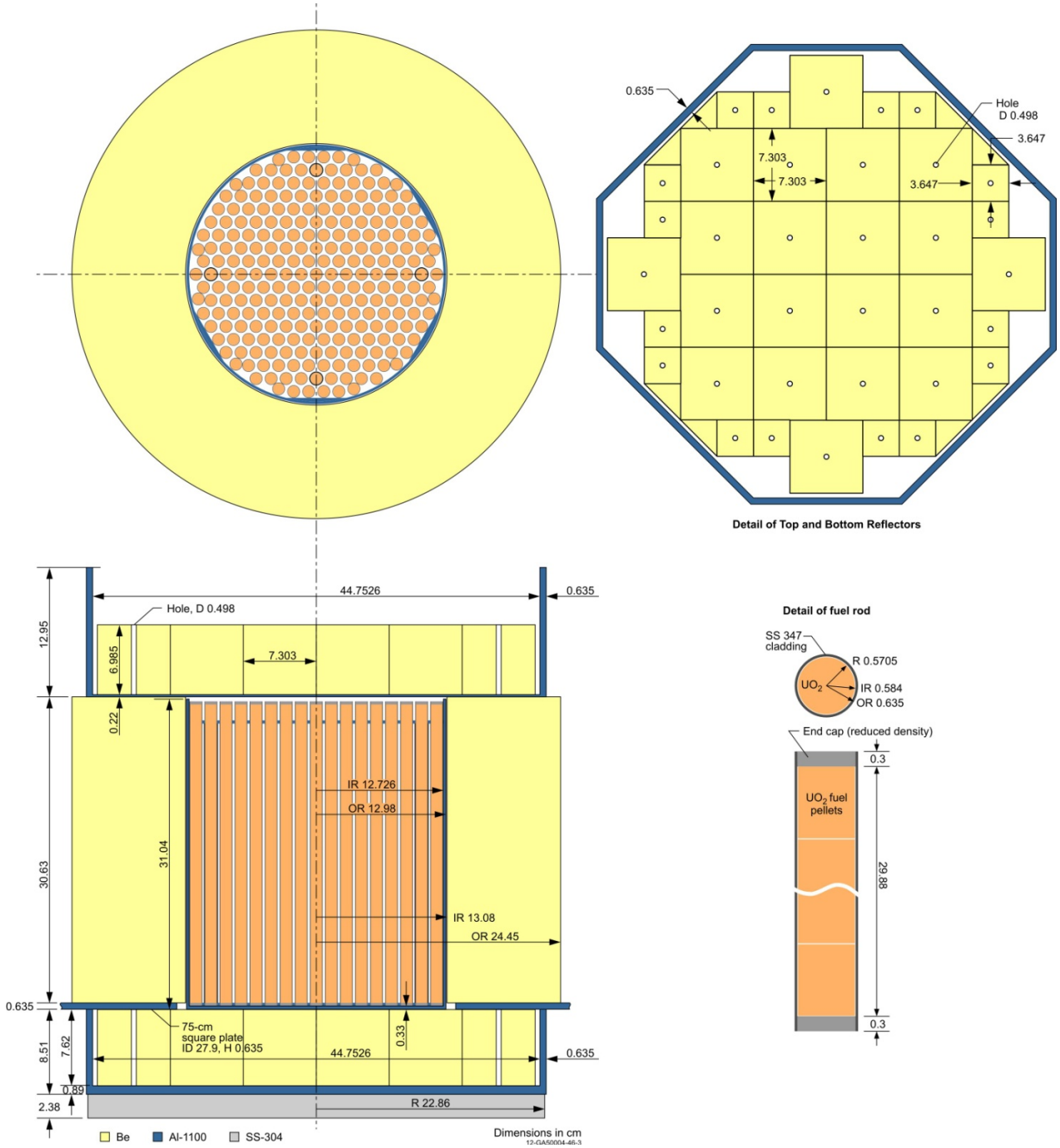

Figure 3.1-1. Detailed Critical Benchmark Model, Case 1.

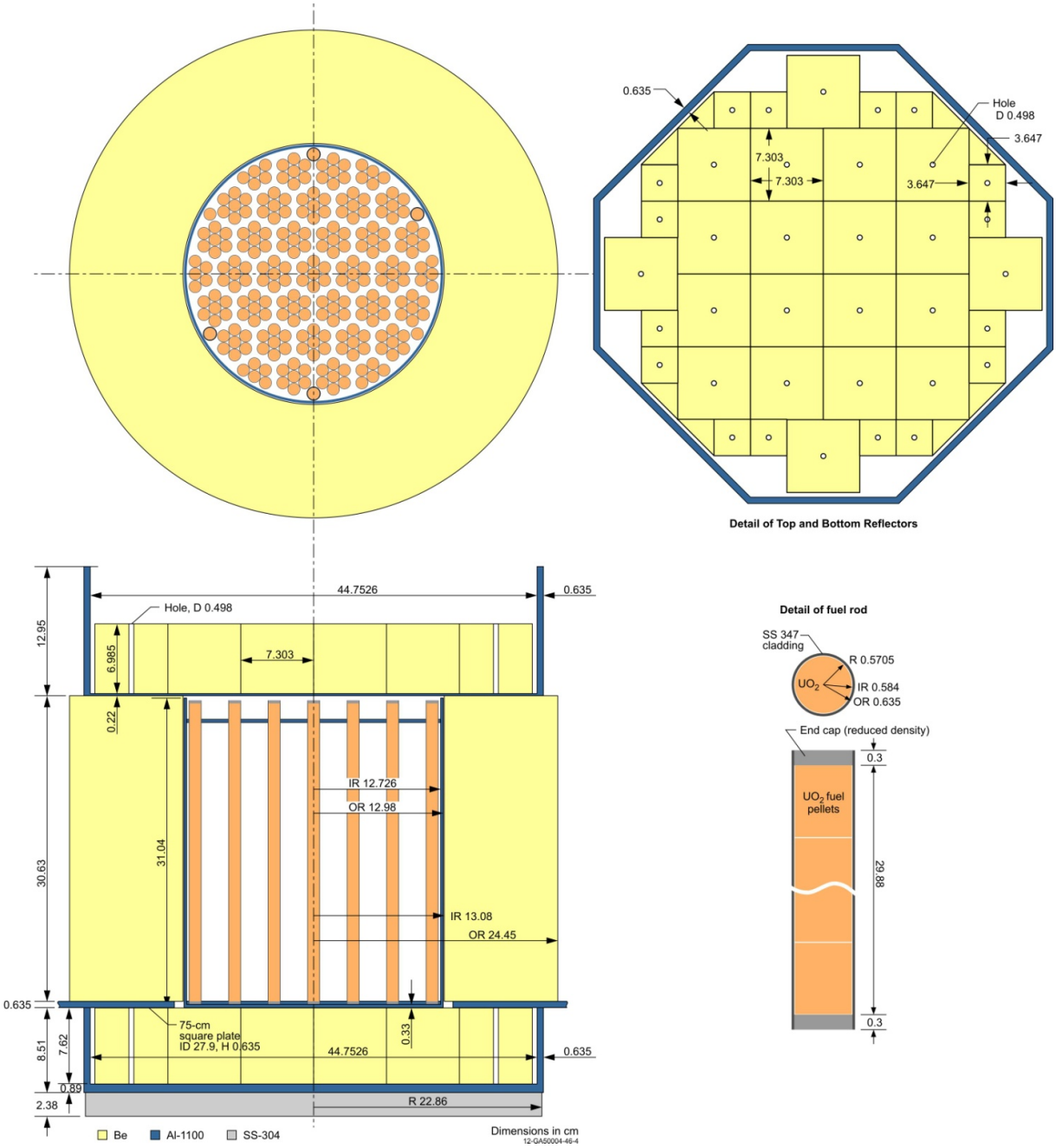

Figure 3.1-2. Detailed Benchmark Model, Case 2.

3.2 Benchmark-Model Specifications for Buckling and Extrapolation-Length Measurements

Buckling and extrapolation-length measurements were not performed.

3.3 Benchmark-Model Specifications for Spectral Characteristics Measurements

3.3.1 Description of the Benchmark-Model Simplifications

The simple and detailed benchmark models were the same as the Case 1 simple detailed benchmark models for the critical configuration described in HEU-COMP-FAST-004. The total simplification biases for the detailed and simple benchmark models were calculated and are given in Table 3.3-1.[a] Biases arising from individual simplifications were not calculated. A bias in the cadmium ratio measurements is considered negligible if it is less than the statistical uncertainty of the Monte Carlo calculation. For biases that are negligible, the bias uncertainty is preserved; as can be seen in Table 3.3-1. The given and modified locations are given in Table 3.3-1 (see Section 2.3 for discussion).

Cadmium ratio measurements were evaluated using explicit modeling of the foils and covers. It should be noted that the foils that were placed on top of the fuel tubes sat inside the end cap wells. In the detailed and simple benchmark models, these wells were not included but rather the mass was homogenized over the total end cap volume. This shifted the position of the foils measurements up by approximately 0.249 cm. The effect of the change in measurement position and the homogenization of the end cap is included in the detailed and simple benchmark model biases. All given modified foil locations correspond to the foils on top of the fuel tubes, not in the end-cap well. Neutron flux calculations were made over the foil and a multiplier for the ^{235}U fission cross section was used.

Table 3.3-1. Simplification Bias of Cadmium Ratios.

Cadmium Ratio				Effect					
Cd Ratio		Given Location (cm)[(a)]	Modified Location (cm)[(b)]	Detailed Benchmark Model Simplification Bias (ΔCd Ratio)			Simple Benchmark Model Simplification Bias (ΔCd Ratio)		
Distribution in Top Beryllium Reflector									
1	H	15.91	15.915	NEG	±	0.021	NEG	±	0.021
2	H	17.18	17.185	NEG	±	0.025	0.080	±	0.026
3	H	18.45	18.455	-0.045	±	0.027	NEG	±	0.028
4	H	19.72	19.725	-0.093	±	0.031	-0.039	±	0.031
5	H	20.99	20.995	0.000	±	0.036	NEG	±	0.036
6	H	22.26	22.265	-0.090	±	0.047	-0.083	±	0.048
Cadmium Ratio at Core Midplane									
7	R	11.35	11.413	NEG	±	0.014	NEG	±	0.014
Distribution at 15.24 cm Above Core Midplane[(c)]									
8	R	3.02	3.02	NEG	±	0.021	0.085	±	0.023
9	R	12.06	12.06	0.212	±	0.033	0.253	±	0.032

(a) Locations were given as axial distance from the center of the fuel tube, height (H), or radial distance from the core center, radius (R).
(b) Many of the foil locations were modified so that the foil was in a feasible location, i.e. not floating in air or in the middle of a solid mass of material.
(c) This height was given as 15.44 cm but was modified so foils lay on top of the fuel tubes and not 0.2 cm above them.

[a] These biases and simplifications are described in HEU-COMP-FAST-004 and include the: room return and air effects; temperature bias; use of nominal diameters for top and bottom reflectors; removal of shims; removal of grid plates and grid plate spacer tubes; grid plate and end cap simplification effect; simplification of the fuel tube; homogenization of the fuel; removal of fuel impurities; and removal of side, top, and bottom reflector impurities.

3.3.2 Dimensions

The simple and detailed benchmark models for the cadmium ratio measurements are the same as the Case 1 benchmark models for the critical configurations given in HEU-COMP-FAST-004 (see Section 3.2.1 for dimensions). Figure 3-3.1 shows the locations for the cadmium ratio measurements. These locations have been adjusted, as described in Section 2.3, from the given locations. The uranium foil and cadmium cover locations are the same for the simple and detailed benchmark models. (Figure 3-3.1 shows the detailed benchmark model.) When bare foils are being measured, the location shown in Figure 3-3.1 is the bottom center of the foils for horizontally positioned foils and the center of the foil surface which is touching the fuel tube for the vertical foil. When the cadmium cover was added the bottom center of the foil shifted up 0.051 cm, the thickness of the cadmium cover, for the horizontal foils and in 0.051 cm radially for the one vertical foil. The locations in Figure 3-3.1 are then the bottom center of the cadmium cover for the horizontally positioned foils and the center of the cadmium cover surface which is touching the fuel tube for the vertical foil.

For both the detailed and simple benchmark models, the uranium foils are 0.75-cm in diameter and 0.01-cm thick. The cadmium covers are 0.051-cm thick on either side of the uranium foil and have a diameter of 0.85 cm. The uranium foil and cadmium cover are shown in Figure 3-3.2.

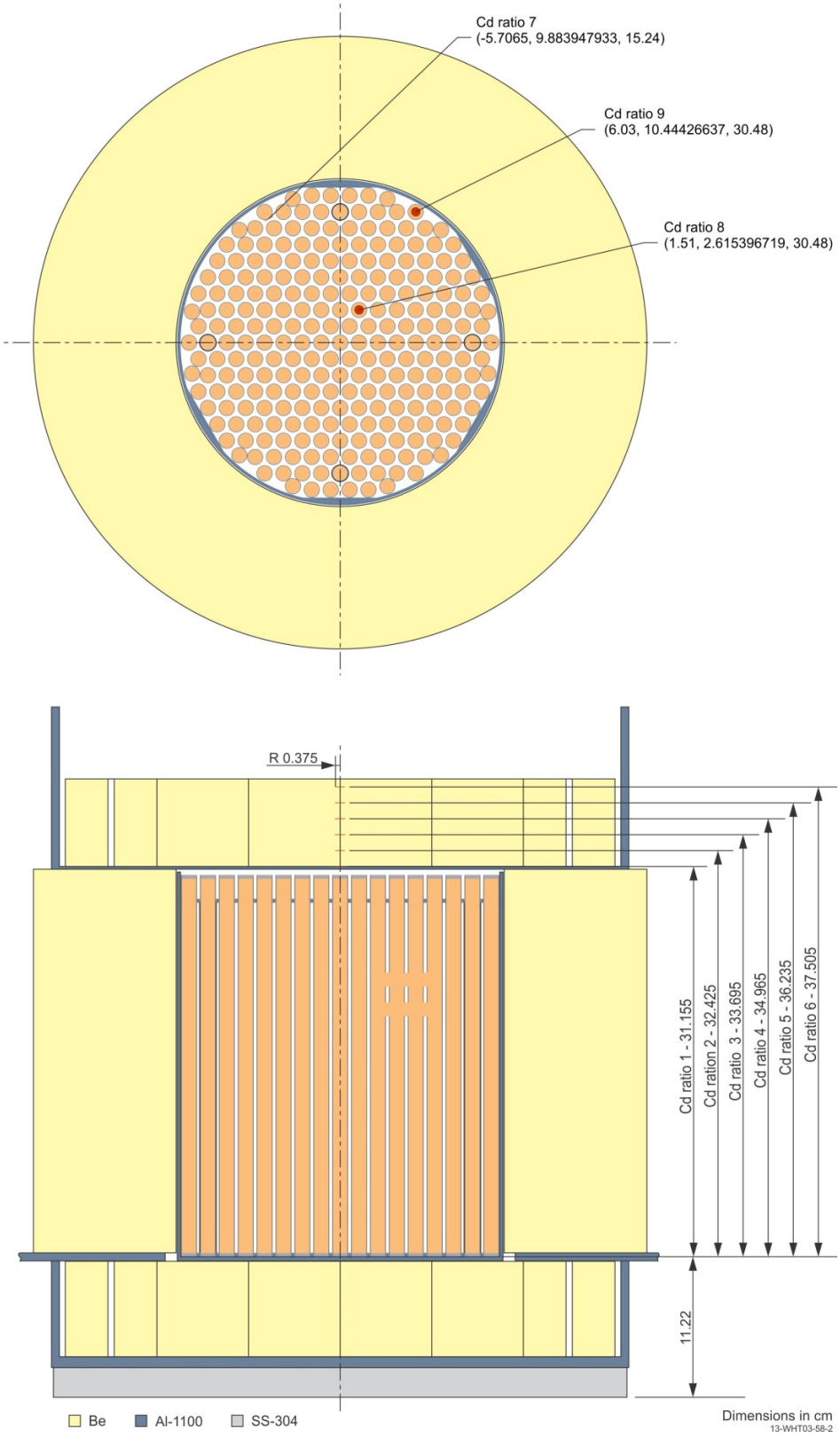

Figure 3.3-1. Uranium Foil and Cadmium Cover Locations.[a]

[a] The foils in the upper reflector are oriented horizontally. The foils at a height of 30.48 cm are horizontally positioned on the top of the fuel tubes. One vertical foil is placed at the midplane of the core (height of 15.24). With sufficient magnification, it can be seen that all foils are explicitly modeled in Figure 3.3-1.

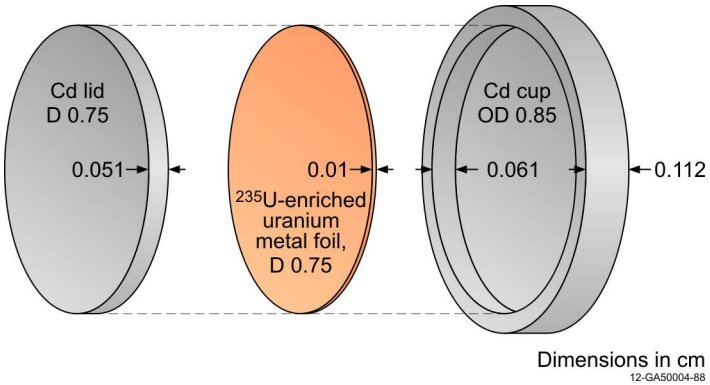

Figure 3.3-2. Uranium Foils and Cadmium Covers.

3.3.3 Material Data

The material data for the simple and detailed benchmark model for the cadmium ratios are the same as the material data for the Case 1 benchmark models for the critical configuration (see HEU-COMP-FAST-004, Section 3.3.1).

For the simple and detailed benchmark models, the uranium foils have a density of 18.75 g/cm^3 (see Section 2.3). The composition is given in Table 3.3-2.

Table 3.3-2. Uranium Metal Foil Composition.

Element	wt.%	Isotopic enrichment	Atoms/barn-cm
U Total	99.95 wt%[(a)]	-	4.7983E-02
^{234}U	-	0.97 wt%	4.6775E-04
^{235}U	-	93.14 wt%	4.4722E-02
^{236}U	-	0.24 wt%	1.1475E-04
^{238}U	-	5.65 wt%	2.6786E-03

(a) The total weight percent is reduced because impurities were replaced with void.

The cadmium covers have a density of 8.65 g/cm^3. The composition is given in Table 3.3-3.

Table 3.3-3. Cadmium Cover Composition.

Element	wt.%	Atoms/barn-cm
Cd Total	99.99911 wt%[(a)]	4.6340E-02

(a) The total weight percent is reduced because impurities were replaced with void.

3.3.4 Temperature Data

The temperature is the same as for the critical configuration, 72°F (22°C).[a]

3.3.5 Experimental and Benchmark-Model Spectral Characteristics Measurements

The benchmark values for the cadmium ratios are found by applying the biases in Table 3.3-1 to the experimental results. The uncertainty in the benchmark model is found by adding in quadrature the uncertainty in the experimental results, discussed in Section 2.3, and the bias uncertainty given in Table 3.3-1. The benchmark results are given in Table 3.3-4.

Table 3.3-4. Benchmark Cadmium Ratios.

Cd Ratio	Given Location (cm)[(a)]		Modified Location (cm)[(b)]	Detailed Benchmark Model Value			Simple Benchmark Model Value		
Distribution in Top Beryllium Reflector									
1	H	15.91	15.915	1.370	±	0.027	1.370	±	0.028
2	H	17.18	17.185	1.560	±	0.029	1.640	±	0.030
3	H	18.45	18.455	1.655	±	0.031	1.700	±	0.031
4	H	19.72	19.725	1.667	±	0.033	1.721	±	0.034
5	H	20.99	20.995	1.970	±	0.038	1.970	±	0.038
6	H	22.26	22.265	1.970	±	0.049	1.977	±	0.050
Cadmium Ratio at Core Midplane									
7	R	11.35	11.413	1.240	±	0.083	1.240	±	0.083
Distribution at 15.24 cm Above Core Midplane[(c)]									
8	R	3.02	3.02	1.390	±	0.023	1.475	±	0.025
9	R	12.06	12.06	2.082	±	0.040	2.123	±	0.040

(a) Locations were given as axial distance from the center of the fuel tube, height (H), or radial distance from the core center, radius (R).
(b) Many of the foil locations were modified so that the foil was in a feasible location, i.e. not floating in air or in the middle of a solid mass of material.
(c) This height was given as 15.44 cm but was modified so foils lay on top of the fuel tubes and not 0.2 cm above them.

3.4 Benchmark-Model Specifications for Reactivity Effects Measurements

3.4.1 Description of the Benchmark-Model Simplifications

3.4.1.1 Fuel Effect Reactivity Measurements

The base models for the reactivity worth measurements were the same as the Case 1 simple and detailed benchmark models for the critical configuration described in HEU-COMP-FAST-004, see Figure 3.1-1 for reference. To obtain the benchmark models for the fuel effect worths, the appropriate fuel rod was removed or moved. The simplifications of the detailed and simple benchmark models were the same as those for the critical configuration. The total simplification biases for the detailed and simple benchmark models were calculated and are given in Table 3.4-1. Many of the calculated biases are less than the 1σ statistical uncertainty of the calculation and the rest were within 2σ. Because of this, and because there was no pattern or consistency across the calculated biases, all biases were judged to be negligible; however, as can be seen in Table 3.4-1 the uncertainty in the calculated bias was preserved.

[a] Personal email communication with J. T. Mihalczo, May 23, 2011.

Table 3.4-1. Fuel Effect Reactivity Measurements and Uncertainties.

Distance from Core Center (Fuel Tube Position)	Detailed Benchmark Model Simplification Bias (Δ¢)	Simple Benchmark Model Simplification Bias (Δ¢)
0 cm (1)	NEG ± 1.668	NEG ± 1.670
2.59 cm (2)	NEG ± 1.668	NEG ± 1.670
5.23 cm (3)	NEG ± 1.668	NEG ± 1.670
7.75 cm (4)	NEG ± 1.668	NEG ± 1.604
10.48 cm (5)	NEG ± 1.667	NEG ± 1.670
10.56 cm (6)	NEG ± 1.667	NEG ± 1.670
11.78 cm (7)	NEG ± 1.602	NEG ± 1.669
Accident Configuration Worth	NEG ± 1.665	NEG ± 1.668

3.4.1.2 Neutron Absorbing and Moderating Material Reactivity Measurements

The base models for the reactivity worth measurements were the same as the Case 1 simple and detailed benchmark models for the critical configuration described in HEU-COMP-FAST-004, see Figure 3.1-1 for reference. To obtain the benchmark models for the material worth measurements the appropriate material was added to the base model. The simplifications of the detailed and simple benchmark models were the same as those for the critical configuration. Additionally, for the tungsten, niobium, and graphite rods and the cadmium lid the impurities were removed for the simple benchmark model but not for the detailed benchmark model. When impurities were removed they were replaced with void thus reducing the total atom density.

The total simplification biases for the detailed and simple benchmark models were calculated and are given in Table 3.4-2. Many of the calculated biases are less than the 1σ statistical uncertainty of the calculation and the rest were within 2σ. Because of this, and because there was no pattern or consistency across the calculated biases, all biases were judged to be negligible; however, as can be seen in Table 3.4-1 the uncertainty in the calculated bias was preserved.

Table 3.4-2. Material Reactivity Measurements and Uncertainties.

Absorbing or Moderating Material	Detailed Benchmark Model Simplification Bias (Δ¢)			Simple Benchmark Model Simplification Bias (Δ¢)		
90 Stainless Steel 347 Rods	NEG	±	1.662	NEG	±	1.664
46 Stainless Steel 347 Rods	NEG	±	1.663	NEG	±	1.665
46 Tungsten Rods	NEG	±	1.600	NEG	±	1.667
90 Niobium Rods	NEG	±	1.663	NEG	±	1.666
8 Polyethylene Rods	NEG	±	1.661	NEG	±	1.664
23 Graphite Rods	NEG	±	1.663	NEG	±	1.666
B_4C Filled Tube	NEG	±	1.668	NEG	±	1.670
Stainless Steel Lid	NEG	±	1.663	NEG	±	1.665
0.3175 cm Thick Al Lid	NEG	±	1.662	NEG	±	1.664
0.315875 cm Thick Al Lid	NEG	±	1.663	NEG	±	1.666
Cadmium Lid	NEG	±	1.603	NEG	±	1.606

3.4.2 Dimensions

3.4.2.1 Fuel Effect Reactivity Measurements

The base model for the benchmark fuel effect reactivity measurements was identical to the Case 1 simple and detailed benchmark models for the critical configuration described in HEU-COMP-FAST-004, see Figure 3.1-1 for reference. The dimensions of the fuel tubes that were removed or moved were identical to the dimensions of the fuel tubes in the base model. Figure 3.4-1 shows the location of the fuel tubes that were removed. For the accident configuration fuel tubes were moved out so that they were touching the core tank wall. When the fuel tubes were moved, the angle of the center of the fuel tube in relation to the center of the core was held constant. Figure 3.4-2 shows the locations of the fuel tubes when they were moved into the accident configuration.

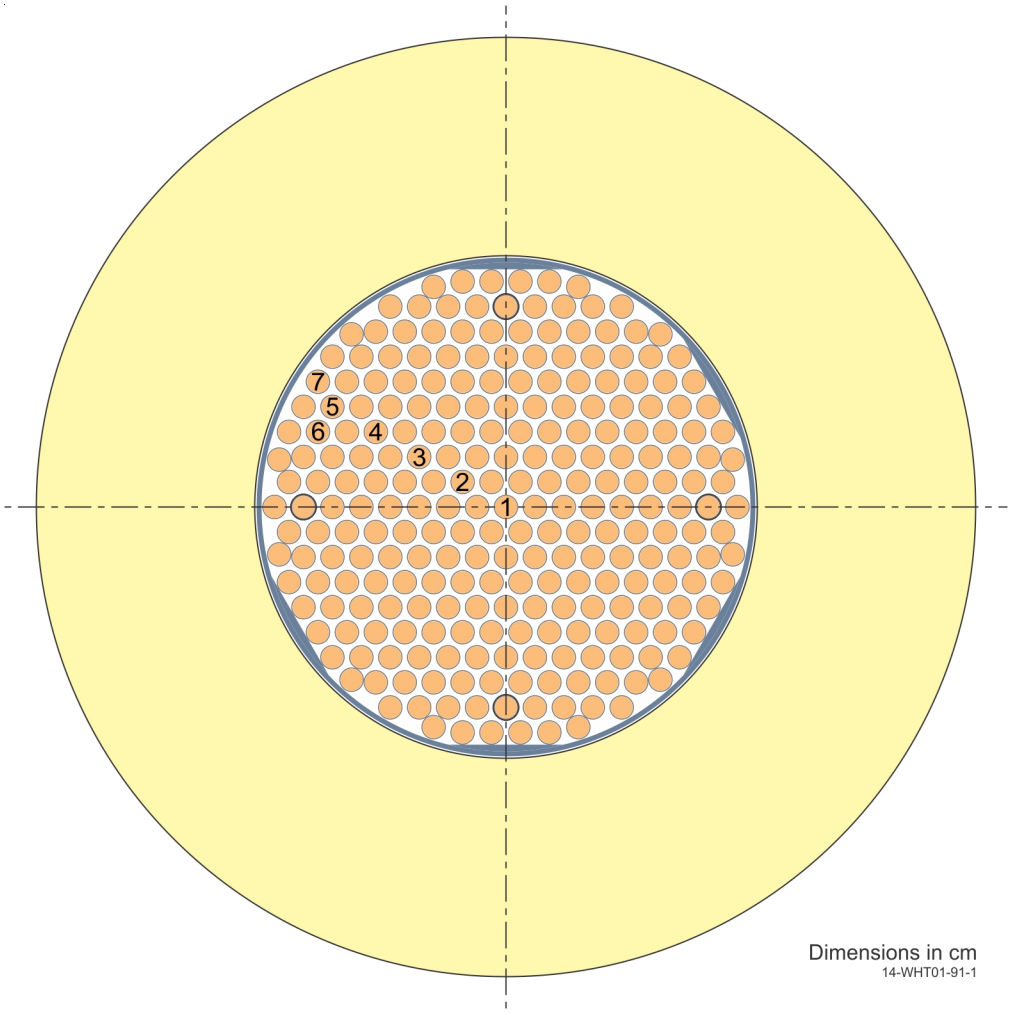

Figure 3.4-1. Location of Removed Fuel Tubes.

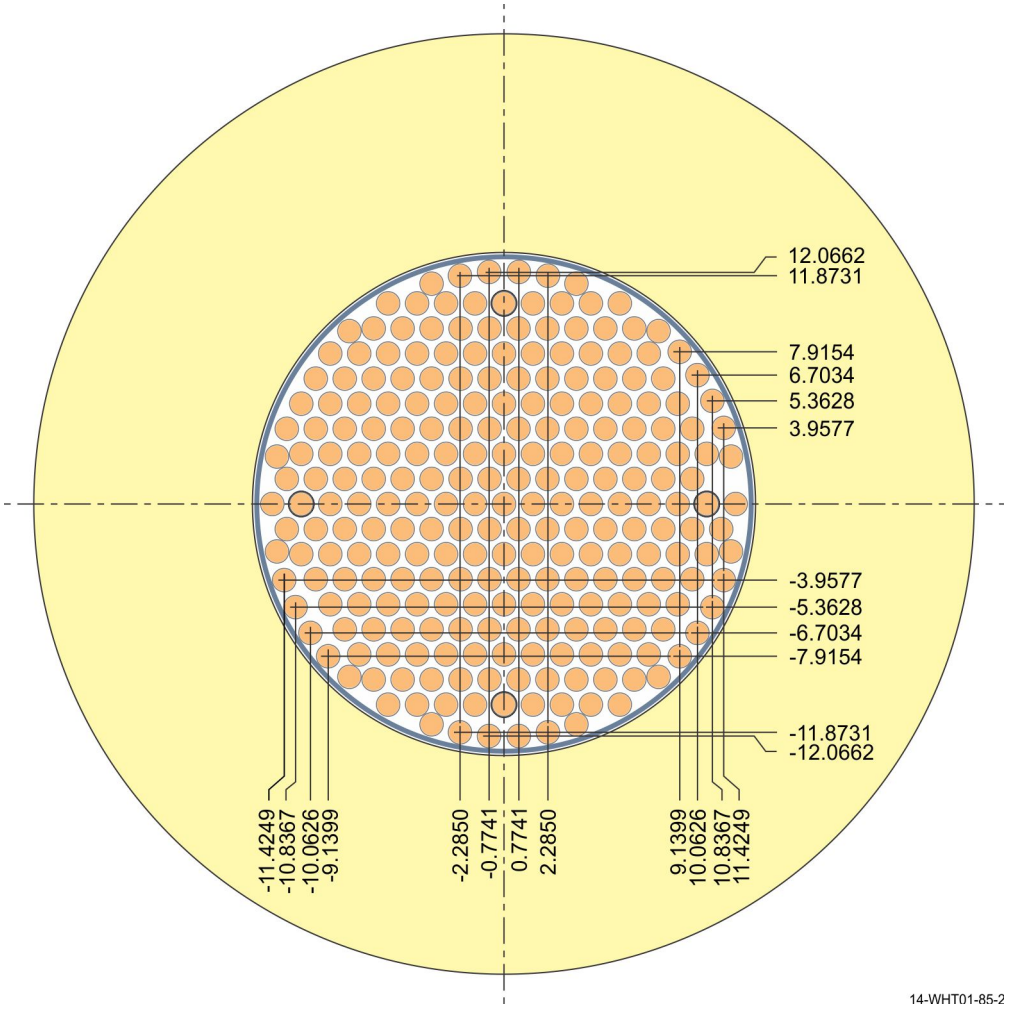

Figure 3.4-2. Location of Fuel Tubes in Accident Configuration.

3.4.2.2 Neutron Absorbing and Moderating Material Reactivity Measurements

The base model for the benchmark fuel effect reactivity measurements was identical to the Case 1 simple and detailed benchmark models for the critical configuration described in HEU-COMP-FAST-004, see Figure 3.1-1 for reference. Materials were added to the core to determine the material worths. The dimensions of the added materials were the same for the simple and detailed benchmark models; only the base model changed. The grid plate was machined to allow for the rods to be inserted into the core. Rods rested on the bottom of the core tank. Lids rested on the top of the fuel tubes. The dimensions of each material are as follows:

Stainless Steel 347 Rods

The stainless steel rods had a diameter of 0.317 cm and were 30.5 cm long. The 90 stainless steel rods filled all 90 rod locations shown in Figure 3.4-3. The 46 stainless steel rods were in every other diagonal-row as is shown in Figure 3.4-4. Other potential arrangements of the 46 rods were evaluated in Section 2.4.2 and are included in the experimental uncertainty.

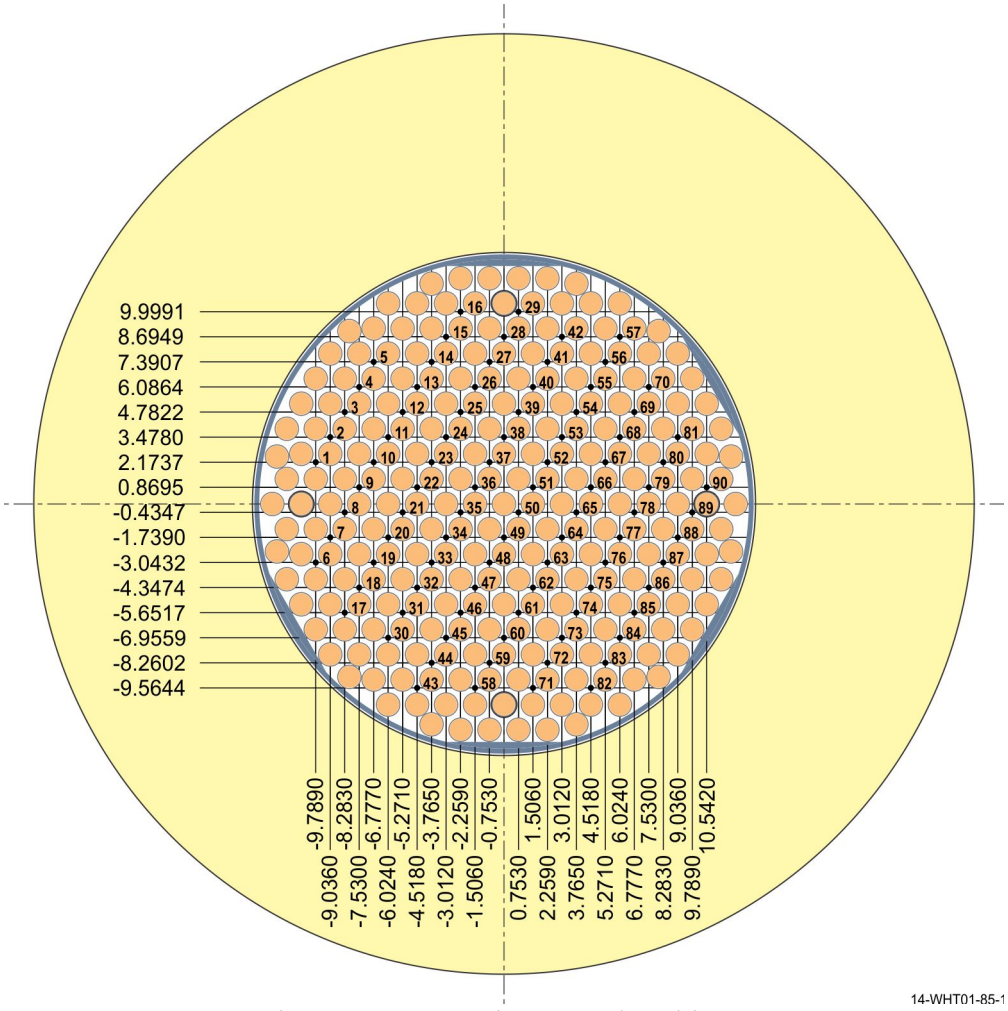

Figure 3.4-3. Location 90 Rod Positions.

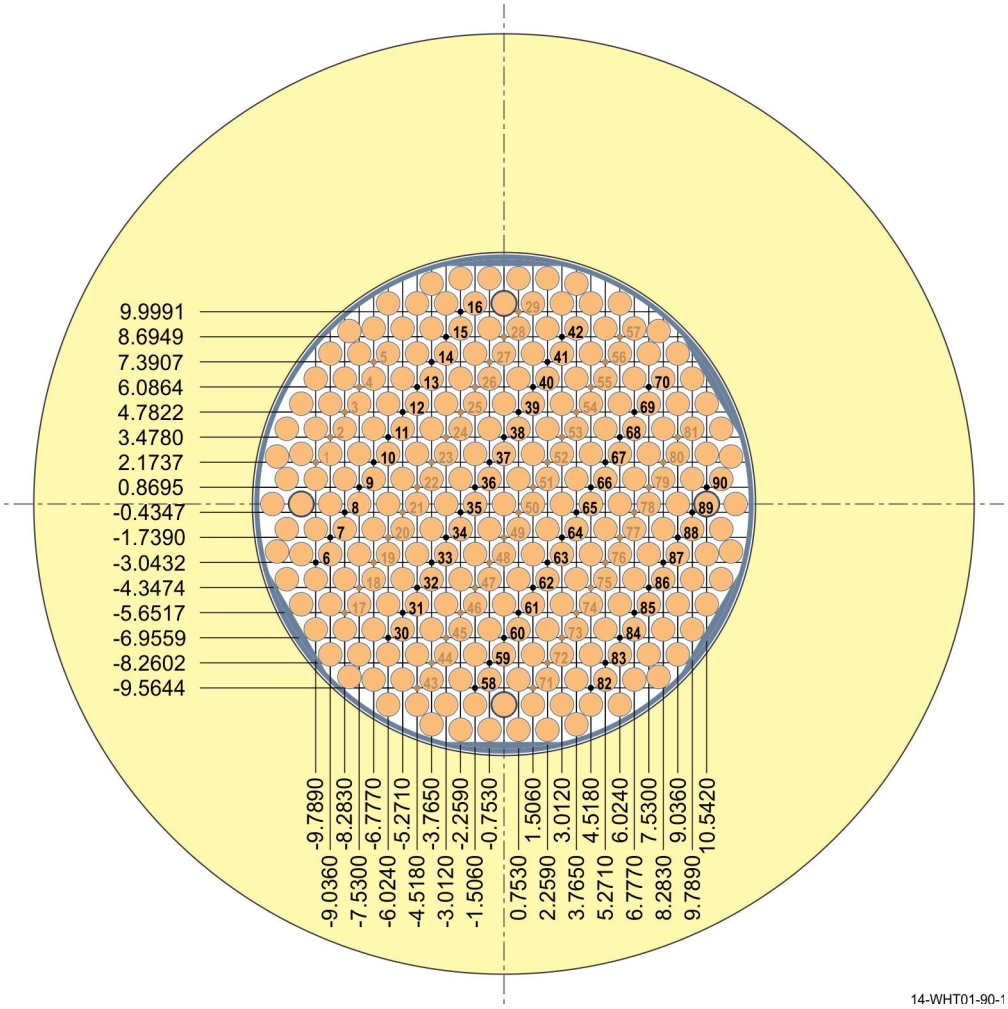

Figure 3.4-4. Location 46 Rod Positions.

Tungsten Rods

The stainless steel rods had a diameter of 0.317 cm and were 30.5 cm long. The 46 tungsten rods were in every other diagonal-row as is shown in Figure 3.4-4. Other potential arrangements of the 46 rods were evaluated in Section 2.4.2 and are included in the experimental uncertainty.

Niobium Rods

The niobium rods had a diameter of 0.238125 cm and were 30.48 cm long. The 90 niobium rods filled all 90 rod locations shown in Figure 3.4-3.

Polyethylene Rods

The polyethylene rods had a diameter of 0.317 cm and were 30.5 cm long. The 8 polyethylene rods were in location43, 45, 47, 49, 51, 53, 55, and 57 in Figure 3.4-3.

Graphite Rods

The graphite rods had a diameter of 0.3048 cm and were 30.5 cm long. The 23 graphite rods filled all the locations as shown in Figure 3.4-5. Other potential arrangements of the 46 rods were evaluated in Section 2.4.2 and are included in the experimental uncertainty.

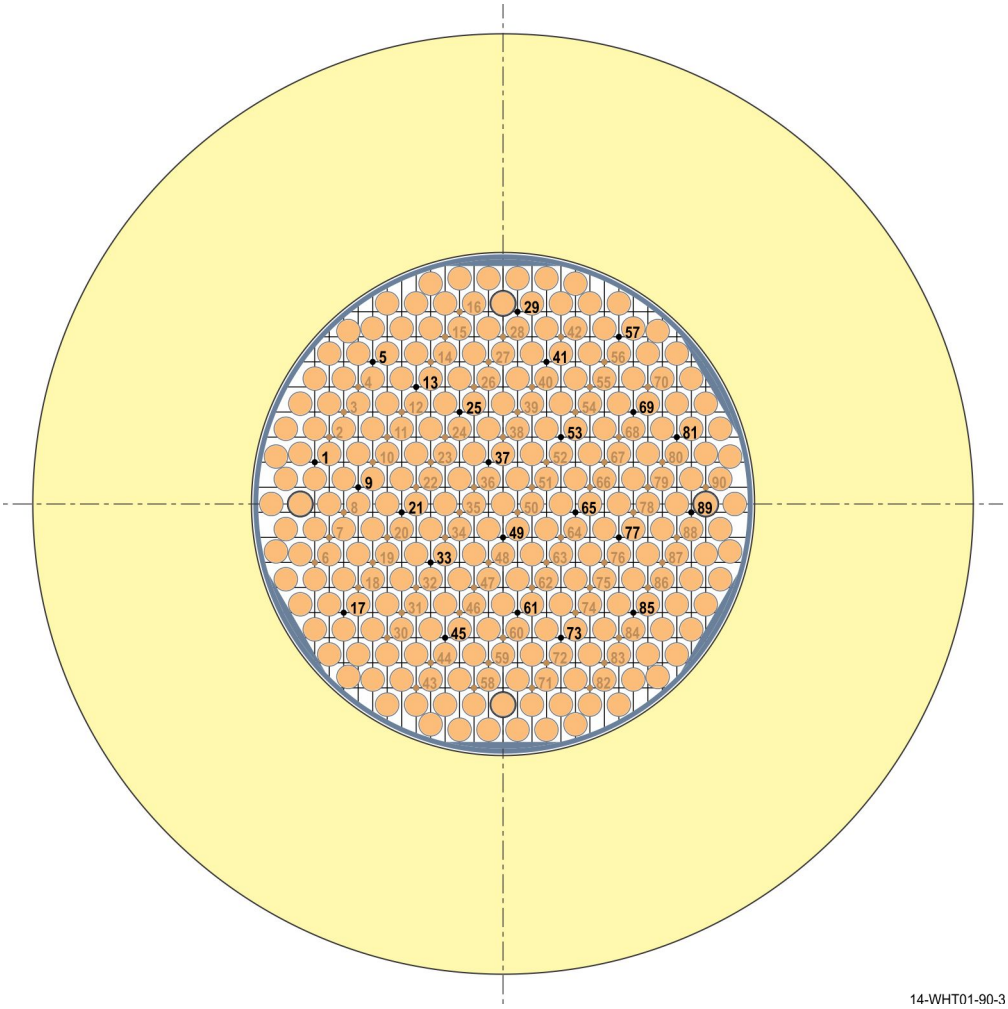

Figure 3.4-5. Location 23 Rod Positions.

B_4C Tube

The B_4C tube was an empty fuel tube fill with B_4C. The dimensions of the fuel tube are given in Figure 3.1-1 and Section 3.2 of HEU-COMP-FAST-004. The volume which the B_4C occupied had a diameter of 1.168 cm and length of 29.88 cm. The center fuel tube was removed and replaced with an empty tube. The tube was then filled B_4C and the change in reactivity between the empty tube and the filled tube represents the worth of the B_4C.

Stainless Steel Lid

The stainless steel lid had a diameter of 25.452 cm and was 0.3175 cm thick. The lid sat inside the core tank and sat on the fuel tubes. The lid was thick enough that it extended into the space above the core tank but did not interfere with the interface of the side reflector and top reflector. A generalized lid is shown in Figure 3.4-6.

Aluminum Lids

The aluminum lids had a diameter of 25.452 cm and were 0.3175 cm and 0.15875 cm thick. The lids sat inside the core tank and sat on the fuel tubes. The 0.3175-cm-thick lid was thick enough that it extended into the space above the core tank but did not interfere with the interface of the side reflector and top reflector. A generalized lid is shown in Figure 3.4-6.

Cadmium Lid

The cadmium lid had a diameter of 25.452 cm and was 0.066 cm thick. The lid sat inside the core tank and sat on the fuel tubes. A generalized lid is shown in Figure 3.4-6.

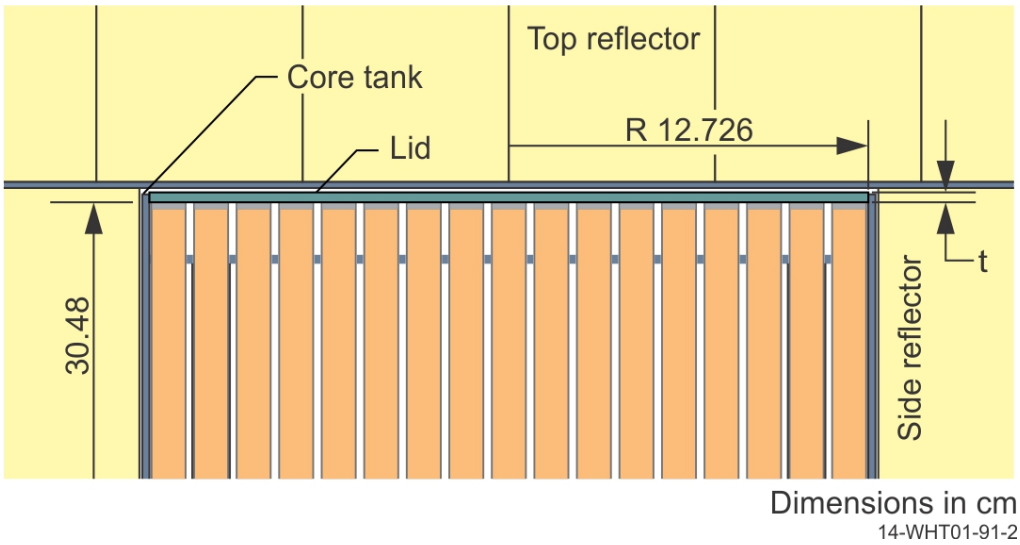

Figure 3.4-6. Diagram of Lid Sitting Atop of Fuel Tubes.

3.4.3 Material Data

The reactivity effect measurements were not evaluated

3.4.3.1 Fuel Effect Reactivity Measurements

The materials for the fuel effect measurements were identical to those in the critical benchmark model. See Section 3.3 of HEU-COMP-FAST-004.

3.4.3.2 Neutron Absorbing and Moderating Material Reactivity Measurements

The materials for the assembly were identical to those in the critical benchmark model. See Section 3.3 of HEU-COMP-FAST-004. The materials for the neutron absorbing and moderating materials are given below. For most materials the detailed and simple benchmark model materials are identical except for tungsten, niobium, graphite, and cadmium. Standard compositions are given in Section 2.4.2.

Table 3.4-3. Rod and Lid Composition.

Element	90 and 46 Stainless Steel 347 Rods (ρ=7.865 g/cm^3)	Stainless Steel Lid (ρ=7.986 g/cm^3)
Fe	5.8286E-02	5.9178E-02
C	1.5774E-04	1.6016E-04
Mn	8.6217E-04	8.7536E-04
Si	8.4325E-04	8.5615E-04
Cr	1.6397E-02	1.6648E-02
Ni	8.8776E-03	9.0134E-03
P	3.4408E-05	3.4934E-05
S	2.2154E-05	2.2493E-05
Nb	3.2816E-04	3.3318E-04
Ta	1.4743E-05	1.4969E-05
Total	8.58236E-02	8.71365E-02

Table 3.4-4. Tungsten Composition.

Element	Detailed Benchmark Model (ρ=19.055 g/cm^3)	Simple Benchmark Model (ρ=19.0519 g/cm^3)[(a)]
W	6.24055E-02	6.24055E-02
K	2.93499E-06	-
Cr	2.20696E-06	-
Ni	2.54181E-05	-
Cu	1.80583E-06	-
Fe	4.10955E-06	-
Total	6.24419E-02	6.24055E-02

(a) For the simple benchmark model, the density is reduced because impurities are removed.

Table 3.4-5. Niobium Composition.

Element	Detailed Benchmark Model (ρ=8.595 g/cm^3)	Simple Benchmark Model (ρ=8.5909 g/cm^3)[(a)]
Nb	5.56856E-02	5.56856E-02
Fe	2.78036E-06	-
Ni	4.40946E-06	-
Si	1.84288E-06	-
Sn	1.09002E-06	-
Ta	8.58119E-06	-
W	7.03811E-07	
Total	5.57050E-02	5.56856E-02

(a) For the simple benchmark model, the density is reduced because impurities are removed.

Table 3.4-6. Polyethylene Composition.

Element	Polyethylene Composition (ρ=0.957 g/cm^3)	
C	85.63 wt.%	4.10658E-02
H	14.37 wt.%	8.21317E-02
Total	5.57050E-02	

Table 3.4-7. Graphite Composition.

Element	Detailed Benchmark Model (ρ=1.603 g/cm^3)	Simple Benchmark Model (ρ=1.5943 g/cm^3)[(a)]
C	7.9936E-02	7.9936E-02
Al	9.6604E-06	-
Ba	1.5466E-07	-
B	4.4648E-08	-
Ca	1.9752E-05	-
Co	4.9143E-08	-
Cr	2.9706E-07	-
Cu	1.5192E-08	-
Fe	6.8108E-05	-
K	1.2346E-07	-
Li	2.7817E-07	-
Lu	5.5175E-09	-
Mg	3.9719E-08	-
Mn	1.7572E-08	-
Mo	5.0312E-08	-
Na	1.2598E-07	-
Ni	4.4412E-07	-
Si	1.8561E-06	-
Sr	5.5089E-08	-
Ti	1.0888E-06	-
V	4.1692E-06	-
Y	1.1944E-07	-
Total	6.1368E-08	7.9936E-02

(a) For the simple benchmark model, the density is reduced because impurities are removed.

Table 3.4-8. B_4C Composition.

Element	Boron Carbide Composition (ρ=0.953 g/cm^3)	
B	78.263 wt.%	4.15317E-02
C	21.737 wt.%	1.03829E-02
Total	5.19147E-02	

Table 3.4-9. Aluminum Composition.

Element	0.3175-cm-Thick Aluminum Plate (ρ=2.87 g/cm^3)	0.15875-cm-Thick Aluminum Plate (ρ=2.80 g/cm^3)
Al	6.36768E-02	6.20300E-02
Cu	3.40260E-05	3.31460E-05
Si	1.46275E-04	1.42492E-04
Fe	7.33543E-05	7.14572E-05
Mn	7.87147E-06	7.66789E-06
Zn	1.32266E-05	1.28845E-05
Total	6.39515E-02	6.22976E-02

Table 3.4-10. Cadmium Composition.

Element	Detailed Benchmark Model (ρ=8.457 g/cm^3)	Simple Benchmark Model (ρ=8.548 g/cm^3)[(a)]
Cd	4.57871E-02	4.57871E-02
Cu	4.04980E-09	
Fe	9.21621E-09	
Pb	4.96812E-08	
Mg	6.35299E-07	
Al	3.81519E-08	-
Si	3.66522E-08	-
Ag	2.38577E-09	-
Ti	2.14995E-08	-
Bi	7.38870E-08	-
Ca	1.28424E-08	
Total	4.57880E-02	4.57871E-02

(a) For the simple benchmark model, the density is reduced because impurities are removed.

3.4.4 Temperature Data

The temperature is the same as for the critical configuration, 72°F (22°C).[a]

3.4.5 Experimental and Benchmark-Model Reactivity Effect Parameters

3.4.5.1 Fuel Effect Reactivity Measurements

The benchmark values for the fuel effect reactivity measurements are found by applying the biases in Table 3.4-1to the experimental results. The uncertainty in the benchmark model is found by adding in quadrature the uncertainty in the experimental results, discussed in Section 2.4, and the bias uncertainty given in Table 3.4-1. The benchmark results, in units of cents, are given in Table 3.4-11.

[a] Personal email communication with J. T. Mihalczo, May 23, 2011.

Table 3.4-11. Benchmark Fuel Effect Reactivity.

Distance from Core Center (Fuel Tube Position)	Detailed Benchmark Model Value (¢)			Simple Benchmark Model Value (¢)		
0 cm (1)	-32.00	±	5.014	-32.00	±	5.015
2.59 cm (2)	-32.00	±	5.014	-32.00	±	5.015
5.23 cm (3)	-30.80	±	4.861	-30.80	±	4.862
7.75 cm (4)	-27.20	±	4.411	-27.20	±	4.387
10.48 cm (5)	-25.50	±	4.203	-25.50	±	4.203
10.56 cm (6)	-25.60	±	4.215	-25.60	±	4.216
11.78 cm (7)	-22.60	±	3.828	-22.60	±	3.857
Accident Configuration Worth	-8.20	±	2.448	-8.20	±	2.450

3.4.5.2 Neutron Absorbing and Moderating Material Reactivity Measurements

The benchmark values for the material reactivity measurements are found by applying the biases in Table 3.4-2to the experimental results. The uncertainty in the benchmark model is found by adding in quadrature the uncertainty in the experimental results, discussed in Section 2.4, and the bias uncertainty given in Table 3.4-2. The benchmark results, in units of cents, are given in Table 3.4-12.

Table 3.4-12. Benchmark Material Reactivity.

Absorbing or Moderating Material	Detailed Benchmark Model Value (¢)			Simple Benchmark Model Value (¢)		
90 Stainless Steel 347 Rods	14.80	±	2.675	14.80	±	2.676
46 Stainless Steel 347 Rods	7.92	±	2.467	7.92	±	2.469
46 Tungsten Rods	-4.27	±	1.776	-4.27	±	1.837
90 Niobium Rods	4.90	±	1.802	4.90	±	1.804
8 Polyethylene Rods	24.43	±	3.841	24.43	±	3.842
23 Graphite Rods	7.50	±	1.997	7.50	±	1.999
B_4C Filled Tube	-6.65	±	1.919	-6.65	±	1.921
Stainless Steel Lid	7.97	±	2.162	7.97	±	2.164
0.3175 cm Thick Al Lid	16.62	±	3.121	16.62	±	3.122
0.315875 cm Thick Al Lid	8.14	±	2.353	8.14	±	2.355
Cadmium Lid	-45.70	±	6.659	-45.70	±	6.659

3.5 Benchmark-Model Specifications for Reactivity Coefficient Measurements

Reactivity coefficient measurements were not evaluated.

3.6 Benchmark-Model Specifications for Kinetics Measurements

Kinetics measurements were not performed.

3.7 Benchmark-Model Specifications for Reaction-Rate Distribution Measurements

3.7.1 Description of the Benchmark-Model Simplifications

The simple and detailed benchmark models are the same as the Case 1 simple and detailed benchmark models for the critical configuration described in HEU-COMP-FAST-004. The total simplification biases for the detailed and simple benchmark models were calculated and are given in Table 3.3-1.[a] Biases arising from individual simplifications were not calculated. A bias in the foil activation measurements is considered negligible if it is less than the statistical uncertainty of the Monte Carlo calculation. For biases that are negligible, the bias uncertainty is preserved; as can be seen in Table 3.7-1.

It should be noted that the foils that were placed on top of the fuel tubes sat inside the end cap wells. In the detailed and simple benchmark models, these wells were not included but rather the mass was homogenized over the total end cap volume. This shifted the position of the foils measurements up by approximately 0.249 cm. The effect of the change in measurement position and the homogenization of the end cap is included in the detailed and simple benchmark model biases. All given modified foil locations correspond to the foils on top of the fuel tubes, not in the end-cap well.

Foil activation measurements were evaluated using explicit modeling of the foils and calculated neutron fluxes over the foil volume and a multiplier for the ^{235}U fission cross section.

[a] These biases and simplifications are described in HEU-COMP-FAST-004 and include: room return and air effects; temperature bias; use of nominal diameters for top and bottom reflectors; removal of shims; removal of grid plates and grid plate spacer tubes; grid plate and end cap simplification effect; simplification of the fuel tube; homogenization of the fuel; removal of fuel impurities; and removal of side, top, and bottom reflector impurities.

Table 3.7-1. Simplification Bias of Foil Activation.

Foil[a]		Given Location (cm)[b]	Modified Location (cm)[c]	Detailed Benchmark Model Simplification Bias			Simple Benchmark Model Simplification Bias		
Axial Foil Activation Distribution									
1	H	-2.54	-2.54	0.012	±	0.003	NEG	±	0.003
2	H	0	0.00	NEG	±	0.003	NEG	±	0.003
3	H	2.54	2.54	NEG	±	0.003	-0.009	±	0.003
4	H	5.08	5.08	NEG	±	0.003	NEG	±	0.003
5	H	7.62	7.62	NEG	±	0.003	NEG	±	0.003
6	H	10.16	10.16	NEG	±	0.003	NEG	±	0.003
7	H	12.7	12.70	NEG	±	0.003	-0.009	±	0.003
8	H	15.44	15.24	0.043	±	0.005	0.155	±	0.005
9	H	15.91	15.915	-0.007	±	0.005	0.071	±	0.005
10	H	17.18	17.185	0.018	±	0.008	0.064	±	0.008
11	H	18.45	18.455	0.014	±	0.009	0.036	±	0.009
12	H	19.72	19.725	-0.013	±	0.008	0.059	±	0.008
13	H	20.99	20.995	-0.090	±	0.007	-0.025	±	0.007
14	H	22.26	22.265	-0.054	±	0.004	-0.006	±	0.004
Radial Foil Activation Distribution at Core Midplane									
16	R	3.25	3.243	0.022	±	0.003	-0.004	±	0.003
17	R	5.87	5.852	0.007	±	0.003	-0.004	±	0.003
18	R	8.53	8.460	-0.008	±	0.003	-0.008	±	0.003
19	R	9.93	9.907	NEG	±	0.004	-0.008	±	0.004
20	R	10.74	10.735	NEG	±	0.004	NEG	±	0.004
21	R	11.12	11.127	-0.006	±	0.004	NEG	±	0.004
22	R	11.2	11.177	0.009	±	0.005	0.022	±	0.005
23	R	11.35	11.413	0.022	±	0.005	0.008	±	0.005
24	R	12.06	12.005	NEG	±	0.012	0.061	±	0.012
25	R	12.47	12.397	-0.035	±	0.014	0.000	±	0.014
26	R	12.62	12.589	0.086	±	0.014	0.124	±	0.014
Foil Activation Distribution at 15.24 cm Above Core Midplane[d]									
28	R	3.02	3.02	0.044	±	0.005	0.145	±	0.006
29	R	12.06	12.06	0.273	±	0.009	0.512	±	0.009

(a) These foil numbers were assigned by the evaluator. Foil number 27 and 15 are skipped because these foils were duplicates of Foil 2 and 8, respectively.
(b) Locations were given as axial distance from the center of the fuel tube, height (H), or radial distance from the core center, radius (R).
(c) Many of the foil locations were modified so that the foil was in a feasible location, i.e. not floating in air or in the middle of a solid mass of material.
(d) This height was given as 15.44 cm but was modified so foils lay on top of the fuel tubes and not 0.2 cm above them.

3.7.2 Dimensions

The simple and detailed benchmark models for the foil activation measurements are the same as the Case 1 benchmark models for the critical configurations given in HEU-COMP-FAST-004 (see Section 3.2.1 for dimensions). Figure 3-7.1 shows the locations for the foils. These locations have been adjusted, as described in Section 2.3 and 2.7, from the given locations. The uranium foil locations are the same for the simple and detailed benchmark models. (Figure 3-7.1 shows the detailed benchmark model.) The location shown in Figure 3-7.1 is the bottom center of the foils for horizontal foils and the center of the foil touching the fuel tube for vertical foils.

For both the detailed and simple benchmark models, the uranium foils are 0.75-cm in diameter and 0.01-cm thick.

3.7.3 Material Data

The material data for the simple and detailed benchmark model for the foil activation measurements are the same as the material data for the Case 1 benchmark models for the critical configuration (see HEU-COMP-FAST-004, Section 3.3.1).

For the simple and detailed benchmark models, the uranium foils have a density of 18.75 g/cm^3 (see Section 2.3). The composition is given in Table 3.7-2.

Table 3.7-2. Uranium Metal Foil Composition.

Element	wt.%	Isotopic enrichment	Atoms/barn-cm
U Total	99.95 wt%[(a)]	-	4.7983E-02
^{234}U	-	0.97 wt%	4.6775E-04
^{235}U	-	93.14 wt%	4.4722E-02
^{236}U	-	0.24 wt%	1.1475E-04
^{238}U	-	5.65 wt%	2.6786E-03

(a) The total weight percent is reduced because impurities were replaced with void.

3.7.4 Temperature Data

The temperature is the same as for the critical configuration, 72°F (22°C).[a]

3.7.5 Experimental and Benchmark-Model Reaction Rate Measurements

The benchmark values for the foil activations are found by applying the biases in Table 3.7-1 to the experimental results. The uncertainty in the benchmark model is found by adding, in quadrature, the uncertainty in the experimental results, discussed in Section 2.7, and the bias uncertainty given in Table 3.7-1. The benchmark results are given in Table 3.7-3.

[a] Personal email communication with J. T. Mihalczo, May 23, 2011.

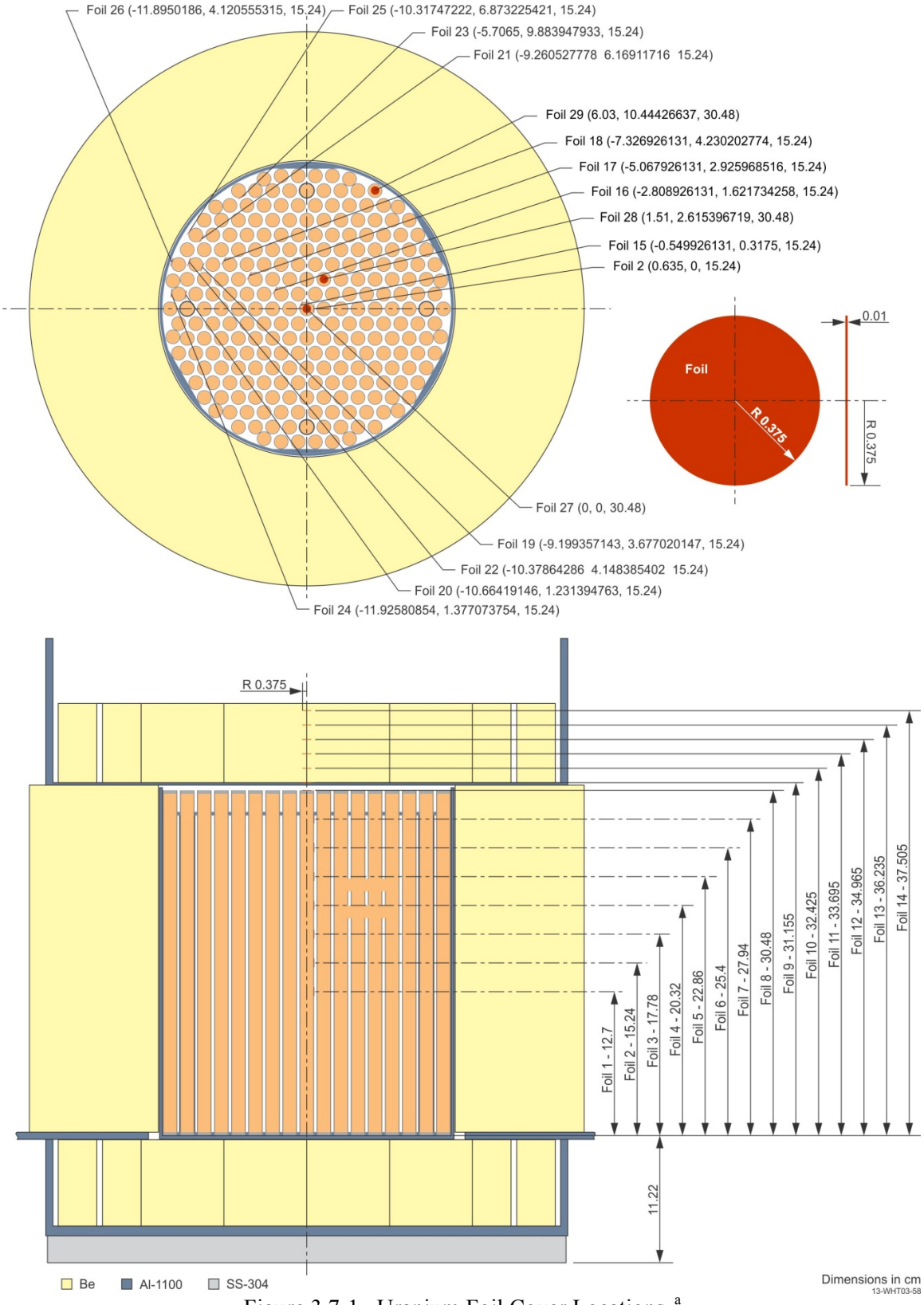

Figure 3.7-1. Uranium Foil Cover Locations. [a]

[a] The foils in the upper reflector are oriented horizontally. The foils at a height of 30.48 cm are horizontally position foils on the top of the fuel tubes. The foils at a height of 15.24) are vertically positions tangent to the side of the fuel tubes. The axial fuel tubes on the center fuel tube are oriented vertically. With sufficient magnification, it can be seen that all foils are explicitly modeled in Figure 3.7-1.

Table 3.7-3. Benchmark Relative Foil Activation.

Foil[(a)]		Given Location (cm)[(b)]	Modified Location (cm)[(c)]	Detailed Benchmark Model Value			Simple Benchmark Model Value		
Axial Foil Activation Distribution									
1	H	-2.54	-2.54	1.032	±	0.029	1.020	±	0.029
2	H	0	0.00	1.000	±	0.019	1.000	±	0.019
3	H	2.54	2.54	1.000	±	0.028	0.991	±	0.028
4	H	5.08	5.08	0.950	±	0.026	0.950	±	0.026
5	H	7.62	7.62	0.910	±	0.024	0.910	±	0.024
6	H	10.16	10.16	0.830	±	0.023	0.830	±	0.023
7	H	12.7	12.70	0.880	±	0.024	0.871	±	0.024
8	H	15.44	15.24	1.553	±	0.041	1.665	±	0.041
9	H	15.91	15.915	1.553	±	0.097	1.631	±	0.097
10	H	17.18	17.185	2.228	±	0.094	2.274	±	0.094
11	H	18.45	18.455	2.544	±	0.101	2.566	±	0.101
12	H	19.72	19.725	2.437	±	0.071	2.509	±	0.071
13	H	20.99	20.995	1.910	±	0.063	1.975	±	0.063
14	H	22.26	22.265	1.146	±	0.093	1.194	±	0.093
Radial Foil Activation Distribution at Core Midplane									
16	R	3.25	3.243	1.002	±	0.027	0.976	±	0.027
17	R	5.87	5.852	0.997	±	0.028	0.986	±	0.028
18	R	8.53	8.460	1.032	±	0.030	1.032	±	0.030
19	R	9.93	9.907	1.060	±	0.036	1.052	±	0.036
20	R	10.74	10.735	1.120	±	0.034	1.120	±	0.034
21	R	11.12	11.127	1.204	±	0.043	1.210	±	0.043
22	R	11.2	11.177	1.559	±	0.053	1.572	±	0.053
23	R	11.35	11.413	1.472	±	0.166	1.458	±	0.166
24	R	12.06	12.005	3.040	±	0.212	3.101	±	0.212
25	R	12.47	12.397	3.645	±	0.162	3.680	±	0.162
26	R	12.62	12.589	3.646	±	0.096	3.684	±	0.096
Foil Activation Distribution at 15.24 cm Above Core Midplane[(d)]									
28	R	3.02	3.02	1.674	±	0.046	1.775	±	0.046
29	R	12.06	12.06	2.773	±	0.133	3.012	±	0.133

(a) These foil numbers were assigned by the evaluator. Foil number 27 and 15 are skipped because these foils were duplicates of Foil 2 and 8, respectively.
(b) Locations were given as axial distance from the center of the fuel tube, height (H), or radial distance from the core center, radius (R).
(c) Many of the foil locations were modified so that the foil was in a feasible location, i.e. not floating in air or in the middle of a solid mass of material.
(d) This height was given as 15.44 cm but was modified so foils lay on top of fuel tube and not 0.2 cm above them.

3.8 Benchmark-Model Specifications for Power Distribution Measurements

The relative power distribution is related to the relative fission rate that was measured in the core region of Assembly 1.

3.9 Benchmark-Model Specifications for Isotopic Measurements

Isotopic measurements were not performed.

3.10 Benchmark-Model Specifications for Other Miscellaneous Types of Measurements

Other miscellaneous types of measurements were not performed.

4.0 RESULTS OF SAMPLE CALCULATIONS

4.1 Results of Calculations of the Critical or Subcritical Configurations

(The criticality portion of this evaluation has been reviewed and approved by the International Criticality Safety Benchmark Evaluation Project (ICSBEP) and has been published under the following identifier: HEU-COMP-FAST-004.[a])

4.2 Results of Buckling and Extrapolation Length Calculations

Buckling and extrapolation-length measurements were not performed.

4.3 Results of Spectral-Characteristics Calculations

The cadmium ratios were calculated using a model as described in Section 3.3 with MCNP5-1.60 and ENDF/B-VII.0 neutron cross section libraries. Foils and covers were explicitly modeled and tallies were taken in the foil cells. Tally multipliers were also used. A total of 2,000 cycles were run, skipping the first 150 cycles, with 1,000,000 histories per cycle. Seven different random numbers were used for each calculation. The variance-weighted average of the seven tally results was taken for the calculated distributions. The tally for the bare and covered foils was divided to find the cadmium ratio. Sample calculation results are given in Table 4.3-1 and 4.3.2. The calculated results agree well with the benchmark results and are all within 3σ. The cadmium ratios in the upper reflector are plotted in Figures 4.3-1 and 4.3-2.

[a] International Handbook of Evaluated Criticality Safety Benchmark Experiments, NEA/NSC/DOC(95)03, OECD-NEA, Paris (2012).

Table 4.3-1. Sample Results for Cadmium Ratio Detailed Benchmark Model.

Cadmium Ratio											
Cd Ratio	Given Location (cm)[a]		Modified Location (cm)[b]	Detailed Benchmark Model Value			Detailed Calculated Value			(C-E)/E [c]	C/E Ratio[c]
Distribution in Top Beryllium Reflector											
1	H	15.91	15.915	1.370	±	0.027	1.358	±	0.015	-0.89%	0.99
2	H	17.18	17.185	1.560	±	0.029	1.557	±	0.018	-0.18%	1.00
3	H	18.45	18.455	1.655	±	0.031	1.669	±	0.019	0.83%	1.01
4	H	19.72	19.725	1.667	±	0.033	1.758	±	0.021	5.47%	1.05
5	H	20.99	20.995	1.970	±	0.038	1.856	±	0.025	-5.79%	0.94
6	H	22.26	22.265	1.970	±	0.049	1.870	±	0.032	-5.07%	0.95
Cadmium Ratio at Core Midplane											
7	R	11.35	11.413	1.240	±	0.083	1.185	±	0.010	-4.42%	0.96
Distribution at 15.24 cm Above Core Midplane[d]											
8	R	3.02	3.02	1.390	±	0.023	1.363	±	0.014	-1.96%	0.98
9	R	12.06	12.06	2.082	±	0.040	2.063	±	0.024	-0.89%	0.99

(a) Locations were given as axial distance from the center of the fuel tube, height (H), or radial distance from the core center, radius (R).
(b) Many of the foil locations were modified so that the foil was in a feasible location, i.e. not floating in air or in the middle of a solid mass of material.
(c) "E" is the expected or benchmark value. "C" is the calculated value.
(d) This height was given as 15.44 cm but was modified so foils lay on top of the fuel tubes and not 0.2 cm above them.

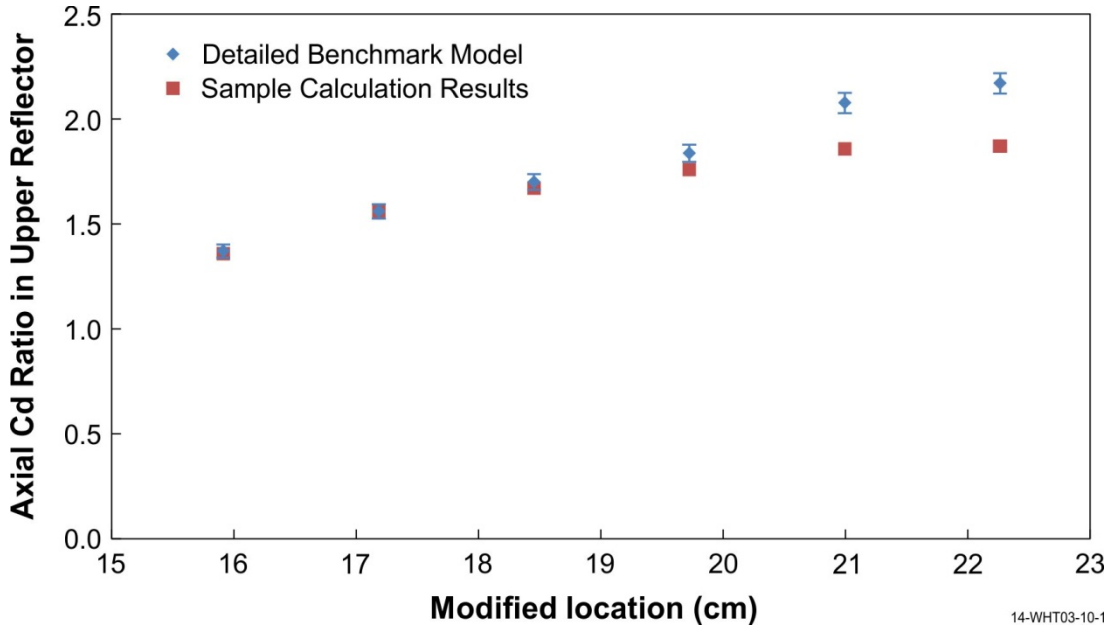

Figure 4.3-1. Benchmark and Calculated Results for Cadmium Ratio in Upper Reflector for Detailed Benchmark Model.

Table 4.3-2. Sample Results for Cadmium Ratio Simple Benchmark Model.

Cadmium Ratio				Effect							
Cd Ratio	Given Location (cm)[a]		Modified Location (cm)[b]	Simple Benchmark Model Value			Simple Calculated Value			(C-E)/E [c]	C/E Ratio[c]
Distribution in Top Beryllium Reflector											
1	H	15.91	15.915	1.370	±	0.028	1.375	±	0.015	0.40%	1.00
2	H	17.18	17.185	1.640	±	0.030	1.624	±	0.019	-0.98%	0.99
3	H	18.45	18.455	1.700	±	0.031	1.738	±	0.020	2.23%	1.02
4	H	19.72	19.725	1.721	±	0.034	1.813	±	0.022	5.30%	1.05
5	H	20.99	20.995	1.970	±	0.038	1.872	±	0.025	-4.99%	0.95
6	H	22.26	22.265	1.977	±	0.050	1.877	±	0.034	-5.05%	0.95
Cadmium Ratio at Core Midplane											
7	R	11.35	11.413	1.240	±	0.083	1.190	±	0.010	-4.02%	0.96
Distribution at 15.24 cm Above Core Midplane[d]											
8	R	3.02	3.02	1.475	±	0.025	1.466	±	0.017	-0.63%	0.99
9	R	12.06	12.06	2.123	±	0.040	2.104	±	0.024	-0.88%	0.99

(a) Locations were given as axial distance from the center of the fuel tube, or height (H), radial distance from the core center, radius (R).
(b) Many of the foil locations were modified so that the foil was in a feasible location, i.e. not floating in air or in the middle of a solid mass of material.
(c) "E" is the expected or benchmark value. "C" is the calculated value.
(d) This height was given as 15.44 cm but was modified so foils lay on top of the fuel tubes and not 0.2 cm above them.

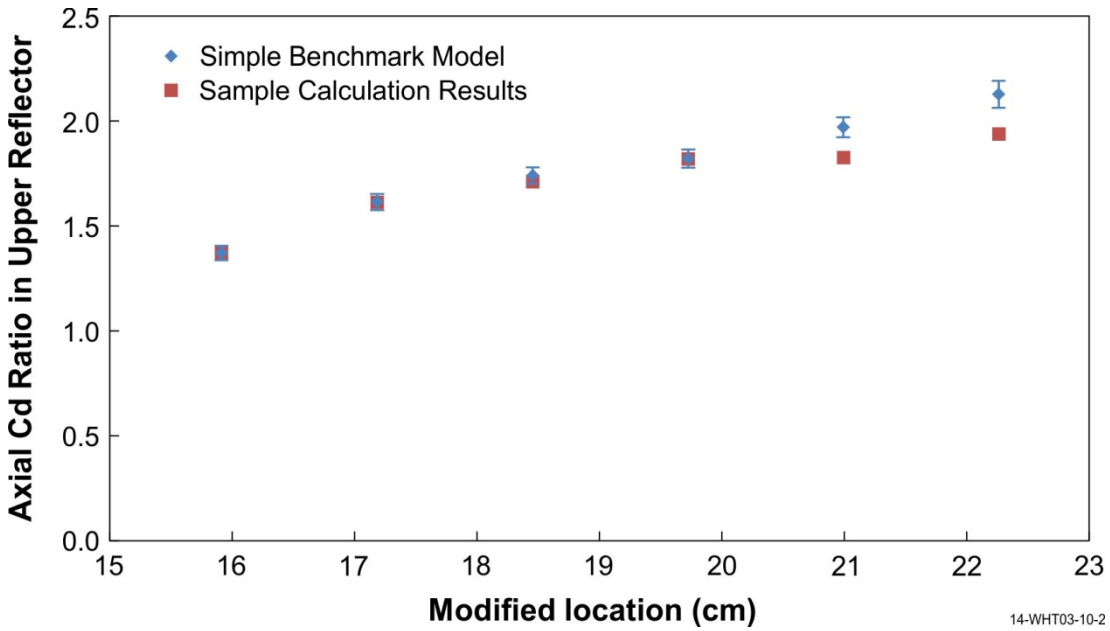

Figure 4.3-2. Benchmark and Calculated Results for Cadmium Ratio in Upper Reflector for Simple Benchmark Model.

4.4 Results of Reactivity-Effects Calculations

The worths were calculated using models, as described in Section 3.4, with MCNP5-1.60 and ENDF/B-VII.0 neutron cross section libraries. For each run, a total of 2,150 cycles were run, skipping the first 150 cycles, with 100,000 histories per cycle. For each reactivity effect measurement the base and perturbed benchmark model eigenvalues were calculated. The change in eigenvalues was then converted to a reactivity in units of cents using β_{eff}, 0.0073± 5% (HEU-COMP-FAST-004, Section 2.1). The fuel effect reactivity calculations are presented in Table 4.4-1 and Table 4.4-2. The calculations agree well with the benchmark results. The material worth calculates are presented in Table 4.4-3 and Table 4.4-4. Some calculated results have a large deviation from the benchmark. This cause for this deviation is not known; however, all results are within 3σ of the benchmark value.

Table 4.4-1. Calculation Results for Fuel Effect Reactivity.

Distance from Core Center (Fuel Tube Position)	Detailed Benchmark Model Value (¢)	Calculated Reactivity (¢)	(C-E)/E [(a)]	C/E Ratio[(a)]
0 cm (1)	-32.00 ± 5.014	-31.67 ± 1.18	-1.0% ± 15.9%	0.99
2.59 cm (2)	-32.00 ± 5.014	-30.14 ± 1.18	-5.8% ± 15.2%	0.94
5.23 cm (3)	-30.80 ± 4.861	-28.47 ± 1.18	-7.6% ± 15.1%	0.92
7.75 cm (4)	-27.20 ± 4.411	-27.21 ± 1.18	0.0% ± 16.8%	1.00
10.48 cm (5)	-25.50 ± 4.203	-24.57 ± 1.18	-3.6% ± 16.5%	0.96
10.56 cm (6)	-25.60 ± 4.215	-23.18 ± 1.18	-9.5% ± 15.6%	0.91
11.78 cm (7)	-22.60 ± 3.828	-20.40 ± 1.08	-9.7% ± 16.0%	0.90
Accident Configuration Worth	-8.20 ± 2.448	-8.04 ± 1.18	-1.9% ± 32.6%	0.98

(a) "E" is the experimental benchmark value. "C" is the calculated value.

Table 4.4-2. Calculation Results for Fuel Effect Reactivity.

Distance from Core Center (Fuel Tube Position)	Simple Benchmark Model Value (¢)	Calculated Reactivity (¢)	(C-E)/E [(a)]	C/E Ratio[(a)]
0 cm (1)	-32.00 ± 5.015	-31.20 ± 1.18	-2.5% ± 15.7%	0.97
2.59 cm (2)	-32.00 ± 5.015	-31.75 ± 1.18	-0.8% ± 16.0%	0.99
5.23 cm (3)	-30.80 ± 4.862	-29.52 ± 1.18	-4.2% ± 15.6%	0.96
7.75 cm (4)	-27.20 ± 4.387	-27.29 ± 1.09	0.3% ± 16.7%	1.00
10.48 cm (5)	-25.50 ± 4.203	-24.50 ± 1.18	-3.9% ± 16.5%	0.96
10.56 cm (6)	-25.60 ± 4.216	-25.06 ± 1.18	-2.1% ± 16.8%	0.98
11.78 cm (7)	-22.60 ± 3.857	-22.69 ± 1.18	0.4% ± 17.9%	1.00
Accident Configuration Worth	-8.20 ± 2.450	-7.79 ± 1.18	-5.1% ± 31.8%	0.95

(a) "E" is the experimental benchmark value. "C" is the calculated value.

Table 4.4-3. Calculation Results for Material Reactivity.

Absorbing or Moderating Material	Detailed Benchmark Model Value (¢)	Calculated Reactivity (¢)	(C-E)/E [(a)]	C/E Ratio[(a)]
90 Stainless Steel 347 Rods	14.80 ± 2.675	21.44 ± 1.18	44.9% ± 27.4%	1.45
46 Stainless Steel 347 Rods	7.92 ± 2.467	8.45 ± 1.18	6.7% ± 36.4%	1.07
46 Tungsten Rods	-4.27 ± 1.776	-1.11 ± 1.08	-74.0% ± 27.6%	0.26
90 Niobium Rods	4.90 ± 1.802	8.45 ± 1.18	72.4% ± 67.8%	1.72
8 Polyethylene Rods	24.43 ± 3.841	22.83 ± 1.18	-6.6% ± 15.5%	0.93
23 Graphite Rods	7.50 ± 1.997	7.76 ± 1.18	3.4% ± 31.7%	1.03
B_4C Filled Tube	-6.65 ± 1.919	-8.22 ± 1.18	23.6% ± 39.8%	1.24
Stainless Steel Lid	7.97 ± 2.162	9.83 ± 1.18	23.4% ± 36.6%	1.23
0.3175 cm Thick Al Lid	16.62 ± 3.121	19.65 ± 1.18	18.2% ± 23.3%	1.18
0.315875 cm Thick Al Lid	8.14 ± 2.353	8.86 ± 1.18	8.9% ± 34.6%	1.09
Cadmium Lid	-45.70 ± 6.659	-31.94 ± 1.18	-30.1% ± 10.5%	0.70

(a) "E" is the experimental benchmark value. "C" is the calculated value.

Table 4.4-4. Calculation Results for Material Reactivity.

Absorbing or Moderating Material	Simple Benchmark Model Value (¢)	Calculated Reactivity (¢)	(C-E)/E [(a)]	C/E Ratio[(a)]
90 Stainless Steel 347 Rods	14.80 ± 2.676	19.15 ± 1.18	29.4% ± 24.7%	1.29
46 Stainless Steel 347 Rods	7.92 ± 2.469	10.00 ± 1.18	26.2% ± 42.1%	1.26
46 Tungsten Rods	-4.27 ± 1.837	-2.92 ± 1.18	-31.6% ± 40.4%	0.68
90 Niobium Rods	4.90 ± 1.804	9.58 ± 1.18	95.5% ± 75.9%	1.96
8 Polyethylene Rods	24.43 ± 3.842	22.06 ± 1.18	-9.7% ± 15.0%	0.90
23 Graphite Rods	7.50 ± 1.999	7.64 ± 1.18	1.8% ± 31.4%	1.02
B_4C Filled Tube	-6.65 ± 1.921	-8.38 ± 1.19	26.0% ± 40.6%	1.26
Stainless Steel Lid	7.97 ± 2.164	9.03 ± 1.18	13.3% ± 34.1%	1.13
0.3175 cm Thick Al Lid	16.62 ± 3.122	18.18 ± 1.18	9.4% ± 21.7%	1.09
0.315875 cm Thick Al Lid	8.14 ± 2.355	9.16 ± 1.18	12.6% ± 35.6%	1.13
Cadmium Lid	-45.70 ± 6.659	-34.83 ± 1.18	-23.8% ± 11.4%	0.76

(a) "E" is the experimental benchmark value. "C" is the calculated value.

4.4.2 Neutron Absorbing and Moderating Material Reactivity Measurements

The reactivity effect measurements were not evaluated

4.5 Results of Reactivity Coefficient Calculations

Reactivity coefficient measurements were not evaluated.

4.6 Results of Kinetics Parameter Calculations

Kinetics measurements were not performed.

4.7 Results of Reaction-Rate Distribution Calculations

The relative foil activations were calculated using a model as described in Section 3.7 with MCNP5-1.60 and ENDF/B-VII.0 neutron cross section libraries. Foils were explicitly modeled and tallies were taken in the foil cells. Tally multipliers were also used. A total of 2,000 cycles were run, skipping the first 150 cycles, with 1,000,000 histories per cycle. Seven different random numbers were used for each calculation. The variance weighted average of the seven tally results was taken for the calculated distributions. The tallies for the foils were normalized. Sample calculation results are given in Table 4.7-1 and 4.7.2 and shown in Figures 4.7-1 through 4.7-4. All sample calculation results are within 3σ of the benchmark value except Foil 26 at the edge of the core midplane, which is 5.6σ high. It is not known why the sample calculation and benchmark model deviate at the peak of the radial flux at the edge of the core midplane. It is interesting to note that the calculated results for the foil that does not match the curve in Figure 1.7-2 (labeled as Foil 8 in Figure 1.7-2) are nearly identical for the simple and detailed benchmark models (see Figure 4.7-2 and 4.7-4). This leads one to believe that the data point is not an outlier, but that foil activity depends on more than just radial position but also factors such as foil position in relation to surrounding fuel tubes (see Figure 1.4-2, foil location 7 vs. 8 vs. 9).

Table 4.7-1. Sample Results for Detailed Benchmark Model Foil Activation Measurements.

Foil[a]		Given Location (cm)[b]	Modified Location (cm)[c]	Detailed Benchmark Model Value	Sample Calculation Results	(C-E)/E [d]	C/E Ratio [d]
Axial Foil Activation Distribution							
1	H	-2.54	-2.54	1.032 ± 0.029	1.008 ± 0.003	-2.33%	0.98
2	H	0	0.00	1.000 ± 0.019	1.000 ± 0.002	0.00%	1.00
3	H	2.54	2.54	1.000 ± 0.028	0.986 ± 0.002	-1.36%	0.99
4	H	5.08	5.08	0.950 ± 0.026	0.954 ± 0.002	0.43%	1.00
5	H	7.62	7.62	0.910 ± 0.024	0.912 ± 0.002	0.17%	1.00
6	H	10.16	10.16	0.830 ± 0.023	0.874 ± 0.002	5.34%	1.05
7	H	12.7	12.70	0.880 ± 0.024	0.880 ± 0.002	-0.03%	1.00
8	H	15.44	15.24	1.553 ± 0.041	1.538 ± 0.004	-0.94%	0.99
9	H	15.91	15.915	1.553 ± 0.097	1.548 ± 0.004	-0.34%	1.00
10	H	17.18	17.185	2.228 ± 0.094	2.249 ± 0.006	0.94%	1.01
11	H	18.45	18.455	2.544 ± 0.101	2.572 ± 0.006	1.10%	1.01
12	H	19.72	19.725	2.437 ± 0.071	2.434 ± 0.006	-0.13%	1.00
13	H	20.99	20.995	1.910 ± 0.063	1.941 ± 0.005	1.61%	1.02
14	H	22.26	22.265	1.146 ± 0.093	1.170 ± 0.003	2.03%	1.02
Radial Foil Activation Distribution at Core Midplane							
16	R	3.25	3.243	1.002 ± 0.027	1.010 ± 0.003	0.72%	1.01
17	R	5.87	5.852	0.997 ± 0.028	0.990 ± 0.002	-0.78%	0.99
18	R	8.53	8.460	1.032 ± 0.030	1.001 ± 0.002	-3.02%	0.97
19	R	9.93	9.907	1.060 ± 0.036	1.046 ± 0.003	-1.35%	0.99
20	R	10.74	10.735	1.120 ± 0.034	1.099 ± 0.003	-1.90%	0.98
21	R	11.12	11.127	1.204 ± 0.043	1.142 ± 0.003	-5.09%	0.95
22	R	11.2	11.177	1.559 ± 0.053	1.547 ± 0.004	-0.81%	0.99
23	R	11.35	11.413	1.472 ± 0.166	1.438 ± 0.004	-2.32%	0.98
24	R	12.06	12.005	3.040 ± 0.212	3.392 ± 0.008	11.59%	1.12
25	R	12.47	12.397	3.645 ± 0.162	3.977 ± 0.010	9.10%	1.09
26	R	12.62	12.589	3.646 ± 0.096	4.075 ± 0.010	11.77%	1.12
Foil Activation Distribution at 15.24 cm Above Core Midplane[e]							
28	R	3.02	3.02	1.674 ± 0.046	1.609 ± 0.004	-3.92%	0.96
29	R	12.06	12.06	2.773 ± 0.133	2.760 ± 0.007	-0.45%	1.00

(a) These foil numbers were assigned by the evaluator. Foil number 27 and 15 are skipped because these foils were duplicates of foil 2 and 8, respectively.
(b) Locations were given as axial distance from the center of the fuel tube, height (H), or radial distance from the core center, radius (R).
(c) Many of the foil locations were modified so that the foil was in a feasible location, i.e. not floating in air or in the middle of a solid mass of material.
(d) "E" is the expected or benchmark value. "C" is the calculated value.
(e) This height was given as 15.44 cm but was modified so foils lay on top of fuel tube and not 0.2 cm above them.

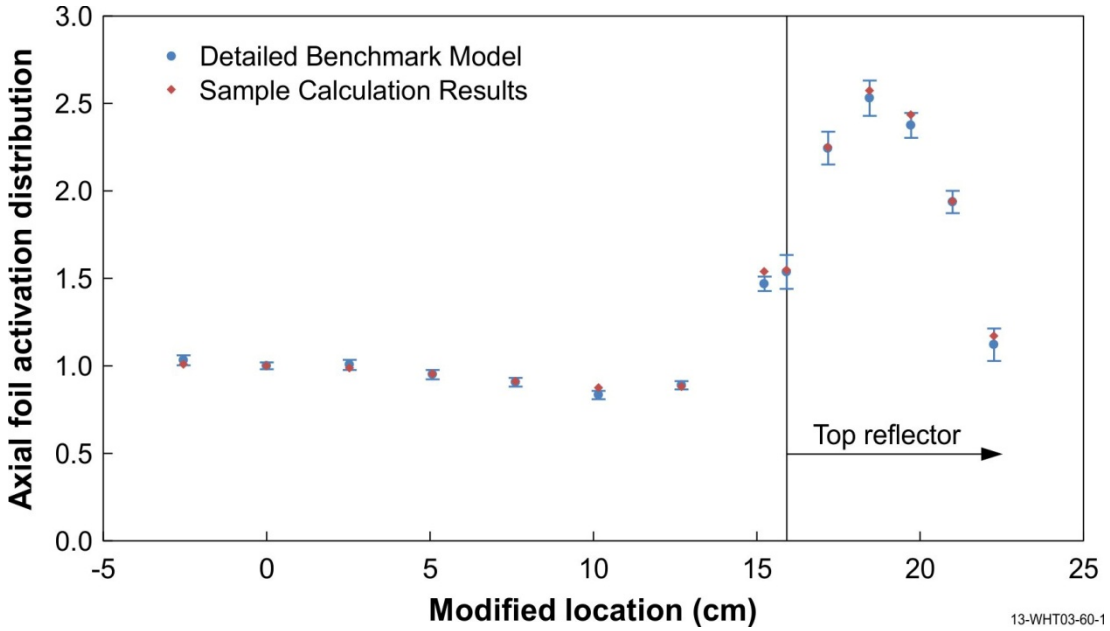

Figure 4.7-1. Benchmark and Calculated Results for Axial Foil Distribution for Detailed Benchmark Model.

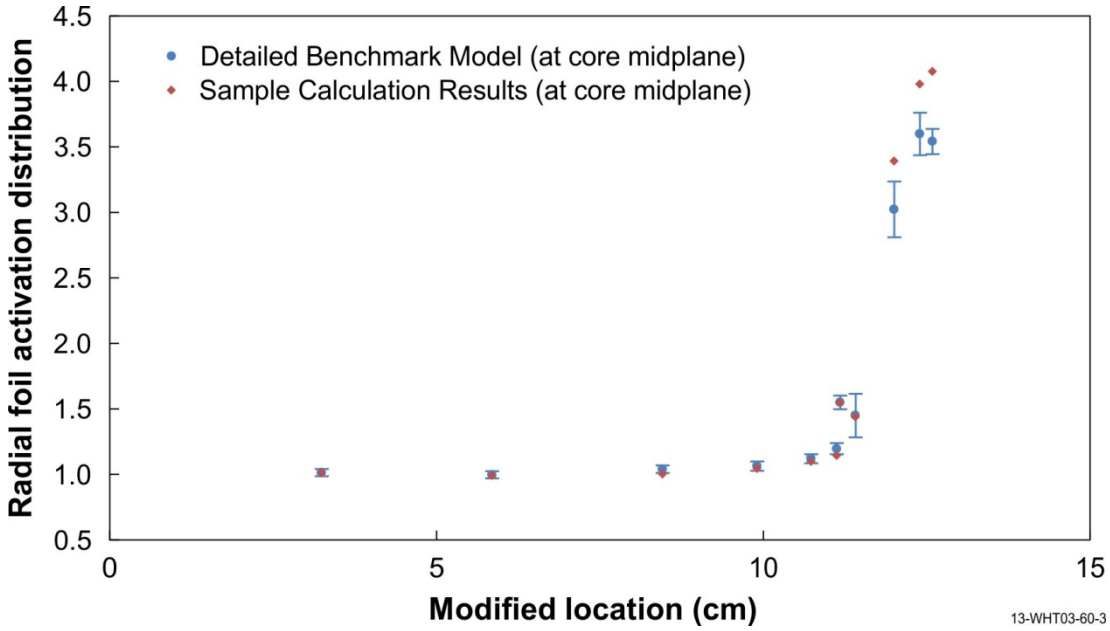

Figure 4.7-2. Benchmark and Calculated Results for Radial Foil Distribution for Detailed Model.

Table 4.7-2. Sample Results for Simple Benchmark Model Foil Activation Measurements.

Foil[a]		Given Location (cm)[b]	Modified Location (cm)[c]	Simple Benchmark Model Value			Sample Calculation Results			(C-E)/E [d]	C/E Ratio[d]
Axial Foil Activation Distribution											
1	H	-2.54	-2.54	1.020	±	0.029	0.995	±	0.002	-2.47%	0.98
2	H	0	0.00	1.000	±	0.019	1.000	±	0.002	0.00%	1.00
3	H	2.54	2.54	0.991	±	0.028	0.980	±	0.002	-1.18%	0.99
4	H	5.08	5.08	0.950	±	0.026	0.953	±	0.002	0.35%	1.00
5	H	7.62	7.62	0.910	±	0.024	0.916	±	0.002	0.63%	1.01
6	H	10.16	10.16	0.830	±	0.023	0.873	±	0.002	5.14%	1.05
7	H	12.7	12.70	0.871	±	0.024	0.872	±	0.002	0.13%	1.00
8	H	15.44	15.24	1.665	±	0.041	1.650	±	0.004	-0.88%	0.99
9	H	15.91	15.915	1.631	±	0.097	1.626	±	0.004	-0.32%	1.00
10	H	17.18	17.185	2.274	±	0.094	2.296	±	0.006	0.92%	1.01
11	H	18.45	18.455	2.566	±	0.101	2.594	±	0.006	1.09%	1.01
12	H	19.72	19.725	2.509	±	0.071	2.506	±	0.006	-0.13%	1.00
13	H	20.99	20.995	1.975	±	0.063	2.006	±	0.005	1.56%	1.02
14	H	22.26	22.265	1.194	±	0.093	1.218	±	0.003	1.95%	1.02
Radial Foil Activation Distribution at Core Midplane											
16	R	3.25	3.243	0.976	±	0.027	0.983	±	0.002	0.74%	1.01
17	R	5.87	5.852	0.986	±	0.028	0.978	±	0.002	-0.79%	0.99
18	R	8.53	8.460	1.032	±	0.030	1.001	±	0.002	-3.02%	0.97
19	R	9.93	9.907	1.052	±	0.036	1.040	±	0.003	-1.16%	0.99
20	R	10.74	10.735	1.120	±	0.034	1.100	±	0.003	-1.77%	0.98
21	R	11.12	11.127	1.210	±	0.043	1.150	±	0.003	-4.94%	0.95
22	R	11.2	11.177	1.572	±	0.053	1.559	±	0.004	-0.80%	0.99
23	R	11.35	11.413	1.458	±	0.166	1.424	±	0.004	-2.34%	0.98
24	R	12.06	12.005	3.101	±	0.212	3.454	±	0.009	11.38%	1.11
25	R	12.47	12.397	3.680	±	0.162	4.001	±	0.010	8.72%	1.09
26	R	12.62	12.589	3.684	±	0.096	4.113	±	0.010	11.64%	1.12
Foil Activation Distribution at 15.24 cm Above Core Midplane[e]											
28	R	3.02	3.02	1.775	±	0.046	1.709	±	0.004	-3.70%	0.96
29	R	12.06	12.06	3.012	±	0.133	3.000	±	0.007	-0.42%	1.00

(a) These foil numbers were assigned by the evaluator. Foil number 27 and 15 are skipped because these foils were duplicates of foil 2 and 8, respectively.
(b) Locations were given as axial distance from the center of the fuel tube, height (H), radial distance from the core center, or radius (R).
(c) Many of the foil locations were modified so that the foil was in a feasible location, i.e. not floating in air or in the middle of a solid mass of material.
(d) "E" is the expected or benchmark value. "C" is the calculated value.
(e) This height was given as 15.44 cm but was modified so foils lay on top of fuel tube and not 0.2 cm above them.

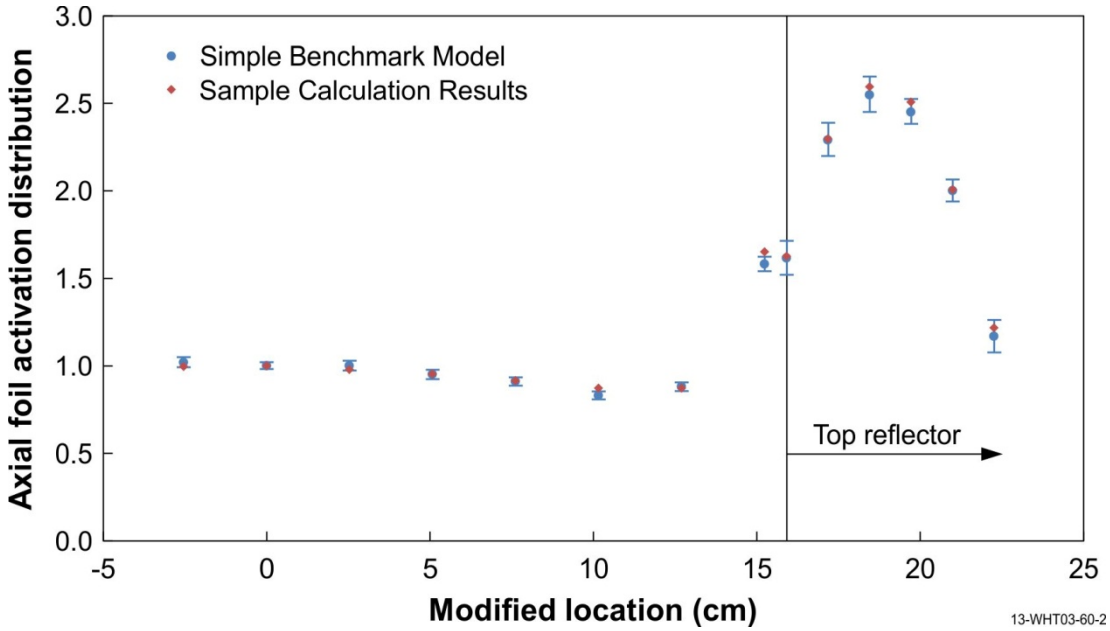

Figure 4.7-3. Benchmark and Calculated Results for Axial Foil Distribution for Simple Benchmark Model.

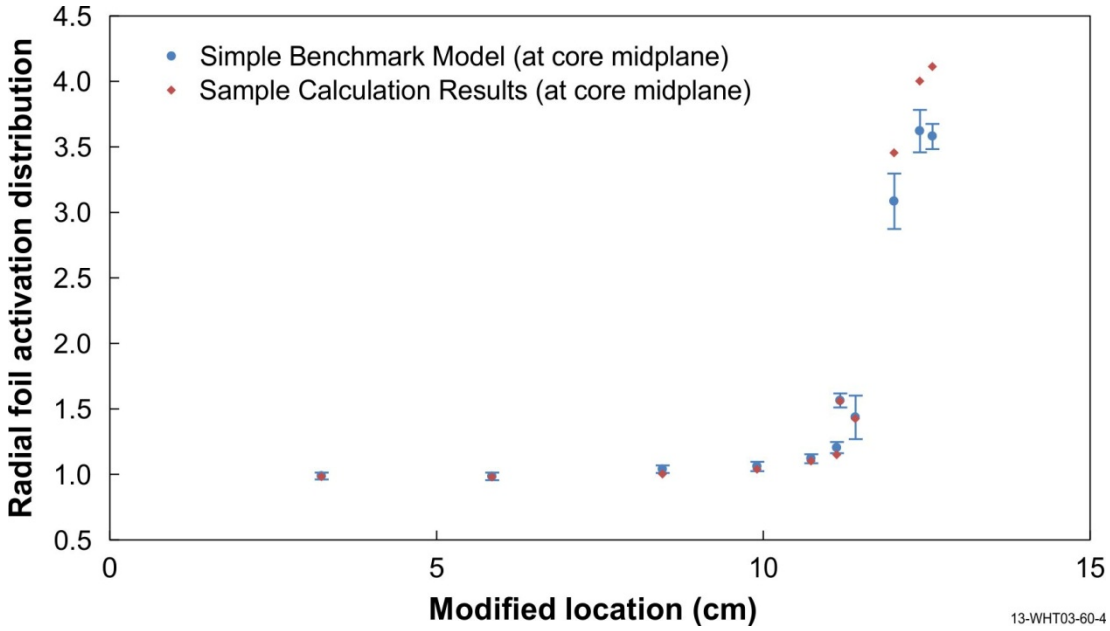

Figure 4.7-4. Benchmark and Calculated Results for Radial Foil Distribution for Simple Benchmark Model.

4.8 Results of Power Distribution Calculations

The relative power distribution is the same as the relative fission rate as was measured in the core region of Assembly 1.

4.9 Results of Isotopic Calculations

Isotopic measurements were not performed.

4.10 Results of Calculations for Other Miscellaneous Types of Measurements

Other miscellaneous types of measurements were not performed.

5.0 REFERENCES

1. J.T. Mihalczo, "A Small Graphite-Reflected UO_2 Critical Assembly," ORNL-TM-450, Oak Ridge National Laboratory (1962).

2. J.T. Mihalczo, "A Small Graphite-Reflected UO_2 Assembly," *Proc. 5th Int. Conf. Nucl. Crit. Safety*, Albuquerque, NM, September 17-21 (1995).

3. J.T. Mihalczo, "A Small Graphite-Reflected UO2 Critical Assembly, Part II," ORNL-TM-561, Oak Ridge National Laboratory (1963).

4. J.T. Mihalczo, "A Small Beryllium-Reflected UO2 Assembly," ORNL-TM-655, Oak Ridge National Laboratory (1963).

5. J.T. Mihalczo, "A Small, Beryllium-Reflected UO_2 Critical Assembly," *Trans. Am. Nucl. Soc.,* **72**, 196-198 (1995).

APPENDIX A: COMPUTER CODES, CROSS SECTIONS, AND TYPICAL INPUT LISTINGS

A.1 Critical/Subcritical Configurations

(The criticality portion of this evaluation has been reviewed and approved by the International Criticality Safety Benchmark Evaluation Project (ICSBEP) and has been published under the following identifier: HEU-COMP-FAST-004[a].)

A.2 Buckling and Extrapolation Length Configurations

Buckling and extrapolation-length measurements were not performed.

A.3 Spectral-Characteristics Configurations

Models were creating using Monte Carlo n-Particle (MCNP), Version 5-1.60, and ENDF/B-VII.0 neutron cross section libraries. Isotopic abundances for all elements except uranium (see Section 3.3.3 for uranium isotopic abundances) were taken from "Nuclides and Isotopes: Chart of the Nuclides," Sixteenth Edition, KAPL, 2002.

A.3.1 Name(s) of Code System(s) Used

1. Monte Carlo n-Particle, Version 5.1.60 (MCNP5).

A.3.2 Bibliographic References for the Codes Used

1. F. B. Brown, R. F. Barrett, T. E. Booth, J. S. Bull, L. J. Cox, R. A. Forster, T. J. Goorley, R. D. Mosteller, S. E. Post, R. E. Prael, E. C. Selcow, A. Sood, and J. Sweezy, "MCNP Version 5," LA-UR-02-3935, Los Alamos National Laboratory (2002).

A.3.3 Origin of Cross-section Data

The evaluated neutron data file library ENDF/B-VII.0[b] was utilized in the benchmark-model analysis.

A.3.4 Spectral Calculations and Data Reduction Methods Used

Not applicable.

A.3.5 Number of Energy Groups or If Continuous-energy Cross Sections are Used in the Different Phases of Calculation

1. Continuous-energy cross sections.

2. Continuous-energy cross sections.

---

[a] International Handbook of Evaluated Criticality Safety Benchmark Experiments, NEA/NSC/DOC(95)03, OECD-NEA, Paris (2012).

[b] M. B. Chadwick, et al., "ENDF/B-VII.0: Next Generation Evaluated Nuclear Data Library for Nuclear Science and Technology," *Nucl. Data Sheets*, **107**: 2931-3060 (2006).

A.3.6 Component Calculations

- Type of cell calculation – reactor core and reflectors
- Geometry – fuel pin and assembly lattice
- Theory used – Not applicable
- Method used – Monte Carlo
- Calculation characteristics
  - MCNP5 – histories/cycles/cycles skipped = 1,000,000/2,000/150 continuous-energy cross sections

A.3.7 Other Assumptions and Characteristics

Not applicable.

A.3.8 Typical Input Listings for Each Code System Type

The input deck for only the simple benchmark model was provided. The input lines for the uranium foils and cadmium covers are identical in the detailed benchmark model. An input deck for the detailed benchmark model of the system is available in HEU-COMP-FAST-004.

MCNP5 Input Deck for Cadmium Ratio Benchmark Models:

Bare Foils

```
SCCA-FUND-EXP-002-001 and HEU-COMP-FAST-002
C
C
C   Cell Cards
1   1  6.54398E-02  (-25 22 -24) u=11 imp:n=1         $fuel pellet
2   0      -22:(25 22 -24 ):24 u=11 imp:n=1  $void around pellet
4   0    -21 22 -23  fill=11 u=12 imp:n=1
C
C  BASIC FUEL TUBE W/ GRID PLATE
15   15 7.50555E-02 (1 -24 -20 21) u=12 imp:n=1  $Fuel tube
16   15 7.50555E-02 (1 -22 -21):(23 -24 -21) u=12 imp:n=1  $end caps
21   0    -1:20:24 u=12 imp:n=1
C     BASIC FUEL TUBES FOR TUBES WHICH ARE MOVED IN
22  0    -21 22 -23  fill=11 u=13 imp:n=1
23   15 7.50555E-02 (21) u=13 imp:n=1  $Fuel tube
24   15 7.50555E-02 (-22 -21):(23 -21) u=13 imp:n=1  $end caps
C   BASIC FUEL TUBES
40  0   -12 fill=12 u=1 imp:n=1
C   FUEL TUBES WHICH ARE MOVED IN
41  0   -13 fill=13 (-3.766 -11.458 0) imp:n=1
42  0   -14 fill=13 (3.766 -11.458 0) imp:n=1
43  0   -15 fill=13 (3.766 11.458 0) imp:n=1
44  0   -16 fill=13 (-3.766 11.458 0) imp:n=1
45  0   -17 fill=13 (-8.039 -8.989 0) imp:n=1
46  0   -18 fill=13 (8.039 -8.989 0) imp:n=1
47  0   -19 fill=13 (-8.039 8.989 0) imp:n=1
48  0   -30 fill=13 (8.039 8.989 0) imp:n=1
49  0   -31 fill=13 (-11.805 -2.467 0) imp:n=1
50  0   -32 fill=13 (11.805 -2.467 0) imp:n=1
51  0   -33 fill=13 (-11.805 2.467 0) imp:n=1
52  0   -34 fill=13 (11.805 2.467 0) imp:n=1
C
C  VOID
```

```
62  0  -999  u=9 imp:n=1
C   Core Assembly
68  0   -11  lat=2  u=2 imp:n=1 fill= -10:10 -10:10 0:0
     9 9 9 9 9 9 9 9 9 9 9 9 9 9 9 9 9 9 9 9 9  $ROW 1
       9 9 9 9 9 9 9 9 9 9 9 9 9 1 1 1 1 9 9 9 9  $ROW 2
        9 9 9 9 9 9 9 9 9 9 1 1 1 1 1 1 1 1 9 9  $ROW 3
         9 9 9 9 9 9 9 9 9 1 1 1 1 1 1 1 1 1 9 9  $ROW 4
          9 9 9 9 9 9 9 9 1 1 1 1 1 1 1 1 1 1 1 9  $ROW 5
           9 9 9 9 9 9 9 1 1 1 1 1 1 1 1 1 1 1 1 9  $ROW 6
            9 9 9 9 9 9 1 1 1 1 1 1 1 1 1 1 1 1 1 9  $ROW 7
             9 9 9 9 9 1 1 1 1 1 1 1 1 1 1 1 1 1 1 9  $ROW 8
              9 9 9 9 1 1 1 1 1 1 1 1 1 1 1 1 1 9 9  $ROW 9
               9 9 9 1 1 1 1 1 1 1 1 1 1 1 1 1 1 9 9  $ROW 10
                9 9 1 1 1 1 1 1 1 1 1 1 1 1 1 1 1 9 9  $ROW 11
                 9 9 1 1 1 1 1 1 1 1 1 1 1 1 1 1 1 9 9 9  $ROW 12
                  9 9 1 1 1 1 1 1 1 1 1 1 1 1 1 1 1 9 9 9 9  $ROW 13
                   9 1 1 1 1 1 1 1 1 1 1 1 1 1 1 1 9 9 9 9  $ROW 14
                    9 1 1 1 1 1 1 1 1 1 1 1 1 1 1 1 9 9 9 9 9  $ROW 15
                     9 1 1 1 1 1 1 1 1 1 1 1 1 1 1 9 9 9 9 9 9  $ROW 16
                      9 1 1 1 1 1 1 1 1 1 1 1 1 1 9 9 9 9 9 9 9  $ROW 17
                       9 9 1 1 1 1 1 1 1 1 1 1 1 9 9 9 9 9 9 9 9  $ROW 18
                        9 9 1 1 1 1 1 1 1 1 1 1 9 9 9 9 9 9 9 9 9  $ROW 19
                         9 9 9 9 1 1 1 1 1 9 9 9 9 9 9 9 9 9 9 9  $ROW 20
                          9 9 9 9 9 9 9 9 9 9 9 9 9 9 9 9 9 9 9 9  $ROW 21
C   Core Tank
70  0 -51 1 -53 13 14 15 16 17 18 19 30 31 32 33 34 706 707 708 fill=2 imp:n=1
74  2 5.88014E-02 (-53 1 -50 51):(-1 52 -50) imp:n=1 $Core Tank
C
C  Reflectors
C  Void Universe
99   0  -999  u=19 imp:n=1
C  Top Reflector
100  8  1.20554E-01 301 -57 -302 700 701 702 703 704 705 imp:n=1
102  0  302 -57 -303  imp:n=1
103  13 7.07826E-02 (301 -303 57 -58):(300 -301 -58) imp:n=1
196  0 -999 300 (58):(-999 303) imp:n=1
C  Bottom Reflector
300  10 1.20636E-01 -57 -304 305  imp:n=1
301  14 6.72481E-02 (57 -58 -304 305):(-305 306 -58) imp:n=1
307  0   58 -304 306 -999 imp:n=1
C   Side Reflector
320  9 1.21199E-01  320 -321 322 -323 imp:n=1
321   0  -300 53 -320 imp:n=1
322   0  -53 50 -320 322 imp:n=1
323   0  -322 50 -326 304 imp:n=1
324   0 -300 52 321 325 -999 imp:n=1
325   0 -306 327 -999 imp:n=1
C  Support Structure/Additional Reflectors
350  30 6.08580E-02 -325 326 imp:n=1 $Support Plate for Be
351  31 8.75101E-02 -327 imp:n=1 $SS304 Plate
C
700 50 4.79835E-02 -700 imp:n=1
701 50 4.79835E-02 -701 imp:n=1
702 50 4.79835E-02 -702 imp:n=1
703 50 4.79835E-02 -703 imp:n=1
704 50 4.79835E-02 -704 imp:n=1
705 50 4.79835E-02 -705 imp:n=1
C
706 50 4.79835E-02 -706 imp:n=1
707 50 4.79835E-02 -707 imp:n=1
708 50 4.79835E-02 -708 imp:n=1
C
999  0  999 imp:n=0

C   Surface Cards
1    pz   0.      $bottom of fuel
11   rhp  0 0 -10  0 0 50   0.753 0 0
12   rhp  0 0 -11  0 0 52   1 0 0
13   rcc  -3.766 -11.458 0  0 0 30.48  0.635
14   rcc  3.766 -11.458 0  0 0 30.48  0.635
15   rcc  3.766 11.458 0  0 0 30.48  0.635
16   rcc  -3.766 11.458 0  0 0 30.48  0.635
17   rcc  -8.039 -8.989 0  0 0 30.48  0.635
18   rcc  8.039 -8.989 0  0 0 30.48  0.635
19   rcc  -8.039 8.989 0  0 0 30.48  0.635
20   cz   0.635   $OR Clad
```

```
21   cz   0.584   $IR Clad
22   pz   0.3     $top of bottom cap
23   pz  30.18    $bottom of top cap
24   pz  30.48    $Top of fuel tube
25   cz   0.5705  $OR of Pellet
30   rcc  8.039 8.989 0  0 0 30.48  0.635
31   rcc  -11.805 -2.467 0  0 0 30.48  0.635
32   rcc  11.805 -2.467 0  0 0 30.48  0.635
33   rcc  -11.805 2.467 0  0 0 30.48  0.635
34   rcc  11.805 2.467 0  0 0 30.48  0.635
C  Core Tank
50  cz  12.98  $OR Core Tank
51  cz  12.726 $IR Core Tank
52  pz  -0.33   $Bottom of Core Tank
53  pz  30.71  $Top of Core Tank
C  simple model to preflector
57   cz 20.65   $Ir upper and lower tank
58   cz 21.285 $OR upper and lower tank
C
300    pz  30.935
301    pz  31.155
302    pz 38.14
303    pz  43.885
C
304    pz -0.33
305    pz -7.95
306    pz -8.84
C   Side Reflector
320    cz  13.08
321    cz  24.45
322    pz 0.305
323    pz 30.935
C
C    Be Support Plate
325  rpp -37.5 37.5  -37.5 37.5  -0.33 0.305
326  cz  13.95
C    SS304 Plate
327  rcc 0. 0. -11.22  0. 0. 2.38  22.86
C
700  rcc  0  0  31.155  0  0  0.01  0.375
701  rcc  0  0  32.425  0  0  0.01  0.375
702  rcc  0  0  33.695  0  0  0.01  0.375
703  rcc  0  0  34.965  0  0  0.01  0.375
704  rcc  0  0  36.235  0  0  0.01  0.375
705  rcc  0  0  37.505  0  0  0.01  0.375
C
706 rcc -5.7065 9.883947933 15.24  0.005 -0.008660254 0  0.375
C
707 rcc 1.51  2.615396719  30.48  0  0  0.01  0.375
708 rcc 6.03  10.44426637  30.48  0  0  0.01  0.375
C
999   rpp  -500 500   -500 500  -500 500

C   Data Cards
m1   92234.70c   2.21403E-04
      92235.70c   2.03324E-02
      92236.70c   1.02154E-04
      92238.70c   1.15733E-03
      8016.70c   4.35205E-02
      8017.70c   1.06012E-04   $ Tot   6.54398E-02
C   Fuel Clad
m15   26054.70c   2.97938E-03
      26056.70c   4.67699E-02
      26057.70c   1.08012E-03
      26058.70c   1.43744E-04
      6000.70c   1.37950E-04
      25055.70c   7.53997E-04
      14028.70c   6.80144E-04
      14029.70c   3.45361E-05
      14030.70c   2.27664E-05
      24050.70c   6.23067E-04
      24052.70c   1.20152E-02
      24053.70c   1.36243E-03
      24054.70c   3.39138E-04
      28058.70c   5.28531E-03
      28060.70c   2.03589E-03
```

```
      28061.70c   8.84989E-05
      28062.70c   2.82173E-04
      28064.70c   7.18612E-05
      15031.70c   3.00906E-05
      16032.70c   1.83924E-05
      16033.70c   1.47248E-07
      16034.70c   8.31174E-07
      16036.70c   3.87494E-09
      41093.70c   2.86989E-04
      73181.70c   1.28933E-05   $tot   7.50555E-02
C   Core Tank
m2   13027.70c   5.85485E-02
      29063.70c   2.16403E-05
      29065.70c   9.64537E-06
      14028.70c   1.24044E-04
      14029.70c   6.29865E-06
      14030.70c   4.15212E-06
      26054.70c   3.95341E-06
      26056.70c   6.20601E-05
      26057.70c   1.43324E-06
      26058.70c   1.90738E-07
      25055.70c   7.23754E-06
      30000.70c   1.21614E-05   $ Tot   5.88014E-02
C   Reflectors
C  ************************************
C  Top Reflector
m8   4009.70c   1.20554E-01
C   Side Reflector
m9   4009.70c   1.21199E-01
C   Bottom Reflector
m10   4009.70c   1.20636E-01
C    ************************************
C  Upper reflector tank
m13   13027.70c   7.04918E-02
      29063.70c   2.60429E-05
      29065.70c   1.16077E-05
      14028.70c   1.49280E-04
      14029.70c   7.58007E-06
      14030.70c   4.99684E-06
      26054.70c   4.75770E-06
      26056.70c   7.46858E-05
      26057.70c   1.72482E-06
      25055.70c   8.70996E-06
      30000.70c   1.46355E-06   $ Tot   7.07826E-02
C  lower reflector tank
m14   13027.70c   6.69718E-02
      29063.70c   2.47424E-05
      29065.70c   1.10280E-05
      14028.70c   1.41826E-04
      14029.70c   7.20156E-06
      14030.70c   4.74732E-06
      26054.70c   4.52013E-06
      26056.70c   7.09564E-05
      26057.70c   1.63869E-06
      25055.70c   8.27504E-06
      30000.70c   1.39047E-06   $ Tot   6.72481E-02
C   ************************************
C  Additional Bottom Reflectors
C   Be Support Plate (Al1100)
m30   13027.70c   6.06080E-02
      29063.70c   2.23913E-05
      29065.70c   9.98012E-06
      14028.70c   1.28349E-04
      14029.70c   6.51725E-06
      14030.70c   4.29622E-06
      26054.70c   4.09062E-06
      26056.70c   6.42139E-05
      26057.70c   1.48298E-06
      25055.70c   7.48872E-06
      30000.70c   1.25834E-06   $ Tot   6.08580E-02
C   SS304 Support Plate
m31   26054.70c   3.51905E-03
      26056.70c   5.52415E-02
      26057.70c   1.27577E-03
      26058.70c   1.69781E-04
      6000.70c   1.60142E-04
```

```
      25055.70c   8.75287E-04
      14028.70c   7.89554E-04
      14029.70c   4.00916E-05
      14030.70c   2.64287E-05
      24050.70c   7.63478E-04
      24052.70c   1.47229E-02
      24053.70c   1.66946E-03
      24054.70c   4.15564E-04
      28058.70c   5.29886E-03
      28060.70c   2.04111E-03
      28061.70c   8.87257E-05
      28062.70c   2.82896E-04
      28064.70c   7.20454E-05
      15031.70c   3.49310E-05
      16032.70c   2.13510E-05
      16033.70c   1.70934E-07
      16034.70c   9.64879E-07
      16034.70c   4.49827E-09   $ tot   8.75101E-02
C    U Foils
m50   92234.70c   4.67753E-04
      92235.70c   4.47223E-02
      92236.70c   1.14750E-04
      92238.70c   2.67865E-03   $ total   4.79835E-02
C    Cd Covers
m55   48106.70c   5.79249E-04
      48108.70c   4.12425E-04
      48110.70c   5.78786E-03
      48111.70c   5.93151E-03
      48112.70c   1.11818E-02
      48113.70c   5.66274E-03
      48114.70c   1.33135E-02
      48116.70c   3.47086E-03   $ total   4.63399E-02
C   Scattering Cards
mt1   o2/u.10t  u/o2.10t
mt2    al27.12t
mt8   be.10t
mt9   be.10t
mt10  be.10t
mt13   al27.12t
mt14   al27.12t
mt20   al27.12t
mt22   al27.12t
C m23    al27.12t
mt30   al27.12t
C
kcode  100000 1 150 2150
ksrc   0.0692  4.5245 0.77787  0  8.8072 0.7787
       0.0692 -4.3864 0.77787  0 -8.7382 0.7787
       3.8736 0 0.7787   7.6780 0 0.7787
      -3.7353 0 0.7787  -7.8510 0 0.7787
f4:n  700
fm4   1 50 -6
C
f14:n   701
fm14   1 50 -6
C
f24:n   702
fm24   1 50 -6
C
f34:n   703
fm34   1 50 -6
C
f44:n   704
fm44   1 50 -6
C
f54:n  705
fm54   1 50 -6
C
f64:n   706
fm64   1 50 -6
c
f74:n   707
fm74   1 50 -6
C
f84:n   708
fm84   1 50 -6
```

```
C  rand  seed=7065399757867  $ r2
C  rand  seed=5724484131590  $ r3
C  rand  seed=417647895433   $ r4
C  rand  seed=8132049697893  $ r5
C  rand  seed=8663498807872  $ r6
C  rand  seed=7447087897166  $ r7
```

Cadmium Covered Foils

```
SCCA-FUND-EXP-002-001 and HEU-COMP-FAST-002
C
C
C   Cell Cards
1   1  6.54398E-02  (-25 22 -24) u=11 imp:n=1         $fuel pellet
2   0      -22:(25 22 -24 ):24 u=11 imp:n=1  $void around pellet
4   0    -21 22 -23  fill=11 u=12 imp:n=1
C
C  BASIC FUEL TUBE W/ GRID PLATE
15   15 7.50555E-02 (1 -24 -20 21) u=12 imp:n=1  $Fuel tube
16   15 7.50555E-02 (1 -22 -21):(23 -24 -21) u=12 imp:n=1  $end caps
21   0    -1:20:24 u=12 imp:n=1
C     BASIC FUEL TUBES FOR TUBES WHICH ARE MOVED IN
22  0    -21 22 -23  fill=11 u=13 imp:n=1
23   15 7.50555E-02 (21) u=13 imp:n=1  $Fuel tube
24   15 7.50555E-02 (-22 -21):(23 -21) u=13 imp:n=1  $end caps
C   BASIC FUEL TUBES
40  0   -12 fill=12 u=1 imp:n=1
C   FUEL TUBES WHICH ARE MOVED IN
41  0   -13 fill=13 (-3.766 -11.458 0) imp:n=1
42  0   -14 fill=13 (3.766 -11.458 0) imp:n=1
43  0   -15 fill=13 (3.766 11.458 0) imp:n=1
44  0   -16 fill=13 (-3.766 11.458 0) imp:n=1
45  0   -17 fill=13 (-8.039 -8.989 0) imp:n=1
46  0   -18 fill=13 (8.039 -8.989 0) imp:n=1
47  0   -19 fill=13 (-8.039 8.989 0) imp:n=1
48  0   -30 fill=13 (8.039 8.989 0) imp:n=1
49  0   -31 fill=13 (-11.805 -2.467 0) imp:n=1
50  0   -32 fill=13 (11.805 -2.467 0) imp:n=1
51  0   -33 fill=13 (-11.805 2.467 0) imp:n=1
52  0   -34 fill=13 (11.805 2.467 0) imp:n=1
C
C  VOID
62  0  -999  u=9 imp:n=1
C   Core Assembly
68  0   -11  lat=2  u=2 imp:n=1 fill= -10:10 -10:10 0:0
     9 9 9 9 9 9 9 9 9 9 9 9 9 9 9 9 9 9 9 9 9 9 9  $ROW 1
       9 9 9 9 9 9 9 9 9 9 9 9 9 1 1 1 1 9 9 9 9  $ROW 2
        9 9 9 9 9 9 9 9 9 9 1 1 1 1 1 1 1 1 1 9 9  $ROW 3
         9 9 9 9 9 9 9 9 9 1 1 1 1 1 1 1 1 1 1 9 9  $ROW 4
          9 9 9 9 9 9 9 9 1 1 1 1 1 1 1 1 1 1 1 9  $ROW 5
           9 9 9 9 9 9 9 1 1 1 1 1 1 1 1 1 1 1 1 9  $ROW 6
            9 9 9 9 9 9 1 1 1 1 1 1 1 1 1 1 1 1 1 9  $ROW 7
             9 9 9 9 1 1 1 1 1 1 1 1 1 1 1 1 1 1 1 9  $ROW 8
              9 9 9 9 1 1 1 1 1 1 1 1 1 1 1 1 1 1 9 9  $ROW 9
               9 9 9 1 1 1 1 1 1 1 1 1 1 1 1 1 1 1 9 9  $ROW 10
                9 9 1 1 1 1 1 1 1 1 1 1 1 1 1 1 1 1 9 9  $ROW 11
                 9 9 1 1 1 1 1 1 1 1 1 1 1 1 1 1 9 9 9  $ROW 12
                  9 9 1 1 1 1 1 1 1 1 1 1 1 1 1 1 9 9 9 9  $ROW 13
                   9 1 1 1 1 1 1 1 1 1 1 1 1 1 1 1 9 9 9 9  $ROW 14
                    9 1 1 1 1 1 1 1 1 1 1 1 1 1 1 1 9 9 9 9 9  $ROW 15
                     9 1 1 1 1 1 1 1 1 1 1 1 1 1 1 9 9 9 9 9 9  $ROW 16
                      9 1 1 1 1 1 1 1 1 1 1 1 1 1 9 9 9 9 9 9 9  $ROW 17
                       9 9 1 1 1 1 1 1 1 1 1 1 9 9 9 9 9 9 9 9 9  $ROW 18
                        9 9 1 1 1 1 1 1 1 1 1 9 9 9 9 9 9 9 9 9 9  $ROW 19
                         9 9 9 9 1 1 1 1 9 9 9 9 9 9 9 9 9 9 9 9  $ROW 20
                          9 9 9 9 9 9 9 9 9 9 9 9 9 9 9 9 9 9 9 9 9  $ROW 21
C   Core Tank
70  0  -51 1 -53 13 14 15 16 17 18 19 30 31 32 33 34 706 707 708 fill=2 imp:n=1
74  2 5.88014E-02 (-53 1 -50 51):(-1 52 -50) imp:n=1 $Core Tank
C
C  Reflectors
C  Void Universe
99   0  -999  u=19 imp:n=1
C  Top Reflector
100  8  1.20554E-01 301 -57 -302 700 701 702 703 704 705 imp:n=1
102  0  302 -57 -303  imp:n=1
103  13 7.07826E-02 (301 -303 57 -58):(300 -301 -58) imp:n=1
```

```
196  0 -999 300 (58):(-999 303) imp:n=1
C  Bottom Reflector
300  10 1.20636E-01 -57 -304 305  imp:n=1
301  14 6.72481E-02 (57 -58 -304 305):(-305 306 -58) imp:n=1
307  0   58 -304 306 -999 imp:n=1
C   Side Reflector
320  9 1.21199E-01  320 -321 322 -323 imp:n=1
321   0  -300 53 -320 imp:n=1
322   0  -53 50 -320 322 imp:n=1
323   0  -322 50 -326 304 imp:n=1
324   0 -300 52 321 325 -999 imp:n=1
325   0 -306 327 -999 imp:n=1
C  Support Structure/Additional Reflectors
350  30 6.08580E-02 -325 326 imp:n=1 $Support Plate for Be
351  31 8.75101E-02 -327 imp:n=1 $SS304 Plate
C
700 55 4.63399E-02 -700 710 imp:n=1
701 55 4.63399E-02 -701 711 imp:n=1
702 55 4.63399E-02 -702 712 imp:n=1
703 55 4.63399E-02 -703 713 imp:n=1
704 55 4.63399E-02 -704 714 imp:n=1
705 55 4.63399E-02 -705 715 imp:n=1
C
706 55 4.63399E-02 -706 716 imp:n=1
707 55 4.63399E-02 -707 717 imp:n=1
708 55 4.63399E-02 -708 718 imp:n=1
C
710 50 4.79835E-02 -710 imp:n=1
711 50 4.79835E-02 -711 imp:n=1
712 50 4.79835E-02 -712 imp:n=1
713 50 4.79835E-02 -713 imp:n=1
714 50 4.79835E-02 -714 imp:n=1
715 50 4.79835E-02 -715 imp:n=1
716 50 4.79835E-02 -716 imp:n=1
717 50 4.79835E-02 -717 imp:n=1
718 50 4.79835E-02 -718 imp:n=1
C
999  0  999 imp:n=0

C   Surface Cards
1    pz   0.      $bottom of fuel
11   rhp  0 0 -10  0 0 50   0.753 0 0
12   rhp  0 0 -11  0 0 52   1 0 0
13   rcc  -3.766 -11.458 0  0 0 30.48  0.635
14   rcc  3.766 -11.458 0  0 0 30.48  0.635
15   rcc  3.766 11.458 0  0 0 30.48  0.635
16   rcc  -3.766 11.458 0  0 0 30.48  0.635
17   rcc  -8.039 -8.989 0  0 0 30.48  0.635
18   rcc  8.039 -8.989 0  0 0 30.48  0.635
19   rcc  -8.039 8.989 0  0 0 30.48  0.635
20   cz   0.635   $OR Clad
21   cz   0.584   $IR Clad
22   pz   0.3     $top of bottom cap
23   pz  30.18    $bottom of top cap
24   pz  30.48    $Top of fuel tube
25   cz   0.5705  $OR of Pellet
30   rcc  8.039 8.989 0  0 0 30.48  0.635
31   rcc  -11.805 -2.467 0  0 0 30.48  0.635
32   rcc  11.805 -2.467 0  0 0 30.48  0.635
33   rcc  -11.805 2.467 0  0 0 30.48  0.635
34   rcc  11.805 2.467 0  0 0 30.48  0.635
C  Core Tank
50  cz  12.98  $OR Core Tank
51  cz  12.726 $IR Core Tank
52  pz  -0.33   $Bottom of Core Tank
53  pz  30.71  $Top of Core Tank
C  simple model to preflector
57   cz 20.65   $Ir upper and lower tank
58   cz 21.285 $OR upper and lower tank
C
300    pz  30.935
301    pz  31.155
302    pz 38.14
303    pz  43.885
C
304    pz -0.33
```

```
305    pz -7.95
306    pz -8.84
C   Side Reflector
320    cz  13.08
321    cz  24.45
322    pz 0.305
323    pz 30.935
C
C    Be Support Plate
325  rpp -37.5 37.5  -37.5 37.5  -0.33 0.305
326  cz  13.95
C    SS304 Plate
327  rcc 0. 0. -11.22  0. 0. 2.38  22.86
C
700  rcc  0  0  31.155  0  0  0.112  0.425
701  rcc  0  0  32.425  0  0  0.112  0.425
702  rcc  0  0  33.695  0  0  0.112  0.425
703  rcc  0  0  34.965  0  0  0.112  0.425
704  rcc  0  0  36.235  0  0  0.112  0.425
705  rcc  0  0  37.505  0  0  0.112  0.425
C
706  rcc  -5.7065  9.883947933  15.24  0.056  -0.096994845  0  0.425
C
707  rcc  1.51  2.615396719  30.48  0  0  0.112  0.425
708  rcc  6.03  10.44426637  30.48  0  0  0.112  0.425
C
710  rcc  0  0  31.206  0  0  0.01  0.375
711  rcc  0  0  32.476  0  0  0.01  0.375
712  rcc  0  0  33.746  0  0  0.01  0.375
713  rcc  0  0  35.016  0  0  0.01  0.375
714  rcc  0  0  36.286  0  0  0.01  0.375
715  rcc  0  0  37.556  0  0  0.01  0.375
C
716  rcc  -5.681  9.839780638  15.24  0.005  -0.008660254  0  0.375
C
717  rcc  1.51  2.615396719  30.531  0  0  0.01  0.375
718  rcc  6.03  10.44426637  30.531  0  0  0.01  0.375
C
999   rpp  -500 500   -500 500  -500 500

C   Data Cards
m1   92234.70c   2.21403E-04
      92235.70c   2.03324E-02
      92236.70c   1.02154E-04
      92238.70c   1.15733E-03
      8016.70c   4.35205E-02
      8017.70c   1.06012E-04   $ Tot   6.54398E-02
C   Fuel Clad
m15   26054.70c   2.97938E-03
      26056.70c   4.67699E-02
      26057.70c   1.08012E-03
      26058.70c   1.43744E-04
      6000.70c   1.37950E-04
      25055.70c   7.53997E-04
      14028.70c   6.80144E-04
      14029.70c   3.45361E-05
      14030.70c   2.27664E-05
      24050.70c   6.23067E-04
      24052.70c   1.20152E-02
      24053.70c   1.36243E-03
      24054.70c   3.39138E-04
      28058.70c   5.28531E-03
      28060.70c   2.03589E-03
      28061.70c   8.84989E-05
      28062.70c   2.82173E-04
      28064.70c   7.18612E-05
      15031.70c   3.00906E-05
      16032.70c   1.83924E-05
      16033.70c   1.47248E-07
      16034.70c   8.31174E-07
      16036.70c   3.87494E-09
      41093.70c   2.86989E-04
      73181.70c   1.28933E-05   $tot   7.50555E-02
C   Core Tank
m2   13027.70c   5.85485E-02
      29063.70c   2.16403E-05
```

```
      29065.70c   9.64537E-06
      14028.70c   1.24044E-04
      14029.70c   6.29865E-06
      14030.70c   4.15212E-06
      26054.70c   3.95341E-06
      26056.70c   6.20601E-05
      26057.70c   1.43324E-06
      26058.70c   1.90738E-07
      25055.70c   7.23754E-06
      30000.70c   1.21614E-05   $ Tot   5.88014E-02
C   Reflectors
C  ***********************************
C  Top Reflector
m8   4009.70c   1.20554E-01
C   Side Reflector
m9   4009.70c   1.21199E-01
C   Bottom Reflector
m10   4009.70c   1.20636E-01
C    ***********************************
C  Upper reflector tank
m13   13027.70c   7.04918E-02
      29063.70c   2.60429E-05
      29065.70c   1.16077E-05
      14028.70c   1.49280E-04
      14029.70c   7.58007E-06
      14030.70c   4.99684E-06
      26054.70c   4.75770E-06
      26056.70c   7.46858E-05
      26057.70c   1.72482E-06
      25055.70c   8.70996E-06
      30000.70c   1.46355E-06   $ Tot   7.07826E-02
C  lower reflector tank
m14   13027.70c   6.69718E-02
      29063.70c   2.47424E-05
      29065.70c   1.10280E-05
      14028.70c   1.41826E-04
      14029.70c   7.20156E-06
      14030.70c   4.74732E-06
      26054.70c   4.52013E-06
      26056.70c   7.09564E-05
      26057.70c   1.63869E-06
      25055.70c   8.27504E-06
      30000.70c   1.39047E-06   $ Tot   6.72481E-02
C   ***************************************
C  Additional Bottom Reflectors
C   Be Support Plate (Al1100)
m30   13027.70c   6.06080E-02
      29063.70c   2.23913E-05
      29065.70c   9.98012E-06
      14028.70c   1.28349E-04
      14029.70c   6.51725E-06
      14030.70c   4.29622E-06
      26054.70c   4.09062E-06
      26056.70c   6.42139E-05
      26057.70c   1.48298E-06
      25055.70c   7.48872E-06
      30000.70c   1.25834E-06   $ Tot   6.08580E-02
C   SS304 Support Plate
m31   26054.70c   3.51905E-03
      26056.70c   5.52415E-02
      26057.70c   1.27577E-03
      26058.70c   1.69781E-04
      6000.70c   1.60142E-04
      25055.70c   8.75287E-04
      14028.70c   7.89554E-04
      14029.70c   4.00916E-05
      14030.70c   2.64287E-05
      24050.70c   7.63478E-04
      24052.70c   1.47229E-02
      24053.70c   1.66946E-03
      24054.70c   4.15564E-04
      28058.70c   5.29886E-03
      28060.70c   2.04111E-03
      28061.70c   8.87257E-05
      28062.70c   2.82896E-04
      28064.70c   7.20454E-05
```

```
      15031.70c   3.49310E-05
      16032.70c   2.13510E-05
      16033.70c   1.70934E-07
      16034.70c   9.64879E-07
      16034.70c   4.49827E-09   $ tot   8.75101E-02
C    U Foils
m50   92234.70c   4.67753E-04
      92235.70c   4.47223E-02
      92236.70c   1.14750E-04
      92238.70c   2.67865E-03   $ total   4.79835E-02
C    Cd Covers
m55   48106.70c   5.79249E-04
      48108.70c   4.12425E-04
      48110.70c   5.78786E-03
      48111.70c   5.93151E-03
      48112.70c   1.11818E-02
      48113.70c   5.66274E-03
      48114.70c   1.33135E-02
      48116.70c   3.47086E-03   $ total   4.63399E-02
C   Scattering Cards
mt1   o2/u.10t  u/o2.10t
mt2    al27.12t
mt8   be.10t
mt9   be.10t
mt10  be.10t
mt13   al27.12t
mt14   al27.12t
mt20   al27.12t
mt22   al27.12t
mt30   al27.12t
C
kcode  100000 1 150 2150
ksrc   0.0692  4.5245 0.77787  0  8.8072 0.7787
       0.0692 -4.3864 0.77787  0 -8.7382 0.7787
       3.8736 0 0.7787   7.6780 0 0.7787
      -3.7353 0 0.7787  -7.8510 0 0.7787
f4:n  710
fm4   1 50 -6
C
f14:n   711
fm14   1 50 -6
C
f24:n   712
fm24   1 50 -6
C
f34:n   713
fm34   1 50 -6
C
f44:n   714
fm44   1 50 -6
C
f54:n  715
fm54   1 50 -6
C
f64:n   716
fm64   1 50 -6
c
f74:n   707
fm74   1 50 -6
C
f84:n   708
fm84   1 50 -6
c
C  rand  seed=7065399757867  $ r2
C  rand  seed=5724484131590  $ r3
C  rand  seed=417647895433   $ r4
C  rand  seed=8132049697893  $ r5
C  rand  seed=8663498807872  $ r6
C  rand  seed=7447087897166  $ r7
```

A.4 Reactivity-Effects Configurations

Models were creating using Monte Carlo n-Particle (MCNP), Version 5-1.60, and ENDF/B-VII.0 neutron cross section libraries. Isotopic abundances for all elements except uranium (see Section 3.3.3 for uranium isotopic abundances) were taken from "Nuclides and Isotopes: Chart of the Nuclides," Sixteenth Edition, KAPL, 2002.

A.4.1 Name(s) of Code System(s) Used

1. Monte Carlo n-Particle, Version 5.1.60 (MCNP5).

A.4.2 Bibliographic References for the Codes Used

1. F. B. Brown, R. F. Barrett, T. E. Booth, J. S. Bull, L. J. Cox, R. A. Forster, T. J. Goorley, R. D. Mosteller, S. E. Post, R. E. Prael, E. C. Selcow, A. Sood, and J. Sweezy, "MCNP Version 5," LA-UR-02-3935, Los Alamos National Laboratory (2002).

A.4.3 Origin of Cross-section Data

The evaluated neutron data file library ENDF/B-VII.0[a] was utilized in the benchmark-model analysis.

A.4.4 Spectral Calculations and Data Reduction Methods Used

Not applicable.

A.4.5 Number of Energy Groups or If Continuous-energy Cross Sections are Used in the Different Phases of Calculation

1. Continuous-energy cross sections.

2. Continuous-energy cross sections.

A.4.6 Component Calculations

- Type of cell calculation – reactor core and reflectors
- Geometry – fuel pin and assembly lattice
- Theory used – Not applicable
- Method used – Monte Carlo
- Calculation characteristics

[a] M. B. Chadwick, et al., "ENDF/B-VII.0: Next Generation Evaluated Nuclear Data Library for Nuclear Science and Technology," *Nucl. Data Sheets*, **107**: 2931-3060 (2006).

- MCNP5 – histories/cycles/cycles skipped = 1,000,000/2,000/150 continuous-energy cross sections

A.4.7 Other Assumptions and Characteristics

Not applicable.

A.4.8 Typical Input Listings for Each Code System Type

The input deck for only the simple benchmark models for the accident configuration, the 90 stainless steel rod worth, and the stainless steel lid worth measurements are provided.

MCNP5 Input Deck for Fuel Effect Reactivity Benchmark Models:
The benchmark model was identical to the critical benchmark model for the fuel tube worth versus position measurements but with a single fuel tube removed at an appropriate location.

The accident configuration worth benchmark model is provided below.

```
SCCA-FUND-EXP-002-001 and HEU-COMP-FAST-002
C
C
C   Cell Cards
1   1  6.54398E-02  (-25 22 -24) u=11 imp:n=1         $fuel pellet
2   0      -22:(25 22 -24 ):24 u=11 imp:n=1  $void around pellet
4   0    -21 22 -23  fill=11 u=12 imp:n=1
C
C  BASIC FUEL TUBE W/ GRID PLATE
15   15 7.50555E-02 (1 -24 -20 21) u=12 imp:n=1  $Fuel tube
16   15 7.50555E-02 (1 -22 -21):(23 -24 -21) u=12 imp:n=1  $end caps
21   0    -1:20:24 u=12 imp:n=1
C     BASIC FUEL TUBES FOR TUBES WHICH ARE MOVED IN
22  0    -21 22 -23  fill=11 u=13 imp:n=1
23   15 7.50555E-02 (21) u=13 imp:n=1  $Fuel tube
24   15 7.50555E-02 (-22 -21):(23 -21) u=13 imp:n=1  $end caps
C   BASIC FUEL TUBES
40  0   -12 fill=12 u=1 imp:n=1
C   FUEL TUBES WHICH ARE MOVED IN
41  0   -13 fill=13 (-3.766 -11.458 0) imp:n=1
42  0   -14 fill=13 (3.766 -11.458 0) imp:n=1
43  0   -15 fill=13 (3.766 11.458 0) imp:n=1
44  0   -16 fill=13 (-3.766 11.458 0) imp:n=1
45  0   -17 fill=13 (-8.039 -8.989 0) imp:n=1
46  0   -18 fill=13 (8.039 -8.989 0) imp:n=1
47  0   -19 fill=13 (-8.039 8.989 0) imp:n=1
48  0   -30 fill=13 (8.039 8.989 0) imp:n=1
49  0   -31 fill=13 (-11.805 -2.467 0) imp:n=1
50  0   -32 fill=13 (11.805 -2.467 0) imp:n=1
51  0   -33 fill=13 (-11.805 2.467 0) imp:n=1
52  0   -34 fill=13 (11.805 2.467 0) imp:n=1
C
C 20 fuel tubes moved out to simulate accident scenario
1000 0   -1000 fill=13 (-2.2850 11.8731 0) imp:n=1
1001 0   -1001 fill=13 (-0.7740 12.0662 0) imp:n=1
1002 0   -1002 fill=13 (0.7740 12.0662 0) imp:n=1
1003 0   -1003 fill=13 (2.2850 11.8731 0) imp:n=1
1004 0   -1004 fill=13 (9.1399 7.9154 0) imp:n=1
1005 0   -1005 fill=13 (10.0626 6.7034 0) imp:n=1
1006 0   -1006 fill=13 (10.8367 5.3628 0) imp:n=1
1007 0   -1007 fill=13 (11.4249 3.9577 0) imp:n=1
1008 0   -1008 fill=13 (11.4249 -3.9577 0) imp:n=1
1009 0   -1009 fill=13 (10.8367 -5.3628 0) imp:n=1
1010 0   -1010 fill=13 (10.0626 -6.7034 0) imp:n=1
1011 0   -1011 fill=13 (9.1399 -7.9154 0) imp:n=1
1012 0   -1012 fill=13 (2.2850 -11.8731 0) imp:n=1
1013 0   -1013 fill=13 (0.7740 -12.0662 0) imp:n=1
1014 0   -1014 fill=13 (-0.7740 -12.0662 0) imp:n=1
1015 0   -1015 fill=13 (-2.2850 -11.8731 0) imp:n=1
1016 0   -1016 fill=13 (-9.1399 -7.9154 0) imp:n=1
```

```
1017 0   -1017 fill=13 (-10.0626 -6.7034 0) imp:n=1
1018 0   -1018 fill=13 (-10.8367 -5.3628 0) imp:n=1
1019 0   -1019 fill=13 (-11.4249 -3.9577 0) imp:n=1
C  VOID
62  0  -999  u=9 imp:n=1
C   Core Assembly
68  0   -11  lat=2  u=2 imp:n=1 fill= -10:10 -10:10 0:0
     9 9 9 9 9 9 9 9 9 9 9 9 9 9 9 9 9 9 9 9 9  $ROW 1
       9 9 9 9 9 9 9 9 9 9 9 9 9 9 9 9 9 9 9 9 9  $ROW 2
        9 9 9 9 9 9 9 9 9 9 1 1 1 1 1 1 1 1 9 9  $ROW 3
         9 9 9 9 9 9 9 9 9 1 1 1 1 1 1 1 1 1 9 9  $ROW 4
          9 9 9 9 9 9 9 9 1 1 1 1 1 1 1 1 1 9 9  $ROW 5
           9 9 9 9 9 9 9 9 1 1 1 1 1 1 1 1 1 9 9  $ROW 6
            9 9 9 9 9 9 9 1 1 1 1 1 1 1 1 1 1 9 9  $ROW 7
             9 9 9 9 9 9 1 1 1 1 1 1 1 1 1 1 1 9 9  $ROW 8
              9 9 9 9 1 1 1 1 1 1 1 1 1 1 1 1 1 9 9  $ROW 9
               9 9 9 1 1 1 1 1 1 1 1 1 1 1 1 1 1 9 9  $ROW 10
                9 9 1 1 1 1 1 1 1 1 1 1 1 1 1 1 1 9 9  $ROW 11
                 9 9 1 1 1 1 1 1 1 1 1 1 1 1 1 1 1 9 9 9  $ROW 12
                  9 9 1 1 1 1 1 1 1 1 1 1 1 1 1 1 1 9 9 9 9  $ROW 13
                   9 1 1 1 1 1 1 1 1 1 1 1 1 1 1 1 9 9 9 9 9  $ROW 14
                    9 1 1 1 1 1 1 1 1 1 1 1 1 1 1 9 9 9 9 9 9  $ROW 15
                     9 1 1 1 1 1 1 1 1 1 1 1 1 1 9 9 9 9 9 9 9  $ROW 16
                      9 1 1 1 1 1 1 1 1 1 1 1 1 9 9 9 9 9 9 9 9  $ROW 17
                       9 9 1 1 1 1 1 1 1 1 1 1 9 9 9 9 9 9 9 9 9  $ROW 18
                        9 9 1 1 1 1 1 1 1 1 1 9 9 9 9 9 9 9 9 9 9  $ROW 19
                         9 9 9 9 9 9 9 9 9 9 9 9 9 9 9 9 9 9 9 9  $ROW 20
                          9 9 9 9 9 9 9 9 9 9 9 9 9 9 9 9 9 9 9 9 9  $ROW 21
C   Core Tank
70  0   -51 1 -53 13 14 15 16 17 18 19 30 31 32 33 34
              1000 1001 1002 1003 1004 1005 1006 1007 1008 1009 1010
               1011 1012 1013 1014 1015 1016 1017 1018 1019 fill=2 imp:n=1
74  2 5.88014E-02 (-53 1 -50 51):(-1 52 -50) imp:n=1 $Core Tank
C
C  Reflectors
C  Void Universe
99   0  -999  u=19 imp:n=1
C  Top Reflector
100  8  1.20554E-01 301 -57 -302  imp:n=1
102  0  302 -57 -303  imp:n=1
103  13 7.07826E-02 (301 -303 57 -58):(300 -301 -58) imp:n=1
196  0 -999 300 (58):(-999 303) imp:n=1
C  Bottom Reflector
300  10 1.20636E-01 -57 -304 305  imp:n=1
301  14 6.72481E-02 (57 -58 -304 305):(-305 306 -58) imp:n=1
307  0   58 -304 306 -999 imp:n=1
C   Side Reflector
320  9 1.21199E-01  320 -321 322 -323 imp:n=1
321   0  -300 53 -320 imp:n=1
322   0  -53 50 -320 322 imp:n=1
323   0  -322 50 -326 304 imp:n=1
324   0 -300 52 321 325 -999 imp:n=1
325   0 -306 327 -999 imp:n=1
C  Support Structure/Additional Reflectors
350  30 6.08580E-02 -325 326 imp:n=1 $Support Plate for Be
351  31 8.75101E-02 -327 imp:n=1 $SS304 Plate
999  0  999 imp:n=0

C   Surface Cards
1    pz   0.      $bottom of fuel
11   rhp  0 0 -10  0 0 50   0.753 0 0
12   rhp  0 0 -11  0 0 52   1 0 0
13   rcc  -3.766 -11.458 0  0 0 30.48  0.635
14   rcc  3.766 -11.458 0  0 0 30.48  0.635
15   rcc  3.766 11.458 0  0 0 30.48  0.635
16   rcc  -3.766 11.458 0  0 0 30.48  0.635
17   rcc  -8.039 -8.989 0  0 0 30.48  0.635
18   rcc  8.039 -8.989 0  0 0 30.48  0.635
19   rcc  -8.039 8.989 0  0 0 30.48  0.635
20   cz   0.635   $OR Clad
21   cz   0.584   $IR Clad
22   pz   0.3     $top of bottom cap
23   pz  30.18    $bottom of top cap
24   pz  30.48    $Top of fuel tube
25   cz   0.5705  $OR of Pellet
30   rcc  8.039 8.989 0  0 0 30.48  0.635
```

```
31   rcc  -11.805 -2.467 0  0 0 30.48  0.635
32   rcc  11.805 -2.467 0  0 0 30.48  0.635
33   rcc  -11.805 2.467 0  0 0 30.48  0.635
34   rcc  11.805 2.467 0  0 0 30.48  0.635
C  Fuel Tubes that have been moved out for accident scenario
1000   rcc  -2.28498403  11.87312532  0  0 0 30.48  0.635
1001   rcc  -0.77404689  12.06619692  0  0 0 30.48  0.635
1002   rcc  0.77404689  12.06619692  0  0 0 30.48  0.635
1003   rcc  2.28498403  11.87312532  0  0 0 30.48  0.635
1004   rcc  9.13993613  7.91541688  0  0 0 30.48  0.635
1005   rcc  10.06260962  6.70344274  0  0 0 30.48  0.635
1006   rcc  10.83665651  5.36275419  0  0 0 30.48  0.635
1007   rcc  11.42492016  3.95770844  0  0 0 30.48  0.635
1008   rcc  11.42492016  -3.95770844  0  0 0 30.48  0.635
1009   rcc  10.83665651  -5.36275419  0  0 0 30.48  0.635
1010   rcc  10.06260962  -6.70344274  0  0 0 30.48  0.635
1011   rcc  9.13993613  -7.91541688  0  0 0 30.48  0.635
1012   rcc  2.28498403  -11.87312532  0  0 0 30.48  0.635
1013   rcc  0.77404689  -12.06619692  0  0 0 30.48  0.635
1014   rcc  -0.77404689  -12.06619692  0  0 0 30.48  0.635
1015   rcc  -2.28498403  -11.87312532  0  0 0 30.48  0.635
1016   rcc  -9.13993613  -7.91541688  0  0 0 30.48  0.635
1017   rcc  -10.06260962  -6.70344274  0  0 0 30.48  0.635
1018   rcc  -10.83665651  -5.36275419  0  0 0 30.48  0.635
1019   rcc  -11.42492016  -3.95770844  0  0 0 30.48  0.635
C  Core Tank
50  cz  12.98  $OR Core Tank
51  cz  12.726 $IR Core Tank
52  pz  -0.33   $Bottom of Core Tank
53  pz  30.71  $Top of Core Tank
C  simple model to preflector
57   cz 20.65   $Ir upper and lower tank
58   cz 21.285 $OR upper and lower tank
C
300    pz  30.935
301    pz  31.155
302    pz 38.14
303    pz  43.885
C
304    pz -0.33
305    pz -7.95
306    pz -8.84
C   Side Reflector
320    cz  13.08
321    cz  24.45
322    pz 0.305
323    pz 30.935
C
C    Be Support Plate
325  rpp -37.5 37.5  -37.5 37.5  -0.33 0.305
326  cz  13.95
C    SS304 Plate
327  rcc 0. 0. -11.22  0. 0. 2.38  22.86
C
999   rpp  -500 500   -500 500  -500 500

C   Data Cards
m1   92234.70c   2.21403E-04
      92235.70c   2.03324E-02
      92236.70c   1.02154E-04
      92238.70c   1.15733E-03
      8016.70c   4.35205E-02
      8017.70c   1.06012E-04   $ Tot   6.54398E-02
C   Fuel Clad
m15   26054.70c   2.97938E-03
      26056.70c   4.67699E-02
      26057.70c   1.08012E-03
      26058.70c   1.43744E-04
      6000.70c   1.37950E-04
      25055.70c   7.53997E-04
      14028.70c   6.80144E-04
      14029.70c   3.45361E-05
      14030.70c   2.27664E-05
      24050.70c   6.23067E-04
      24052.70c   1.20152E-02
      24053.70c   1.36243E-03
```

```
      24054.70c   3.39138E-04
      28058.70c   5.28531E-03
      28060.70c   2.03589E-03
      28061.70c   8.84989E-05
      28062.70c   2.82173E-04
      28064.70c   7.18612E-05
      15031.70c   3.00906E-05
      16032.70c   1.83924E-05
      16033.70c   1.47248E-07
      16034.70c   8.31174E-07
      16036.70c   3.87494E-09
      41093.70c   2.86989E-04
      73181.70c   1.28933E-05   $tot   7.50555E-02
C   Core Tank
m2   13027.70c   5.85485E-02
      29063.70c   2.16403E-05
      29065.70c   9.64537E-06
      14028.70c   1.24044E-04
      14029.70c   6.29865E-06
      14030.70c   4.15212E-06
      26054.70c   3.95341E-06
      26056.70c   6.20601E-05
      26057.70c   1.43324E-06
      26058.70c   1.90738E-07
      25055.70c   7.23754E-06
      30000.70c   1.21614E-05   $ Tot   5.88014E-02
C   Reflectors
C  ***********************************
C  Top Reflector
m8   4009.70c   1.20554E-01
C   Side Reflector
m9   4009.70c   1.21199E-01
C   Bottom Reflector
m10   4009.70c   1.20636E-01
C    ***********************************
C  Upper reflector tank
m13   13027.70c   7.04918E-02
      29063.70c   2.60429E-05
      29065.70c   1.16077E-05
      14028.70c   1.49280E-04
      14029.70c   7.58007E-06
      14030.70c   4.99684E-06
      26054.70c   4.75770E-06
      26056.70c   7.46858E-05
      26057.70c   1.72482E-06
      25055.70c   8.70996E-06
      30000.70c   1.46355E-06   $ Tot   7.07826E-02
C  lower reflector tank
m14   13027.70c   6.69718E-02
      29063.70c   2.47424E-05
      29065.70c   1.10280E-05
      14028.70c   1.41826E-04
      14029.70c   7.20156E-06
      14030.70c   4.74732E-06
      26054.70c   4.52013E-06
      26056.70c   7.09564E-05
      26057.70c   1.63869E-06
      25055.70c   8.27504E-06
      30000.70c   1.39047E-06   $ Tot   6.72481E-02
C   ************************************
C  Additional Bottom Reflectors
C   Be Support Plate (Al1100)
m30   13027.70c   6.06080E-02
      29063.70c   2.23913E-05
      29065.70c   9.98012E-06
      14028.70c   1.28349E-04
      14029.70c   6.51725E-06
      14030.70c   4.29622E-06
      26054.70c   4.09062E-06
      26056.70c   6.42139E-05
      26057.70c   1.48298E-06
      25055.70c   7.48872E-06
      30000.70c   1.25834E-06   $ Tot   6.08580E-02
C   SS304 Support Plate
m31   26054.70c   3.51905E-03
      26056.70c   5.52415E-02
```

```
      26057.70c   1.27577E-03
      26058.70c   1.69781E-04
      6000.70c   1.60142E-04
      25055.70c   8.75287E-04
      14028.70c   7.89554E-04
      14029.70c   4.00916E-05
      14030.70c   2.64287E-05
      24050.70c   7.63478E-04
      24052.70c   1.47229E-02
      24053.70c   1.66946E-03
      24054.70c   4.15564E-04
      28058.70c   5.29886E-03
      28060.70c   2.04111E-03
      28061.70c   8.87257E-05
      28062.70c   2.82896E-04
      28064.70c   7.20454E-05
      15031.70c   3.49310E-05
      16032.70c   2.13510E-05
      16033.70c   1.70934E-07
      16034.70c   9.64879E-07
      16034.70c   4.49827E-09   $ tot   8.75101E-02
C   Scattering Cards
mt1   o2/u.10t  u/o2.10t
mt2    al27.12t
mt8   be.10t
mt9   be.10t
mt10  be.10t
mt13   al27.12t
mt14   al27.12t
mt20   al27.12t
mt22   al27.12t
mt23    al27.12t
mt30   al27.12t
C
kcode  100000 1 150 2150
ksrc   0.0692  4.5245 0.77787  0  8.8072 0.7787
       0.0692 -4.3864 0.77787  0 -8.7382 0.7787
       3.8736 0 0.7787   7.6780 0 0.7787
      -3.7353 0 0.7787  -7.8510 0 0.7787
```

MCNP5 Input Deck for Material Reactivity Benchmark Models:
An example input deck is given below for the 90 stainless steel rod worth measurement. The other rod worth measurements would have had a similar input deck but modified accordingly.

```
SCCA-FUND-EXP-002-001 and HEU-COMP-FAST-002
C
C
C   Cell Cards
1   1  6.54398E-02  (-25 22 -24) u=11 imp:n=1         $fuel pellet
2   0      -22:(25 22 -24 ):24 u=11 imp:n=1  $void around pellet
4   0    -21 22 -23  fill=11 u=12 imp:n=1
C
C  BASIC FUEL TUBE W/ GRID PLATE
15   15 7.50555E-02 (1 -24 -20 21) u=12 imp:n=1  $Fuel tube
16   15 7.50555E-02 (1 -22 -21):(23 -24 -21) u=12 imp:n=1  $end caps
21   0    -1:20:24 u=12 imp:n=1
C     BASIC FUEL TUBES FOR TUBES WHICH ARE MOVED IN
22  0    -21 22 -23  fill=11 u=13 imp:n=1
23   15 7.50555E-02 (21) u=13 imp:n=1  $Fuel tube
24   15 7.50555E-02 (-22 -21):(23 -21) u=13 imp:n=1  $end caps
C   BASIC FUEL TUBES
40  0   -12 fill=12 u=1 imp:n=1
C   FUEL TUBES WHICH ARE MOVED IN
41  0   -13 fill=13 (-3.766 -11.458 0) imp:n=1
42  0   -14 fill=13 (3.766 -11.458 0) imp:n=1
43  0   -15 fill=13 (3.766 11.458 0) imp:n=1
44  0   -16 fill=13 (-3.766 11.458 0) imp:n=1
45  0   -17 fill=13 (-8.039 -8.989 0) imp:n=1
46  0   -18 fill=13 (8.039 -8.989 0) imp:n=1
47  0   -19 fill=13 (-8.039 8.989 0) imp:n=1
48  0   -30 fill=13 (8.039 8.989 0) imp:n=1
49  0   -31 fill=13 (-11.805 -2.467 0) imp:n=1
50  0   -32 fill=13 (11.805 -2.467 0) imp:n=1
51  0   -33 fill=13 (-11.805 2.467 0) imp:n=1
52  0   -34 fill=13 (11.805 2.467 0) imp:n=1
```

```
C
C   Reactivity Effect Rods
1000 1000 8.58236E-02 -1001:-1002:-1003:-1004:-1005:-1006:-1007:-1008:-1009:
        -1010:-1011:-1012:-1013:-1014:-1015:-1016:-1017:-1018:-1019:
        -1020:-1021:-1022:-1023:-1024:-1025:-1026:-1027:-1028:-1029:
        -1030:-1031:-1032:-1033:-1034:-1035:-1036:-1037:-1038:-1039:
        -1040:-1041:-1042:-1043:-1044:-1045:-1046:-1047:-1048:-1049:
        -1050:-1051:-1052:-1053:-1054:-1055:-1056:-1057:-1058:-1059:
        -1060:-1061:-1062:-1063:-1064:-1065:-1066:-1067:-1068:-1069:
        -1070:-1071:-1072:-1073:-1074:-1075:-1076:-1077:-1078:-1079:
        -1080:-1081:-1082:-1083:-1084:-1085:-1086:-1087:-1088:-1089:-1090
         imp:n=1
C  VOID
62  0  -999  u=9 imp:n=1
C   Core Assembly
68  0   -11  lat=2  u=2 imp:n=1 fill= -10:10 -10:10 0:0
     9 9 9 9 9 9 9 9 9 9 9 9 9 9 9 9 9 9 9 9 9  $ROW 1
       9 9 9 9 9 9 9 9 9 9 9 9 1 1 1 1 9 9 9 9  $ROW 2
        9 9 9 9 9 9 9 9 9 9 1 1 1 1 1 1 1 1 9 9  $ROW 3
         9 9 9 9 9 9 9 9 9 1 1 1 1 1 1 1 1 1 9 9  $ROW 4
          9 9 9 9 9 9 9 9 1 1 1 1 1 1 1 1 1 1 1 9  $ROW 5
           9 9 9 9 9 9 9 1 1 1 1 1 1 1 1 1 1 1 1 9  $ROW 6
            9 9 9 9 9 9 1 1 1 1 1 1 1 1 1 1 1 1 1 9  $ROW 7
             9 9 9 9 9 1 1 1 1 1 1 1 1 1 1 1 1 1 1 9  $ROW 8
              9 9 9 9 1 1 1 1 1 1 1 1 1 1 1 1 1 1 9 9  $ROW 9
               9 9 9 1 1 1 1 1 1 1 1 1 1 1 1 1 1 1 9 9  $ROW 10
                9 9 1 1 1 1 1 1 1 1 1 1 1 1 1 1 1 9 9  $ROW 11
                 9 9 1 1 1 1 1 1 1 1 1 1 1 1 1 1 1 9 9 9  $ROW 12
                  9 9 1 1 1 1 1 1 1 1 1 1 1 1 1 1 9 9 9 9  $ROW 13
                   9 1 1 1 1 1 1 1 1 1 1 1 1 1 1 1 9 9 9 9  $ROW 14
                    9 1 1 1 1 1 1 1 1 1 1 1 1 1 1 1 9 9 9 9 9  $ROW 15
                     9 1 1 1 1 1 1 1 1 1 1 1 1 1 1 9 9 9 9 9 9  $ROW 16
                      9 1 1 1 1 1 1 1 1 1 1 1 1 1 9 9 9 9 9 9 9  $ROW 17
                       9 9 1 1 1 1 1 1 1 1 1 1 1 9 9 9 9 9 9 9 9  $ROW 18
                        9 9 1 1 1 1 1 1 1 1 1 1 9 9 9 9 9 9 9 9 9  $ROW 19
                         9 9 9 9 1 1 1 1 9 9 9 9 9 9 9 9 9 9 9 9  $ROW 20
                          9 9 9 9 9 9 9 9 9 9 9 9 9 9 9 9 9 9 9 9  $ROW 21
C   Core Tank
70  0   -51 1 -53 13 14 15 16 17 18 19 30 31 32 33 34
             1001 1002 1003 1004 1005 1006 1007 1008 1009
        1010 1011 1012 1013 1014 1015 1016 1017 1018 1019
        1020 1021 1022 1023 1024 1025 1026 1027 1028 1029
        1030 1031 1032 1033 1034 1035 1036 1037 1038 1039
        1040 1041 1042 1043 1044 1045 1046 1047 1048 1049
        1050 1051 1052 1053 1054 1055 1056 1057 1058 1059
        1060 1061 1062 1063 1064 1065 1066 1067 1068 1069
        1070 1071 1072 1073 1074 1075 1076 1077 1078 1079
        1080 1081 1082 1083 1084 1085 1086 1087 1088 1089 1090 fill=2 imp:n=1
74  2 5.88014E-02 (-53 1 -50 51):(-1 52 -50) imp:n=1 $Core Tank
C
C  Reflectors
C  Void Universe
99   0  -999  u=19 imp:n=1
C  Top Reflector
100  8  1.20554E-01 301 -57 -302  imp:n=1
102  0  302 -57 -303  imp:n=1
103  13 7.07826E-02 (301 -303 57 -58):(300 -301 -58) imp:n=1
196  0 -999 300 (58):(-999 303) imp:n=1
C  Bottom Reflector
300  10 1.20636E-01 -57 -304 305  imp:n=1
301  14 6.72481E-02 (57 -58 -304 305):(-305 306 -58) imp:n=1
307  0   58 -304 306 -999 imp:n=1
C   Side Reflector
320  9 1.21199E-01  320 -321 322 -323 imp:n=1
321   0  -300 53 -320 imp:n=1
322   0  -53 50 -320 322 imp:n=1
323   0  -322 50 -326 304 imp:n=1
324   0 -300 52 321 325 -999 imp:n=1
325   0 -306 327 -999 imp:n=1
C  Support Structure/Additional Reflectors
350  30 6.08580E-02 -325 326 imp:n=1 $Support Plate for Be
351  31 8.75101E-02 -327 imp:n=1 $SS304 Plate
999  0  999 imp:n=0

C   Surface Cards
1    pz   0.      $bottom of fuel
```

```
11   rhp  0 0 -10  0 0 50   0.753 0 0
12   rhp  0 0 -11  0 0 52   1 0 0
13   rcc  -3.766 -11.458 0  0 0 30.48  0.635
14   rcc  3.766 -11.458 0  0 0 30.48  0.635
15   rcc  3.766 11.458 0  0 0 30.48  0.635
16   rcc  -3.766 11.458 0  0 0 30.48  0.635
17   rcc  -8.039 -8.989 0  0 0 30.48  0.635
18   rcc  8.039 -8.989 0  0 0 30.48  0.635
19   rcc  -8.039 8.989 0  0 0 30.48  0.635
20   cz   0.635   $OR Clad
21   cz   0.584   $IR Clad
22   pz   0.3     $top of bottom cap
23   pz  30.18    $bottom of top cap
24   pz  30.48    $Top of fuel tube
25   cz   0.5705  $OR of Pellet
30   rcc  8.039 8.989 0  0 0 30.48  0.635
31   rcc  -11.805 -2.467 0  0 0 30.48  0.635
32   rcc  11.805 -2.467 0  0 0 30.48  0.635
33   rcc  -11.805 2.467 0  0 0 30.48  0.635
34   rcc  11.805 2.467 0  0 0 30.48  0.635
C  Core Tank
50  cz  12.98  $OR Core Tank
51  cz  12.726 $IR Core Tank
52  pz  -0.33   $Bottom of Core Tank
C   Worth Measurement Rods
1001    rcc  -9.7890   2.1737  0  0 0 30.50  0.1585                          $ Rod Worth
Measurement Position 1
1002    rcc  -9.0360   3.4780  0  0 0 30.50  0.1585                          $ Rod Worth
Measurement Position 2
1003    rcc  -8.2830   4.7822  0  0 0 30.50  0.1585                          $ Rod Worth
Measurement Position 3
1004    rcc  -7.5300   6.0864  0  0 0 30.50  0.1585                          $ Rod Worth
Measurement Position 4
1005    rcc  -6.7770   7.3907  0  0 0 30.50  0.1585                          $ Rod Worth
Measurement Position 5
1006    rcc  -9.7890  -3.0432  0  0 0 30.50  0.1585                          $ Rod Worth
Measurement Position 6
1007    rcc  -9.0360  -1.7390  0  0 0 30.50  0.1585                          $ Rod Worth
Measurement Position 7
1008    rcc  -8.2830  -0.4347  0  0 0 30.50  0.1585                          $ Rod Worth
Measurement Position 8
1009    rcc  -7.5300   0.8695  0  0 0 30.50  0.1585                          $ Rod Worth
Measurement Position 9
1010    rcc  -6.7770   2.1737  0  0 0 30.50  0.1585                          $ Rod Worth
Measurement Position 10
1011    rcc  -6.0240   3.4780  0  0 0 30.50  0.1585                          $ Rod Worth
Measurement Position 11
1012    rcc  -5.2710   4.7822  0  0 0 30.50  0.1585                          $ Rod Worth
Measurement Position 12
1013    rcc  -4.5180   6.0864  0  0 0 30.50  0.1585                          $ Rod Worth
Measurement Position 13
1014    rcc  -3.7650   7.3907  0  0 0 30.50  0.1585                          $ Rod Worth
Measurement Position 14
1015    rcc  -3.0120   8.6949  0  0 0 30.50  0.1585                          $ Rod Worth
Measurement Position 15
1016    rcc  -2.2590   9.9991  0  0 0 30.50  0.1585                          $ Rod Worth
Measurement Position 16
1017    rcc  -8.2830  -5.6517  0  0 0 30.50  0.1585                          $ Rod Worth
Measurement Position 17
1018    rcc  -7.5300  -4.3474  0  0 0 30.50  0.1585                          $ Rod Worth
Measurement Position 18
1019    rcc  -6.7770  -3.0432  0  0 0 30.50  0.1585                          $ Rod Worth
Measurement Position 19
1020    rcc  -6.0240  -1.7390  0  0 0 30.50  0.1585                          $ Rod Worth
Measurement Position 20
1021    rcc  -5.2710  -0.4347  0  0 0 30.50  0.1585                          $ Rod Worth
Measurement Position 21
1022    rcc  -4.5180   0.8695  0  0 0 30.50  0.1585                          $ Rod Worth
Measurement Position 22
1023    rcc  -3.7650   2.1737  0  0 0 30.50  0.1585                          $ Rod Worth
Measurement Position 23
1024    rcc  -3.0120   3.4780  0  0 0 30.50  0.1585                          $ Rod Worth
Measurement Position 24
1025    rcc  -2.2590   4.7822  0  0 0 30.50  0.1585                          $ Rod Worth
Measurement Position 25
1026    rcc  -1.5060   6.0864  0  0 0 30.50  0.1585                          $ Rod Worth
```

```
Measurement Position 26
1027    rcc  -0.7530   7.3907  0  0 0 30.50  0.1585                              $ Rod Worth
Measurement Position 27
1028    rcc   0.0000   8.6949  0  0 0 30.50  0.1585                              $ Rod Worth
Measurement Position 28
1029    rcc   0.7530   9.9991  0  0 0 30.50  0.1585                              $ Rod Worth
Measurement Position 29
1030    rcc  -6.0240  -6.9559  0  0 0 30.50  0.1585                              $ Rod Worth
Measurement Position 30
1031    rcc  -5.2710  -5.6517  0  0 0 30.50  0.1585                              $ Rod Worth
Measurement Position 31
1032    rcc  -4.5180  -4.3474  0  0 0 30.50  0.1585                              $ Rod Worth
Measurement Position 32
1033    rcc  -3.7650  -3.0432  0  0 0 30.50  0.1585                              $ Rod Worth
Measurement Position 33
1034    rcc  -3.0120  -1.7390  0  0 0 30.50  0.1585                              $ Rod Worth
Measurement Position 34
1035    rcc  -2.2590  -0.4347  0  0 0 30.50  0.1585                              $ Rod Worth
Measurement Position 35
1036    rcc  -1.5060   0.8695  0  0 0 30.50  0.1585                              $ Rod Worth
Measurement Position 36
1037    rcc  -0.7530   2.1737  0  0 0 30.50  0.1585                              $ Rod Worth
Measurement Position 37
1038    rcc   0.0000   3.4780  0  0 0 30.50  0.1585                              $ Rod Worth
Measurement Position 38
1039    rcc   0.7530   4.7822  0  0 0 30.50  0.1585                              $ Rod Worth
Measurement Position 39
1040    rcc   1.5060   6.0864  0  0 0 30.50  0.1585                              $ Rod Worth
Measurement Position 40
1041    rcc   2.2590   7.3907  0  0 0 30.50  0.1585                              $ Rod Worth
Measurement Position 41
1042    rcc   3.0120   8.6949  0  0 0 30.50  0.1585                              $ Rod Worth
Measurement Position 42
1043    rcc  -4.5180  -9.5644  0  0 0 30.50  0.1585                              $ Rod Worth
Measurement Position 43
1044    rcc  -3.7650  -8.2602  0  0 0 30.50  0.1585                              $ Rod Worth
Measurement Position 44
1045    rcc  -3.0120  -6.9559  0  0 0 30.50  0.1585                              $ Rod Worth
Measurement Position 45
1046    rcc  -2.2590  -5.6517  0  0 0 30.50  0.1585                              $ Rod Worth
Measurement Position 46
1047    rcc  -1.5060  -4.3474  0  0 0 30.50  0.1585                              $ Rod Worth
Measurement Position 47
1048    rcc  -0.7530  -3.0432  0  0 0 30.50  0.1585                              $ Rod Worth
Measurement Position 48
1049    rcc   0.0000  -1.7390  0  0 0 30.50  0.1585                              $ Rod Worth
Measurement Position 49
1050    rcc   0.7530  -0.4347  0  0 0 30.50  0.1585                              $ Rod Worth
Measurement Position 50
1051    rcc   1.5060   0.8695  0  0 0 30.50  0.1585                              $ Rod Worth
Measurement Position 51
1052    rcc   2.2590   2.1737  0  0 0 30.50  0.1585                              $ Rod Worth
Measurement Position 52
1053    rcc   3.0120   3.4780  0  0 0 30.50  0.1585                              $ Rod Worth
Measurement Position 53
1054    rcc   3.7650   4.7822  0  0 0 30.50  0.1585                              $ Rod Worth
Measurement Position 54
1055    rcc   4.5180   6.0864  0  0 0 30.50  0.1585                              $ Rod Worth
Measurement Position 55
1056    rcc   5.2710   7.3907  0  0 0 30.50  0.1585                              $ Rod Worth
Measurement Position 56
1057    rcc   6.0240   8.6949  0  0 0 30.50  0.1585                              $ Rod Worth
Measurement Position 57
1058    rcc  -1.5060  -9.5644  0  0 0 30.50  0.1585                              $ Rod Worth
Measurement Position 58
1059    rcc  -0.7530  -8.2602  0  0 0 30.50  0.1585                              $ Rod Worth
Measurement Position 59
1060    rcc   0.0000  -6.9559  0  0 0 30.50  0.1585                              $ Rod Worth
Measurement Position 60
1061    rcc   0.7530  -5.6517  0  0 0 30.50  0.1585                              $ Rod Worth
Measurement Position 61
1062    rcc   1.5060  -4.3474  0  0 0 30.50  0.1585                              $ Rod Worth
Measurement Position 62
1063    rcc   2.2590  -3.0432  0  0 0 30.50  0.1585                              $ Rod Worth
Measurement Position 63
1064    rcc   3.0120  -1.7390  0  0 0 30.50  0.1585                              $ Rod Worth
```

```
Measurement Position 64
1065    rcc   3.7650  -0.4347  0  0 0 30.50  0.1585                                  $ Rod Worth
Measurement Position 65
1066    rcc   4.5180   0.8695  0  0 0 30.50  0.1585                                  $ Rod Worth
Measurement Position 66
1067    rcc   5.2710   2.1737  0  0 0 30.50  0.1585                                  $ Rod Worth
Measurement Position 67
1068    rcc   6.0240   3.4780  0  0 0 30.50  0.1585                                  $ Rod Worth
Measurement Position 68
1069    rcc   6.7770   4.7822  0  0 0 30.50  0.1585                                  $ Rod Worth
Measurement Position 69
1070    rcc   7.5300   6.0864  0  0 0 30.50  0.1585                                  $ Rod Worth
Measurement Position 70
1071    rcc   1.5060  -9.5644  0  0 0 30.50  0.1585                                  $ Rod Worth
Measurement Position 71
1072    rcc   2.2590  -8.2602  0  0 0 30.50  0.1585                                  $ Rod Worth
Measurement Position 72
1073    rcc   3.0120  -6.9559  0  0 0 30.50  0.1585                                  $ Rod Worth
Measurement Position 73
1074    rcc   3.7650  -5.6517  0  0 0 30.50  0.1585                                  $ Rod Worth
Measurement Position 74
1075    rcc   4.5180  -4.3474  0  0 0 30.50  0.1585                                  $ Rod Worth
Measurement Position 75
1076    rcc   5.2710  -3.0432  0  0 0 30.50  0.1585                                  $ Rod Worth
Measurement Position 76
1077    rcc   6.0240  -1.7390  0  0 0 30.50  0.1585                                  $ Rod Worth
Measurement Position 77
1078    rcc   6.7770  -0.4347  0  0 0 30.50  0.1585                                  $ Rod Worth
Measurement Position 78
1079    rcc   7.5300   0.8695  0  0 0 30.50  0.1585                                  $ Rod Worth
Measurement Position 79
1080    rcc   8.2830   2.1737  0  0 0 30.50  0.1585                                  $ Rod Worth
Measurement Position 80
1081    rcc   9.0360   3.4780  0  0 0 30.50  0.1585                                  $ Rod Worth
Measurement Position 81
1082    rcc   4.5180  -9.5644  0  0 0 30.50  0.1585                                  $ Rod Worth
Measurement Position 82
1083    rcc   5.2710  -8.2602  0  0 0 30.50  0.1585                                  $ Rod Worth
Measurement Position 83
1084    rcc   6.0240  -6.9559  0  0 0 30.50  0.1585                                  $ Rod Worth
Measurement Position 84
1085    rcc   6.7770  -5.6517  0  0 0 30.50  0.1585                                  $ Rod Worth
Measurement Position 85
1086    rcc   7.5300  -4.3474  0  0 0 30.50  0.1585                                  $ Rod Worth
Measurement Position 86
1087    rcc   8.2830  -3.0432  0  0 0 30.50  0.1585                                  $ Rod Worth
Measurement Position 87
1088    rcc   9.0360  -1.7390  0  0 0 30.50  0.1585                                  $ Rod Worth
Measurement Position 88
1089    rcc   9.7890  -0.4347  0  0 0 30.50  0.1585                                  $ Rod Worth
Measurement Position 89
1090    rcc   10.5420   0.8695  0  0 0 30.50  0.1585                                  $ Rod Worth
Measurement Position 90
C
53  pz  30.71  $Top of Core Tank
C  simple model to preflector
57   cz 20.65   $Ir upper and lower tank
58   cz 21.285 $OR upper and lower tank
C
300    pz  30.935
301    pz  31.155
302    pz 38.14
303    pz  43.885
C
304    pz -0.33
305    pz -7.95
306    pz -8.84
C   Side Reflector
320    cz  13.08
321    cz  24.45
322    pz 0.305
323    pz 30.935
C
C    Be Support Plate
325  rpp -37.5 37.5  -37.5 37.5  -0.33 0.305
326  cz  13.95
```

```
C    SS304 Plate
327  rcc 0. 0. -11.22  0. 0. 2.38  22.86
C
999   rpp  -500 500   -500 500  -500 500

C   Data Cards
m1   92234.70c   2.21403E-04
      92235.70c   2.03324E-02
      92236.70c   1.02154E-04
      92238.70c   1.15733E-03
      8016.70c   4.35205E-02
      8017.70c   1.06012E-04   $ Tot   6.54398E-02
C   Fuel Clad
m15   26054.70c   2.97938E-03
      26056.70c   4.67699E-02
      26057.70c   1.08012E-03
      26058.70c   1.43744E-04
      6000.70c   1.37950E-04
      25055.70c   7.53997E-04
      14028.70c   6.80144E-04
      14029.70c   3.45361E-05
      14030.70c   2.27664E-05
      24050.70c   6.23067E-04
      24052.70c   1.20152E-02
      24053.70c   1.36243E-03
      24054.70c   3.39138E-04
      28058.70c   5.28531E-03
      28060.70c   2.03589E-03
      28061.70c   8.84989E-05
      28062.70c   2.82173E-04
      28064.70c   7.18612E-05
      15031.70c   3.00906E-05
      16032.70c   1.83924E-05
      16033.70c   1.47248E-07
      16034.70c   8.31174E-07
      16036.70c   3.87494E-09
      41093.70c   2.86989E-04
      73181.70c   1.28933E-05   $tot   7.50555E-02
C   Core Tank
m2   13027.70c   5.85485E-02
      29063.70c   2.16403E-05
      29065.70c   9.64537E-06
      14028.70c   1.24044E-04
      14029.70c   6.29865E-06
      14030.70c   4.15212E-06
      26054.70c   3.95341E-06
      26056.70c   6.20601E-05
      26057.70c   1.43324E-06
      26058.70c   1.90738E-07
      25055.70c   7.23754E-06
      30000.70c   1.21614E-05   $ Tot   5.88014E-02
C   Reflectors
C  ***********************************
C  Top Reflector
m8   4009.70c   1.20554E-01
C   Side Reflector
m9   4009.70c   1.21199E-01
C   Bottom Reflector
m10   4009.70c   1.20636E-01
C    ***********************************
C  Upper reflector tank
m13   13027.70c   7.04918E-02
      29063.70c   2.60429E-05
      29065.70c   1.16077E-05
      14028.70c   1.49280E-04
      14029.70c   7.58007E-06
      14030.70c   4.99684E-06
      26054.70c   4.75770E-06
      26056.70c   7.46858E-05
      26057.70c   1.72482E-06
      25055.70c   8.70996E-06
      30000.70c   1.46355E-06   $ Tot   7.07826E-02
C  lower reflector tank
m14   13027.70c   6.69718E-02
      29063.70c   2.47424E-05
      29065.70c   1.10280E-05
```

```
      14028.70c   1.41826E-04
      14029.70c   7.20156E-06
      14030.70c   4.74732E-06
      26054.70c   4.52013E-06
      26056.70c   7.09564E-05
      26057.70c   1.63869E-06
      25055.70c   8.27504E-06
      30000.70c   1.39047E-06   $ Tot   6.72481E-02
C   ************************************
C  Additional Bottom Reflectors
C   Be Support Plate (Al1100)
m30   13027.70c   6.06080E-02
      29063.70c   2.23913E-05
      29065.70c   9.98012E-06
      14028.70c   1.28349E-04
      14029.70c   6.51725E-06
      14030.70c   4.29622E-06
      26054.70c   4.09062E-06
      26056.70c   6.42139E-05
      26057.70c   1.48298E-06
      25055.70c   7.48872E-06
      30000.70c   1.25834E-06   $ Tot   6.08580E-02
C   SS304 Support Plate
m31   26054.70c   3.51905E-03
      26056.70c   5.52415E-02
      26057.70c   1.27577E-03
      26058.70c   1.69781E-04
      6000.70c   1.60142E-04
      25055.70c   8.75287E-04
      14028.70c   7.89554E-04
      14029.70c   4.00916E-05
      14030.70c   2.64287E-05
      24050.70c   7.63478E-04
      24052.70c   1.47229E-02
      24053.70c   1.66946E-03
      24054.70c   4.15564E-04
      28058.70c   5.29886E-03
      28060.70c   2.04111E-03
      28061.70c   8.87257E-05
      28062.70c   2.82896E-04
      28064.70c   7.20454E-05
      15031.70c   3.49310E-05
      16032.70c   2.13510E-05
      16033.70c   1.70934E-07
      16034.70c   9.64879E-07
      16034.70c   4.49827E-09   $ tot   8.75101E-02
C   SS90 Rod Material
m1000   26054.70c   3.40683E-03
      26056.70c   5.34799E-02
      26057.70c   1.23509E-03
      26058.70c   1.64367E-04
      6000.70c   1.57742E-04
      25055.70c   8.62172E-04
      14028.70c   7.77724E-04
      14029.70c   3.94909E-05
      14030.70c   2.60327E-05
      24050.70c   7.12458E-04
      24052.70c   1.37390E-02
      24053.70c   1.55790E-03
      24054.70c   3.87793E-04
      28058.70c   6.04359E-03
      28060.70c   2.32798E-03
      28061.70c   1.01196E-04
      28062.70c   3.22656E-04
      28064.70c   8.21710E-05
      15031.70c   3.44076E-05
      16032.70c   2.10311E-05
      16033.70c   1.68373E-07
      16034.70c   9.50422E-07
      16036.70c   4.43087E-09
      41093.70c   3.28163E-04
      73181.70c   1.47431E-05   $ tot   8.58236E-02
C   Scattering Cards
mt1   o2/u.10t  u/o2.10t
mt2    al27.12t
mt8   be.10t
```

```
mt9   be.10t
mt10  be.10t
mt13   al27.12t
mt14   al27.12t
mt20   al27.12t
mt22   al27.12t
mt23    al27.12t
mt30   al27.12t
C
kcode  100000 1 150 2150
ksrc   0.0692  4.5245 0.77787  0  8.8072 0.7787
       0.0692 -4.3864 0.77787  0 -8.7382 0.7787
       3.8736 0 0.7787   7.6780 0 0.7787
      -3.7353 0 0.7787  -7.8510 0 0.7787
```

MCNP5 Input Deck for Material Reactivity Benchmark Models:
An example input deck is given below for the stainless steel lid. The other lid worth measurements would have had a similar input deck but modified accordingly.

```
SCCA-FUND-EXP-002-001 and HEU-COMP-FAST-002
C
C
C   Cell Cards
1   1  6.54398E-02  (-25 22 -24) u=11 imp:n=1         $fuel pellet
2   0      -22:(25 22 -24 ):24 u=11 imp:n=1  $void around pellet
4   0    -21 22 -23  fill=11 u=12 imp:n=1
C
C  BASIC FUEL TUBE W/ GRID PLATE
15   15 7.50555E-02 (1 -24 -20 21) u=12 imp:n=1  $Fuel tube
16   15 7.50555E-02 (1 -22 -21):(23 -24 -21) u=12 imp:n=1  $end caps
21   0    -1:20:24 u=12 imp:n=1
C     BASIC FUEL TUBES FOR TUBES WHICH ARE MOVED IN
22  0    -21 22 -23  fill=11 u=13 imp:n=1
23   15 7.50555E-02 (21) u=13 imp:n=1  $Fuel tube
24   15 7.50555E-02 (-22 -21):(23 -21) u=13 imp:n=1  $end caps
C   BASIC FUEL TUBES
40  0   -12 fill=12 u=1 imp:n=1
C   FUEL TUBES WHICH ARE MOVED IN
41  0   -13 fill=13 (-3.766 -11.458 0) imp:n=1
42  0   -14 fill=13 (3.766 -11.458 0) imp:n=1
43  0   -15 fill=13 (3.766 11.458 0) imp:n=1
44  0   -16 fill=13 (-3.766 11.458 0) imp:n=1
45  0   -17 fill=13 (-8.039 -8.989 0) imp:n=1
46  0   -18 fill=13 (8.039 -8.989 0) imp:n=1
47  0   -19 fill=13 (-8.039 8.989 0) imp:n=1
48  0   -30 fill=13 (8.039 8.989 0) imp:n=1
49  0   -31 fill=13 (-11.805 -2.467 0) imp:n=1
50  0   -32 fill=13 (11.805 -2.467 0) imp:n=1
51  0   -33 fill=13 (-11.805 2.467 0) imp:n=1
52  0   -34 fill=13 (11.805 2.467 0) imp:n=1
C
C  VOID
62  0  -999  u=9 imp:n=1
C   Core Assembly
68  0   -11  lat=2  u=2 imp:n=1 fill= -10:10 -10:10 0:0
     9 9 9 9 9 9 9 9 9 9 9 9 9 9 9 9 9 9 9 9 9  $ROW 1
       9 9 9 9 9 9 9 9 9 9 9 9 9 9 1 1 1 1 9 9 9 9  $ROW 2
        9 9 9 9 9 9 9 9 9 9 1 1 1 1 1 1 1 1 1 9 9  $ROW 3
         9 9 9 9 9 9 9 9 9 1 1 1 1 1 1 1 1 1 1 9 9  $ROW 4
          9 9 9 9 9 9 9 9 1 1 1 1 1 1 1 1 1 1 1 1 9  $ROW 5
           9 9 9 9 9 9 9 1 1 1 1 1 1 1 1 1 1 1 1 1 9  $ROW 6
            9 9 9 9 9 9 1 1 1 1 1 1 1 1 1 1 1 1 1 1 9  $ROW 7
             9 9 9 9 9 1 1 1 1 1 1 1 1 1 1 1 1 1 1 1 9  $ROW 8
              9 9 9 9 9 1 1 1 1 1 1 1 1 1 1 1 1 1 1 9 9  $ROW 9
               9 9 9 1 1 1 1 1 1 1 1 1 1 1 1 1 1 1 9 9  $ROW 10
                9 9 1 1 1 1 1 1 1 1 1 1 1 1 1 1 1 1 9 9  $ROW 11
                 9 9 1 1 1 1 1 1 1 1 1 1 1 1 1 1 1 9 9 9  $ROW 12
                  9 9 1 1 1 1 1 1 1 1 1 1 1 1 1 1 9 9 9 9  $ROW 13
                   9 1 1 1 1 1 1 1 1 1 1 1 1 1 1 1 9 9 9 9  $ROW 14
                    9 1 1 1 1 1 1 1 1 1 1 1 1 1 1 9 9 9 9 9  $ROW 15
                     9 1 1 1 1 1 1 1 1 1 1 1 1 1 1 9 9 9 9 9 9  $ROW 16
                      9 1 1 1 1 1 1 1 1 1 1 1 1 1 1 9 9 9 9 9 9 9  $ROW 17
                       9 9 1 1 1 1 1 1 1 1 1 1 1 9 9 9 9 9 9 9 9 9  $ROW 18
                        9 9 1 1 1 1 1 1 1 1 1 1 9 9 9 9 9 9 9 9 9 9  $ROW 19
                         9 9 9 9 1 1 1 1 9 9 9 9 9 9 9 9 9 9 9 9 9  $ROW 20
```

```
                        9 9 9 9 9 9 9 9 9 9 9 9 9 9 9 9 9 9 9 9 9  $ROW 21
C   Core Tank
70  0   -51 1 -53 13 14 15 16 17 18 19 30 31 32 33 34 1000  fill=2 imp:n=1
74  2 5.88014E-02 (-53 1 -50 51):(-1 52 -50) imp:n=1 $Core Tank
C   SS Lid
1000 1006 8.71365E-02  -1000 imp:n=1
1001 0                 323 -300 1000 -321 imp:n=1
C  Reflectors
C  Void Universe
99   0  -999  u=19 imp:n=1
C  Top Reflector
100  8  1.20554E-01 301 -57 -302  imp:n=1
102  0  302 -57 -303  imp:n=1
103  13 7.07826E-02 (301 -303 57 -58):(300 -301 -58) imp:n=1
196  0 -999 300 (58):(-999 303) imp:n=1
C  Bottom Reflector
300  10 1.20636E-01 -57 -304 305  imp:n=1
301  14 6.72481E-02 (57 -58 -304 305):(-305 306 -58) imp:n=1
307  0   58 -304 306 -999 imp:n=1
C   Side Reflector
320  9 1.21199E-01  320 -321 322 -323 imp:n=1
321   0  -300 53 -320 1000 imp:n=1
322   0  -53 50 -320 322 imp:n=1
323   0  -322 50 -326 304 imp:n=1
324   0 -300 52 321 325 -999 imp:n=1
325   0 -306 327 -999 imp:n=1
C  Support Structure/Additional Reflectors
350  30 6.08580E-02 -325 326 imp:n=1 $Support Plate for Be
351  31 8.75101E-02 -327 imp:n=1 $SS304 Plate
999  0  999 imp:n=0

C   Surface Cards
1    pz   0.      $bottom of fuel
11   rhp  0 0 -10  0 0 50   0.753 0 0
12   rhp  0 0 -11  0 0 52   1 0 0
13   rcc  -3.766 -11.458 0  0 0 30.48  0.635
14   rcc  3.766 -11.458 0  0 0 30.48  0.635
15   rcc  3.766 11.458 0  0 0 30.48  0.635
16   rcc  -3.766 11.458 0  0 0 30.48  0.635
17   rcc  -8.039 -8.989 0  0 0 30.48  0.635
18   rcc  8.039 -8.989 0  0 0 30.48  0.635
19   rcc  -8.039 8.989 0  0 0 30.48  0.635
20   cz   0.635   $OR Clad
21   cz   0.584   $IR Clad
22   pz   0.3     $top of bottom cap
23   pz  30.18    $bottom of top cap
24   pz  30.48    $Top of fuel tube
25   cz   0.5705  $OR of Pellet
30   rcc  8.039 8.989 0  0 0 30.48  0.635
31   rcc  -11.805 -2.467 0  0 0 30.48  0.635
32   rcc  11.805 -2.467 0  0 0 30.48  0.635
33   rcc  -11.805 2.467 0  0 0 30.48  0.635
34   rcc  11.805 2.467 0  0 0 30.48  0.635
C  Core Tank
50  cz  12.98  $OR Core Tank
51  cz  12.726 $IR Core Tank
52  pz  -0.33   $Bottom of Core Tank
53  pz  30.71  $Top of Core Tank
C  SS Lid
1000  rcc 0 0 30.48  0 0 0.3175  12.726
C  simple model to preflector
57   cz 20.65   $Ir upper and lower tank
58   cz 21.285 $OR upper and lower tank
C   Top Reflector Z Plates
300    pz  30.935
301    pz  31.155
302    pz 38.14
303    pz  43.885
C
304    pz -0.33
305    pz -7.95
306    pz -8.84
C   Side Reflector
320    cz  13.08
321    cz  24.45
322    pz 0.305
```

```
323    pz 30.935
C
C    Be Support Plate
325  rpp -37.5 37.5  -37.5 37.5  -0.33 0.305
326  cz  13.95
C    SS304 Plate
327  rcc 0. 0. -11.22  0. 0. 2.38  22.86
C
999   rpp  -500 500   -500 500  -500 500

C   Data Cards
m1   92234.70c   2.21403E-04
      92235.70c   2.03324E-02
      92236.70c   1.02154E-04
      92238.70c   1.15733E-03
      8016.70c   4.35205E-02
      8017.70c   1.06012E-04   $ Tot   6.54398E-02
C   Fuel Clad
m15   26054.70c   2.97938E-03
      26056.70c   4.67699E-02
      26057.70c   1.08012E-03
      26058.70c   1.43744E-04
      6000.70c   1.37950E-04
      25055.70c   7.53997E-04
      14028.70c   6.80144E-04
      14029.70c   3.45361E-05
      14030.70c   2.27664E-05
      24050.70c   6.23067E-04
      24052.70c   1.20152E-02
      24053.70c   1.36243E-03
      24054.70c   3.39138E-04
      28058.70c   5.28531E-03
      28060.70c   2.03589E-03
      28061.70c   8.84989E-05
      28062.70c   2.82173E-04
      28064.70c   7.18612E-05
      15031.70c   3.00906E-05
      16032.70c   1.83924E-05
      16033.70c   1.47248E-07
      16034.70c   8.31174E-07
      16036.70c   3.87494E-09
      41093.70c   2.86989E-04
      73181.70c   1.28933E-05   $tot   7.50555E-02
C   Core Tank
m2   13027.70c   5.85485E-02
      29063.70c   2.16403E-05
      29065.70c   9.64537E-06
      14028.70c   1.24044E-04
      14029.70c   6.29865E-06
      14030.70c   4.15212E-06
      26054.70c   3.95341E-06
      26056.70c   6.20601E-05
      26057.70c   1.43324E-06
      26058.70c   1.90738E-07
      25055.70c   7.23754E-06
      30000.70c   1.21614E-05   $ Tot   5.88014E-02
C   Reflectors
C  ************************************
C  Top Reflector
m8   4009.70c   1.20554E-01
C   Side Reflector
m9   4009.70c   1.21199E-01
C   Bottom Reflector
m10   4009.70c   1.20636E-01
C    ************************************
C  Upper reflector tank
m13   13027.70c   7.04918E-02
      29063.70c   2.60429E-05
      29065.70c   1.16077E-05
      14028.70c   1.49280E-04
      14029.70c   7.58007E-06
      14030.70c   4.99684E-06
      26054.70c   4.75770E-06
      26056.70c   7.46858E-05
      26057.70c   1.72482E-06
      25055.70c   8.70996E-06
```

```
      30000.70c   1.46355E-06   $ Tot   7.07826E-02
C  lower reflector tank
m14   13027.70c   6.69718E-02
      29063.70c   2.47424E-05
      29065.70c   1.10280E-05
      14028.70c   1.41826E-04
      14029.70c   7.20156E-06
      14030.70c   4.74732E-06
      26054.70c   4.52013E-06
      26056.70c   7.09564E-05
      26057.70c   1.63869E-06
      25055.70c   8.27504E-06
      30000.70c   1.39047E-06   $ Tot   6.72481E-02
C   ************************************
C  Additional Bottom Reflectors
C   Be Support Plate (Al1100)
m30   13027.70c   6.06080E-02
      29063.70c   2.23913E-05
      29065.70c   9.98012E-06
      14028.70c   1.28349E-04
      14029.70c   6.51725E-06
      14030.70c   4.29622E-06
      26054.70c   4.09062E-06
      26056.70c   6.42139E-05
      26057.70c   1.48298E-06
      25055.70c   7.48872E-06
      30000.70c   1.25834E-06   $ Tot   6.08580E-02
C   SS304 Support Plate
m31   26054.70c   3.51905E-03
      26056.70c   5.52415E-02
      26057.70c   1.27577E-03
      26058.70c   1.69781E-04
      6000.70c   1.60142E-04
      25055.70c   8.75287E-04
      14028.70c   7.89554E-04
      14029.70c   4.00916E-05
      14030.70c   2.64287E-05
      24050.70c   7.63478E-04
      24052.70c   1.47229E-02
      24053.70c   1.66946E-03
      24054.70c   4.15564E-04
      28058.70c   5.29886E-03
      28060.70c   2.04111E-03
      28061.70c   8.87257E-05
      28062.70c   2.82896E-04
      28064.70c   7.20454E-05
      15031.70c   3.49310E-05
      16032.70c   2.13510E-05
      16033.70c   1.70934E-07
      16034.70c   9.64879E-07
      16034.70c   4.49827E-09   $ tot   8.75101E-02
C   SS347 Lid
m1006   26054.70c   3.45895E-03                                                $ Total atom
density, atom/b-cm,   8.71365E-02
        26056.70c   5.42981E-02
        26057.70c   1.25398E-03
        26058.70c   1.66882E-04
        6000.70c   1.60155E-04
        25055.70c   8.75361E-04
        14028.70c   7.89621E-04
        14029.70c   4.00951E-05
        14030.70c   2.64310E-05
        24050.70c   7.23357E-04
        24052.70c   1.39492E-02
        24053.70c   1.58173E-03
        24054.70c   3.93726E-04
        28058.70c   6.13605E-03
        28060.70c   2.36359E-03
        28061.70c   1.02744E-04
        28062.70c   3.27592E-04
        28064.70c   8.34281E-05
        15031.70c   3.49340E-05
        16032.70c   2.13529E-05
        16033.70c   1.70949E-07
        16034.70c   9.64961E-07
        16036.70c   4.49865E-09
```

```
        41093.70c   3.33183E-04
        73181.70c   1.49687E-05
C   Scattering Cards
mt1   o2/u.10t  u/o2.10t
mt2    al27.12t
mt8   be.10t
mt9   be.10t
mt10  be.10t
mt13   al27.12t
mt14   al27.12t
mt20   al27.12t
mt22   al27.12t
mt23    al27.12t
mt30   al27.12t
C
kcode  100000 1 150 2150
ksrc   0.0692  4.5245 0.77787  0  8.8072 0.7787
       0.0692 -4.3864 0.77787  0 -8.7382 0.7787
       3.8736 0 0.7787   7.6780 0 0.7787
      -3.7353 0 0.7787  -7.8510 0 0.7787
```

A.5 Reactivity Coefficient Configurations

Reactivity coefficient measurements were not evaluated.

A.6 Kinetics Parameter Configurations

Kinetics measurements were not performed.

A.7 Reaction-Rate Configurations

Models were creating using Monte Carlo n-Particle (MCNP), Version 5-1.60, and ENDF/B-VII.0 neutron cross section libraries. Isotopic abundances for all elements except uranium (see Section 3.3.3 for uranium isotopic abundances) were taken from "Nuclides and Isotopes: Chart of the Nuclides," Sixteenth Edition, KAPL, 2002.

A.7.1 Name(s) of Code System(s) Used

1. Monte Carlo n-Particle, Version 5.1.60 (MCNP5).

A.7.2 Bibliographic References for the Codes Used

1. F. B. Brown, R. F. Barrett, T. E. Booth, J. S. Bull, L. J. Cox, R. A. Forster, T. J. Goorley, R. D. Mosteller, S. E. Post, R. E. Prael, E. C. Selcow, A. Sood, and J. Sweezy, "MCNP Version 5," LA-UR-02-3935, Los Alamos National Laboratory (2002).

A.7.3 Origin of Cross-section Data

The evaluated neutron data file library ENDF/B-VII.0[a] was utilized in the benchmark-model analysis.

[a] M. B. Chadwick, et al., "ENDF/B-VII.0: Next Generation Evaluated Nuclear Data Library for Nuclear Science and Technology," *Nucl. Data Sheets*, **107**: 2931-3060 (2006).

A.7.4 Spectral Calculations and Data Reduction Methods Used

Not applicable.

A.7.5 Number of Energy Groups or If Continuous-energy Cross Sections are Used in the Different Phases of Calculation

1. Continuous-energy cross sections.

2. Continuous-energy cross sections.

A.7.6 Component Calculations

- Type of cell calculation – reactor core and reflectors
- Geometry – fuel pin and assembly lattice
- Theory used – Not applicable
- Method used – Monte Carlo
- Calculation characteristics
  - MCNP5 – histories/cycles/cycles skipped = 1,000,000/2,000/150 continuous-energy cross sections

A.7.7 Other Assumptions and Characteristics

Not applicable.

A.7.8 Typical Input Listings for Each Code System Type

The input deck for only the simple benchmark model is provided. The input lines for the uranium foils are identical in the detailed benchmark model. An input deck for the detailed benchmark model of the system is available in HEU-COMP-FAST-004.

MCNP5 Input Deck for Cadmium Ratio Benchmark Models:

```
Bare Foils
SCCA-FUND-EXP-002-001 and HEU-COMP-FAST-002
C
C
C   Cell Cards
1   1  6.54398E-02  (-25 22 -24) u=11 imp:n=1         $fuel pellet
2   0      -22:(25 22 -24 ):24 u=11 imp:n=1  $void around pellet
4   0    -21 22 -23  fill=11 u=12 imp:n=1
C
C  BASIC FUEL TUBE W/ GRID PLATE
15   15 7.50555E-02 (1 -24 -20 21) u=12 imp:n=1  $Fuel tube
16   15 7.50555E-02 (1 -22 -21):(23 -24 -21) u=12 imp:n=1  $end caps
21   0    -1:20:24 u=12 imp:n=1
C     BASIC FUEL TUBES FOR TUBES WHICH ARE MOVED IN
22  0    -21 22 -23  fill=11 u=13 imp:n=1
23   15 7.50555E-02 (21) u=13 imp:n=1  $Fuel tube
```

```
24   15 7.50555E-02 (-22 -21):(23 -21) u=13 imp:n=1  $end caps
C   BASIC FUEL TUBES
40  0   -12 fill=12 u=1 imp:n=1
C   FUEL TUBES WHICH ARE MOVED IN
41  0   -13 fill=13 (-3.766 -11.458 0) imp:n=1
42  0   -14 fill=13 (3.766 -11.458 0) imp:n=1
43  0   -15 fill=13 (3.766 11.458 0) imp:n=1
44  0   -16 fill=13 (-3.766 11.458 0) imp:n=1
45  0   -17 fill=13 (-8.039 -8.989 0) imp:n=1
46  0   -18 fill=13 (8.039 -8.989 0) imp:n=1
47  0   -19 fill=13 (-8.039 8.989 0) imp:n=1
48  0   -30 fill=13 (8.039 8.989 0) imp:n=1
49  0   -31 fill=13 (-11.805 -2.467 0) imp:n=1
50  0   -32 fill=13 (11.805 -2.467 0) imp:n=1
51  0   -33 fill=13 (-11.805 2.467 0) imp:n=1
52  0   -34 fill=13 (11.805 2.467 0) imp:n=1
C
C  VOID
62  0  -999  u=9 imp:n=1
C   Core Assembly
68  0   -11  lat=2  u=2 imp:n=1 fill= -10:10 -10:10 0:0
     9 9 9 9 9 9 9 9 9 9 9 9 9 9 9 9 9 9 9 9 9  $ROW 1
       9 9 9 9 9 9 9 9 9 9 9 9 9 1 1 1 1 9 9 9 9  $ROW 2
        9 9 9 9 9 9 9 9 9 9 1 1 1 1 1 1 1 1 9 9  $ROW 3
         9 9 9 9 9 9 9 9 9 1 1 1 1 1 1 1 1 1 9 9  $ROW 4
          9 9 9 9 9 9 9 9 1 1 1 1 1 1 1 1 1 1 1 9  $ROW 5
           9 9 9 9 9 9 9 1 1 1 1 1 1 1 1 1 1 1 1 9  $ROW 6
            9 9 9 9 9 9 1 1 1 1 1 1 1 1 1 1 1 1 1 9  $ROW 7
             9 9 9 9 1 1 1 1 1 1 1 1 1 1 1 1 1 1 1 9  $ROW 8
              9 9 9 9 1 1 1 1 1 1 1 1 1 1 1 1 1 1 9 9  $ROW 9
               9 9 9 1 1 1 1 1 1 1 1 1 1 1 1 1 1 1 9 9  $ROW 10
                9 9 1 1 1 1 1 1 1 1 1 1 1 1 1 1 1 1 9 9  $ROW 11
                 9 9 1 1 1 1 1 1 1 1 1 1 1 1 1 1 1 9 9 9  $ROW 12
                  9 9 1 1 1 1 1 1 1 1 1 1 1 1 1 1 9 9 9 9  $ROW 13
                   9 1 1 1 1 1 1 1 1 1 1 1 1 1 1 1 1 9 9 9 9  $ROW 14
                    9 1 1 1 1 1 1 1 1 1 1 1 1 1 1 1 9 9 9 9 9  $ROW 15
                     9 1 1 1 1 1 1 1 1 1 1 1 1 1 1 9 9 9 9 9 9  $ROW 16
                      9 1 1 1 1 1 1 1 1 1 1 1 1 1 9 9 9 9 9 9 9  $ROW 17
                       9 9 1 1 1 1 1 1 1 1 1 1 1 9 9 9 9 9 9 9 9 9  $ROW 18
                        9 9 1 1 1 1 1 1 1 1 1 1 9 9 9 9 9 9 9 9 9 9  $ROW 19
                         9 9 9 9 1 1 1 1 9 9 9 9 9 9 9 9 9 9 9 9 9  $ROW 20
                          9 9 9 9 9 9 9 9 9 9 9 9 9 9 9 9 9 9 9 9 9  $ROW 21
C   Core Tank
70  0   -51 1 -53 13 14 15 16 17 18 19 30 31 32 33 34
     700 701 702 703 704 705 706 707 720 721 722 723 724 725 726 727 728 729
        730 731  741 742 fill=2 imp:n=1
74  2 5.88014E-02 (-53 1 -50 51):(-1 52 -50) imp:n=1 $Core Tank
C
C  Reflectors
C  Void Universe
99   0  -999  u=19 imp:n=1
C  Top Reflector
100  8  1.20554E-01 301 -57 -302 707 708 709 710 711 712 713 imp:n=1
102  0  302 -57 -303  imp:n=1
103  13 7.07826E-02 (301 -303 57 -58):(300 -301 -58) imp:n=1
196  0 -999 300 (58):(-999 303) imp:n=1
C  Bottom Reflector
300  10 1.20636E-01 -57 -304 305  imp:n=1
301  14 6.72481E-02 (57 -58 -304 305):(-305 306 -58) imp:n=1
307  0   58 -304 306 -999 imp:n=1
C   Side Reflector
320  9 1.21199E-01  320 -321 322 -323 imp:n=1
321   0  -300 53 -320 imp:n=1
322   0  -53 50 -320 322 imp:n=1
323   0  -322 50 -326 304 imp:n=1
324   0 -300 52 321 325 -999 imp:n=1
325   0 -306 327 -999 imp:n=1
C  Support Structure/Additional Reflectors
350  30 6.08580E-02 -325 326 imp:n=1 $Support Plate for Be
351  31 8.75101E-02 -327 imp:n=1 $SS304 Plate
C
700  50 4.79835E-02 -700 imp:n=1
701  50 4.79835E-02 -701 imp:n=1
702  50 4.79835E-02 -702 imp:n=1
703  50 4.79835E-02 -703 imp:n=1
704  50 4.79835E-02 -704 imp:n=1
```

```
705  50 4.79835E-02 -705 imp:n=1
706  50 4.79835E-02 -706 imp:n=1
707  50 4.79835E-02 -707 imp:n=1
708  50 4.79835E-02 -708 imp:n=1
709  50 4.79835E-02 -709 imp:n=1
710  50 4.79835E-02 -710 imp:n=1
711  50 4.79835E-02 -711 imp:n=1
712  50 4.79835E-02 -712 imp:n=1
713  50 4.79835E-02 -713 imp:n=1
720  50 4.79835E-02 -720 imp:n=1
721  50 4.79835E-02 -721 imp:n=1
722  50 4.79835E-02 -722 imp:n=1
723  50 4.79835E-02 -723 imp:n=1
724  50 4.79835E-02 -724 imp:n=1
725  50 4.79835E-02 -725 imp:n=1
726  50 4.79835E-02 -726 imp:n=1
727  50 4.79835E-02 -727 imp:n=1
728  50 4.79835E-02 -728 imp:n=1
729  50 4.79835E-02 -729 imp:n=1
730  50 4.79835E-02 -730 imp:n=1
731  50 4.79835E-02 -731 imp:n=1
741  50 4.79835E-02 -741 imp:n=1
742  50 4.79835E-02 -742 imp:n=1
C
999  0  999 imp:n=0

C   Surface Cards
1    pz   0.      $bottom of fuel
11   rhp  0 0 -10  0 0 50   0.753 0 0
12   rhp  0 0 -11  0 0 52   1 0 0
13   rcc  -3.766 -11.458 0  0 0 30.48  0.635
14   rcc  3.766 -11.458 0  0 0 30.48  0.635
15   rcc  3.766 11.458 0  0 0 30.48  0.635
16   rcc  -3.766 11.458 0  0 0 30.48  0.635
17   rcc  -8.039 -8.989 0  0 0 30.48  0.635
18   rcc  8.039 -8.989 0  0 0 30.48  0.635
19   rcc  -8.039 8.989 0  0 0 30.48  0.635
20   cz   0.635   $OR Clad
21   cz   0.584   $IR Clad
22   pz   0.3     $top of bottom cap
23   pz  30.18    $bottom of top cap
24   pz  30.48    $Top of fuel tube
25   cz   0.5705  $OR of Pellet
30   rcc  8.039 8.989 0  0 0 30.48  0.635
31   rcc  -11.805 -2.467 0  0 0 30.48  0.635
32   rcc  11.805 -2.467 0  0 0 30.48  0.635
33   rcc  -11.805 2.467 0  0 0 30.48  0.635
34   rcc  11.805 2.467 0  0 0 30.48  0.635
C  Core Tank
50  cz  12.98  $OR Core Tank
51  cz  12.726 $IR Core Tank
52  pz  -0.33   $Bottom of Core Tank
53  pz  30.71  $Top of Core Tank
C  simple model to preflector
57   cz 20.65   $Ir upper and lower tank
58   cz 21.285 $OR upper and lower tank
C
300    pz  30.935
301    pz  31.155
302    pz 38.14
303    pz  43.885
C
304    pz -0.33
305    pz -7.95
306    pz -8.84
C   Side Reflector
320    cz  13.08
321    cz  24.45
322    pz 0.305
323    pz 30.935
C
C    Be Support Plate
325  rpp -37.5 37.5  -37.5 37.5  -0.33 0.305
326  cz  13.95
C    SS304 Plate
327  rcc 0. 0. -11.22  0. 0. 2.38  22.86
```

```
C
700  rcc  0.635  0  12.7  0.01  0  0  0.375
701  rcc  0.635  0  15.24  0.01  0  0  0.375
702  rcc  0.635  0  17.78  0.01  0  0  0.375
703  rcc  0.635  0  20.32  0.01  0  0  0.375
704  rcc  0.635  0  22.86  0.01  0  0  0.375
705  rcc  0.635  0  25.4  0.01  0  0  0.375
706  rcc  0.635  0  27.94  0.01  0  0  0.375
C
707  rcc  0  0  30.48  0  0  0.01  0.375
708  rcc  0  0  31.155  0  0  0.01  0.375
709  rcc  0  0  32.425  0  0  0.01  0.375
710  rcc  0  0  33.695  0  0  0.01  0.375
711  rcc  0  0  34.965  0  0  0.01  0.375
712  rcc  0  0  36.235  0  0  0.01  0.375
713  rcc  0  0  37.505  0  0  0.01  0.375
C
720  rcc  -0.549926131  0.3175  15.24  -0.008660254  0.005  0  0.375
721  rcc  -2.808926131  1.621734258  15.24  -0.008660254  0.005  0  0.375
722  rcc  -5.067926131  2.925968516  15.24  -0.008660254  0.005  0  0.375
723  rcc  -7.326926131  4.230202774  15.24  -0.008660254  0.005  0  0.375
724  rcc  -9.199357143  3.677020147  15.24  0.009285714  -0.003711537  0  0.375
725  rcc  -10.66419146  1.231394763  15.24  0.009933993  -0.001147079  0  0.375
726  rcc  -9.260527778  6.16911716  15.24  0.008322397  -0.00554416  0  0.375
727  rcc  -10.37864286  4.148385402  15.24  -0.009285714  0.003711537  0  0.375
728  rcc  -5.7065  9.883947933  15.24  0.005  -0.008660254  0  0.375
729  rcc  -11.92580854  1.377073754  15.24  -0.009933993  0.001147079  0  0.375
730  rcc  -10.31747222  6.873225421  15.24  -0.008322397  0.00554416  0  0.375
731  rcc  -11.8950186  4.120555315  15.24  -0.009449112  0.003273268  0  0.375
C
741  rcc  1.51  2.615396719  30.48  0  0  0.01  0.375
742  rcc  6.03  10.44426637  30.48  0  0  0.01  0.375
C
999   rpp  -500 500   -500 500  -500 500

C   Data Cards
m1   92234.70c   2.21403E-04
      92235.70c   2.03324E-02
      92236.70c   1.02154E-04
      92238.70c   1.15733E-03
      8016.70c   4.35205E-02
      8017.70c   1.06012E-04   $ Tot   6.54398E-02
C   Fuel Clad
m15   26054.70c   2.97938E-03
      26056.70c   4.67699E-02
      26057.70c   1.08012E-03
      26058.70c   1.43744E-04
      6000.70c   1.37950E-04
      25055.70c   7.53997E-04
      14028.70c   6.80144E-04
      14029.70c   3.45361E-05
      14030.70c   2.27664E-05
      24050.70c   6.23067E-04
      24052.70c   1.20152E-02
      24053.70c   1.36243E-03
      24054.70c   3.39138E-04
      28058.70c   5.28531E-03
      28060.70c   2.03589E-03
      28061.70c   8.84989E-05
      28062.70c   2.82173E-04
      28064.70c   7.18612E-05
      15031.70c   3.00906E-05
      16032.70c   1.83924E-05
      16033.70c   1.47248E-07
      16034.70c   8.31174E-07
      16036.70c   3.87494E-09
      41093.70c   2.86989E-04
      73181.70c   1.28933E-05   $tot   7.50555E-02
C   Core Tank
m2   13027.70c   5.85485E-02
      29063.70c   2.16403E-05
      29065.70c   9.64537E-06
      14028.70c   1.24044E-04
      14029.70c   6.29865E-06
      14030.70c   4.15212E-06
      26054.70c   3.95341E-06
```

```
      26056.70c   6.20601E-05
      26057.70c   1.43324E-06
      26058.70c   1.90738E-07
      25055.70c   7.23754E-06
      30000.70c   1.21614E-05   $ Tot   5.88014E-02
C   Reflectors
C  ***********************************
C  Top Reflector
m8   4009.70c   1.20554E-01
C   Side Reflector
m9   4009.70c   1.21199E-01
C   Bottom Reflector
m10   4009.70c   1.20636E-01
C    ***********************************
C  Upper reflector tank
m13   13027.70c   7.04918E-02
      29063.70c   2.60429E-05
      29065.70c   1.16077E-05
      14028.70c   1.49280E-04
      14029.70c   7.58007E-06
      14030.70c   4.99684E-06
      26054.70c   4.75770E-06
      26056.70c   7.46858E-05
      26057.70c   1.72482E-06
      25055.70c   8.70996E-06
      30000.70c   1.46355E-06   $ Tot   7.07826E-02
C  lower reflector tank
m14   13027.70c   6.69718E-02
      29063.70c   2.47424E-05
      29065.70c   1.10280E-05
      14028.70c   1.41826E-04
      14029.70c   7.20156E-06
      14030.70c   4.74732E-06
      26054.70c   4.52013E-06
      26056.70c   7.09564E-05
      26057.70c   1.63869E-06
      25055.70c   8.27504E-06
      30000.70c   1.39047E-06   $ Tot   6.72481E-02
C   ************************************
C  Additional Bottom Reflectors
C   Be Support Plate (Al1100)
m30   13027.70c   6.06080E-02
      29063.70c   2.23913E-05
      29065.70c   9.98012E-06
      14028.70c   1.28349E-04
      14029.70c   6.51725E-06
      14030.70c   4.29622E-06
      26054.70c   4.09062E-06
      26056.70c   6.42139E-05
      26057.70c   1.48298E-06
      25055.70c   7.48872E-06
      30000.70c   1.25834E-06   $ Tot   6.08580E-02
C   SS304 Support Plate
m31   26054.70c   3.51905E-03
      26056.70c   5.52415E-02
      26057.70c   1.27577E-03
      26058.70c   1.69781E-04
      6000.70c   1.60142E-04
      25055.70c   8.75287E-04
      14028.70c   7.89554E-04
      14029.70c   4.00916E-05
      14030.70c   2.64287E-05
      24050.70c   7.63478E-04
      24052.70c   1.47229E-02
      24053.70c   1.66946E-03
      24054.70c   4.15564E-04
      28058.70c   5.29886E-03
      28060.70c   2.04111E-03
      28061.70c   8.87257E-05
      28062.70c   2.82896E-04
      28064.70c   7.20454E-05
      15031.70c   3.49310E-05
      16032.70c   2.13510E-05
      16033.70c   1.70934E-07
      16034.70c   9.64879E-07
      16034.70c   4.49827E-09   $ tot   8.75101E-02
```

```
C    U Foils
m50   92234.70c   4.67753E-04
      92235.70c   4.47223E-02
      92236.70c   1.14750E-04
      92238.70c   2.67865E-03   $ total   4.79835E-02
C    Cd Covers
m55   48106.70c   5.79249E-04
      48108.70c   4.12425E-04
      48110.70c   5.78786E-03
      48111.70c   5.93151E-03
      48112.70c   1.11818E-02
      48113.70c   5.66274E-03
      48114.70c   1.33135E-02
      48116.70c   3.47086E-03   $ total   4.63399E-02
C   Scattering Cards
mt1   o2/u.10t  u/o2.10t
mt2    al27.12t
mt8   be.10t
mt9   be.10t
mt10  be.10t
mt13   al27.12t
mt14   al27.12t
C mt20   al27.12t
C mt22   al27.12t
C m23    al27.12t
mt30   al27.12t
C
kcode  100000 1 150 2150
ksrc   0.0692  4.5245 0.77787  0  8.8072 0.7787
       0.0692 -4.3864 0.77787  0 -8.7382 0.7787
       3.8736 0 0.7787   7.6780 0 0.7787
      -3.7353 0 0.7787  -7.8510 0 0.7787
f4:n  700
fm4   1 50 -6
C
f14:n   701
fm14   1 50 -6
C
f24:n   702
fm24   1 50 -6
C
f34:n   703
fm34   1 50 -6
C
f44:n   704
fm44   1 50 -6
C
f54:n  705
fm54   1 50 -6
C
f64:n   706
fm64   1 50 -6
C
f74:n   707
fm74   1 50 -6
C
f84:n   708
fm84   1 50 -6
C
f94:n   709
fm94   1 50 -6
C
f104:n   710
fm104   1 50 -6
C
f114:n   711
fm114   1 50 -6
C
f124:n   712
fm124   1 50 -6
C
f134:n   713
fm134   1 50 -6
C
f144:n   720
fm144   1 50 -6
```

```
C
f154:n   721
fm154   1 50 -6
C
f164:n   722
fm164   1 50 -6
C
f174:n   723
fm174   1 50 -6
C
f184:n   724
fm184   1 50 -6
C
f194:n   725
fm194   1 50 -6
C
f204:n   726
fm204   1 50 -6
C
f214:n   727
fm214   1 50 -6
C
f224:n   728
fm224   1 50 -6
C
f234:n   729
fm234   1 50 -6
C
f244:n   730
fm244   1 50 -6
C
f254:n   731
fm254   1 50 -6
C
f264:n   741
fm264   1 50 -6
C
f274:n   742
fm274   1 50 -6
C  rand  seed=7065399757867  $ r2
C  rand  seed=5724484131590  $ r3
C  rand  seed=417647895433   $ r4
C  rand  seed=8132049697893  $ r5
C  rand  seed=8663498807872  $ r6
C  rand  seed=7447087897166  $ r7
```

A.8 Power Distribution Configurations

The axial relative power distribution is the same as the relative fission rate as was measured in the core region of Assembly 1 (see Section A.7).

A.9 Isotopic Configurations

Isotopic measurements were not performed.

A.10 Configurations of Other Miscellaneous Types of Measurements

Other miscellaneous types of measurements were not performed.